Politecnico di Milano

Energy Department

Doctoral Program in
Energy and Nuclear Science and Technology

Operation and design optimization for off-grid hybrid microgrids with high RES penetration

Author:
Simone Mazzola

Supervisor:
Prof. Ennio Macchi

Tutor:
Prof. Paolo Chiesa

Doctoral Program Coordinator:
Prof. Enrico Bottani

2017 - XXIX Cycle

Abstract

Nowadays, electricity production in off-grid contexts is mainly based on fossil fuels, especially diesel. Considering that diesel oil cost is considerably higher than on mainland, this entails very high electricity costs together with other drawbacks, as the energy dependence from the outside and possible environmental concerns. Renewable energy sources (RES) have proven to be effective in order to reduce the overall electricity costs in remote contexts and to ensure a sustainable energy access, characterized by low emissions of pollutants and carbon dioxide. For these reasons, we are witnessing at numerous projects worldwide aiming at 100% production from renewables. Unfortunately, this goal is not feasible in a cost-effective way relying only traditional RES as sun and wind, which are characterized by a strong intermittency and it would require huge energy storages.

The thesis starts from this background and investigates two possible approaches to increase RES penetration without incurring in a sharp increase of electricity cost. First, the possibility to include in the scheduling some programmable loads has been considered. The concept of "multi-good system" has been introduced, enabling the possibility to optimize the operation of microgrids in which all valuable goods (as electricity, heating and potable water) are taken into account. Second, the potential related to dispatchable RES generators (as biomass-based generators and Concentrating solar power with thermal energy storage) which do not suffer intermittency have been evaluated. Both options have been studied using an original simulation mathematical model developed by the author and based on consecutive resolutions of the unit commitment problem with a limited time horizon following a rolling horizon approach.

The two options have been assessed analyzing two different case studies, a rural village and an island community. Results show that programmable loads are effective in mitigating the intermittency of PV, shifting in time a part of the energy consumption. This entails that the allowable RES share increases to values around 40-50%. The second option appears to be even more effective: thanks to the capability to produce energy when it is needed, dispatchable RES generators allows to break 70-80% RES penetration maintaining a cost-saving respect to fossil-fuel solutions. The results show also that optimal solutions do not rely on a single technology and synergy among intermittent and dispatchable RESs allows to reach nearly 90% RES penetration.

Contents

Chapter 1

Introduction

The lack of reliable and affordable electricity access is experienced in many rural regions of developing countries (Kanagawa and Nakata, 2008). This problem is very widespread and affects over 1 billion people across the world, according to an IEA estimate (IEA, 2012). Grid extension has been the most common pathway for universal energy access in developed countries but it faces many difficulties in developing countries context (Mainali and Silveira, 2013). The main reason is that grid extension is a capital intensive option, which needs a considerable energy volume to make sense. In addition to this, even in cases where the grid is already present, the quality of service can be so low due to frequent outages to become a barrier to electricity access. Providing electricity in remote locations is not related only to developing countries but also to other contexts as islands and remote areas. In most of these cases, grid extension is practically unfeasible and other solutions are needed.

A possible option is given by off-grid microgrids. These energy systems rely on local power generators, avoiding the need of the infrastructure to reach the existing grid and its associated energy losses. Internal combustion engines fueled by diesel are the most common generation technology due to properties such as a wide operating range and high reliability. However, diesel-generated electricity is usually more expensive than the average cost of grid electricity due to the inherently high oil fuel cost, which can increase significantly when it has to be transported to isolated locations. Motivated by the cost decrease of generation technologies based on renewable energy resources (RES), the use of hybrid microgrids with intermittent renewable energy sources (i.e. photovoltaic (PV) panels, wind turbines) has been addressed in literature (B. Zhao, X. Zhang, Li, et al., 2014; Bekele and Palm, 2010) and implemented in many locations (Schnitzer et al., 2014), usually in combination with a battery energy storage system (BESS) to cope with the natural variability of wind and solar generators.

In addition to this, looking from a wider perspective, it would be more cost-effective to push RES in remote contexts rather than on large grids in developed countries to reduce anthropogenic carbon dioxide emissions. An important metric to support this argument is the cost of CO_2 avoided, given by the ratio between the increase of the electricity cost (comparing traditional sources and RES) and the amount of CO_2 avoided. Since the electricity cost from traditional fossil fuel sources is usually very low in industrialized countries, in most of the cases the cost of the CO_2 avoided could be high, braking the development of RES. A perfect example is Italy, where, after an investment boom caused by massive incentives, new RES capacity is slowing down[1]. On the other hand, if we consider remote contexts, the cost of

[1] New capacity from RES has declined from +11 GW/year in 2010 to +0.9 GW/year in 2015 (Terna, 2016)

electricity by traditional sources (mainly diesel oil) is very high and the cost of CO_2 avoided could be very low or even negative if RES electricity costs is lower than traditional one.

However, even if capable of reducing overall electricity costs with a negative cost of CO_2 avoided, most common RES show strong limitations. In fact their intermittent nature is a barrier to reach high degrees of RES penetration, which is the share of total energy produced only by RES. This aspect is confirmed by numerous real projects, which show how difficult is to design systems which can produce more than half of their energy from intermittent RES as PV and wind turbines (Bunker et al., 2015a; IRENA, 2015b).

Two options could play a relevant role to overcome this limit. On one hand, we have the possibility to develop more advanced microgrid management strategies, which can take into account short-term forecast (around 1 day) to manage optimally generators and controllable loads and finally lower the operating costs. On the other hand, we can consider the implementation of dispatchable RES generators, namely technologies which can adjust their power output according to system requests (i.e. biomass-based generators, concentrating solar power). Only few studies in literature deal with this topic (Ho, Hashim, and Lim, 2014) and there is a lack of tools to properly simulate this kind of technologies in a microgrid environment. The thesis work aimed to close this gap and, consequently, give an actual contribution to the development of hybrid microgrid systems.

Scope and objectives

This thesis work investigates the possibility to use advanced mathematical tools for the successful operation and design of hybrid microgrid systems. As a secondary objective, these tools are also applied on two different test-cases in order to test their effectiveness and to evaluate dispatchable RES technologies feasibility. Given the background described in the previous section, this thesis work aims to contribute at answering the following question: *Which are the tools and technologies to make off-grid microgrids a more competitive and sustainable solution?* In order to accomplish the main objective, the following set of sub-tasks is listed:

- Analyzing the current state of art status related to microgrids, with a focus on optimizations models applied in management and design.
- Developing simulation and optimization tools capable of handling complex systems, made by different generation technologies and programmable loads.
- Performing system analysis in order to evaluate the potential impact in both technical and economic terms of dispatchable RES (biomass-based generators and concentrating solar power) in an off-grid system environment.

In relation to the initial scope and objectives, the main thesis contributions can be summarized as follows:

- Assessment of the potential advantages related to operation strategies based on forecast in comparison with non-predictive ones. This comparison is made using an ad-hoc

simulation framework which evaluates the cost saving related to forecast-based strategies using perfect forecast (*Paper I*) and real forecast datasets with different levels of accuracy (*Paper III*).

- Development of a mathematical model for the optimal operation of complex microgrid systems (*Paper I*). The most innovative aspect is that not only electricity but multiple goods (as potable water or wood-chips) are taken into account in the optimization, enabling the possibility to define the optimal schedule of both loads and complex generators and consequently achieve higher cost savings.

- Integration of the developed mathematical model in a simulation framework and application to two different test-cases in order to test the feasibility of dispatchable RES generators. In the first case (*Paper II*), the installation of two biomass-based technologies is investigated, evaluating their performance in an advanced microgrid, in which a relevant part of the loads is schedulable. In the second case (*Paper IV*), a comparison between PV and Concentrating Solar Power technologies on the capability to provide energy to an island community is performed, taking into account potential synergies with desalination facilities.

Thesis structure

This thesis includes eight chapters. Chapter 1 is an introduction to the thesis, giving a brief overview of the background, a description of the scope and a list of the publications developed concurrently with this thesis work. In Chapter 2 the technical background is defined. The concept of microgrid is introduced, exploring its field of application and possible architectures. Then, the most relevant technologies in the fields of power generation and energy storage are described, focusing on both traditional and innovative ones. Chapter 3 offers a description of most common mathematical tools, used for microgrid operations and design. In the first part, the algorithms used for microgrid operation (the dispatch strategies) are introduced, showing and describing the most interesting examples of both non-predictive and predictive ones. In the second part, the focus is shifted on the mathematical tools proposed in literature to perform long-term simulation and design of hybrid microgrids. Chapter 4 describes the methodology developed in the thesis work, highlighting the potential advantages compared with state of the art mathematical models. In Chapter 5 a comparative analysis on how predictive and non-predictive strategies perform is given. After the analysis of a case with perfect forecast, the remaining part of the chapter is devoted to assess qualitatively the impact of forecast accuracy on the performance of a microgrid running with a predictive strategy. Chapter 6 reports the first application of the methodology developed in the thesis to a peculiar test-case, a rural village located India. In addition to exploring the capability of the model to handle a system with numerous programmable units, this study evaluates how biomass-based generators (an example of dispachable RES generators) could perform in an off-grid environment. Chapter 7 has a structure similar to the previous one, but the test-case is a remote island. In this chapter the potential of Concentrating solar power is

assessed, making a comparison with PV technologies and exploring possible synergies with most popular desalination technologies. Finally Chapter 8 gives the conclusions to the work and offers some starting points for future works.

Publications

The papers included in this thesis are *Paper I*, *Paper II*, *Paper III* and *Paper IV* of the list below. With regard to these, I am the first author, responsible of the modeling, the simulations and part of the writing. Significant parts of the Chapters 4, 5, 6, 7 are self-citations from previous mentioned papers. As reported in Elsevier policy[2], as author of these articles, I retain the right to include the journal article, full or in part, in a thesis or dissertation without any permission. An additional paper has been realized during this thesis work but not included in the final manuscript (*Paper V*).

Paper I

Simone Mazzola, Marco Astolfi, and Ennio Macchi (2015a). "A detailed model for the optimal management of a multigood microgrid". In: *Applied Energy* 154, pp. 862–873

Paper II

Simone Mazzola, Marco Astolfi, and Ennio Macchi (2016). "The potential role of solid biomass for rural electrification: A techno economic analysis for a hybrid microgrid in India". In: *Applied Energy* 169, pp. 370–383

Paper III

Simone Mazzola, Claudio Ricardo Vergara, et al. (2017). "Assessing the value of forecast-based dispatch in the operation of off-grid rural microgrids". In: *under review*

Paper IV

Simone Mazzola, Marco Astolfi, Paolo Silva, et al. (2017). "Solar energy for electricity and water production in islands". In: *under review*

Paper V

Simone Mazzola, Marco Astolfi, and Ennio Macchi (2015b). "Techno-Economic Optimization of a Stand-alone Hybrid Microgrid for the Rural Electrification in Sub Saharan Africa". In: *3rd Southern African Solar Energy Conference*

[2]URL:`http://www.elsevier.com/wps/find/authorsview.authors/copyright#whatrights`; Date of access: 28 Jun 2016

Chapter 2

Off-grid microgrids overview

Microgrids (MGs) are energy systems made by power generators, energy storages, loads and an electric network which connect all the components, able to self-produce and fulfill the energy demand (or a part of it). Different definitions have been proposed to outline the MG concept and one of the most popular, coming from the U.S. Department of Energy, is hereafter reported:

"A microgrid is a group of interconnected loads and distributed energy resources within clearly defined electrical boundaries that acts as a single controllable entity with respect to the grid. A microgrid can connect and disconnect from the grid to enable it to operate in both grid-connected or island-mode."

U.S. Department of Energy, 2012

Two pillars can be extracted from this definition. First, the capability of the MG to act a single controllable entity and hence the possibility to manage efficiently its components. Second, the possibility to operate in both grid-connected or island mode.

Grid-connected MGs are expected to play an important role in the future of energy field, especially for the integration of low carbon technologies (Farhangi, 2010). The aim of grid-connected MGs is to coordinate optimally different distributed generators (including controllable entities as storage or programmable loads) considering the interaction with the existing grid. Power generation can be delocalized, moving from large scale centralized power generation systems to small scale renewable energy sources system, as PV or wind turbines, and small-scale combined heat and power (CHP) generators. This will bring potential benefits in increased energy efficiency and reduced carbon emissions (Hatziargyriou et al., 2007). In case of grid faults, MGs could be able to work in island mode, hence ensuring high level of energy supply reliability.

The other branch is off-grid MGs. These systems have been in use since long time to provide energy in remote locations, which can not be easily connected to an existing grid or in case of very low reliability of the grid. In the last decade the interest in this kind of systems has grown thanks to the development of cheap and reliable renewable energy based systems, potentially capable of replacing fossil fuels in these contexts. In the next sections, an overview on off-grid MGs will be given, focusing on application fields, most common system architectures and components.

2.1 Application fields

Off-grid MGs can be installed for different purposes. Following the segmentation proposed in Navigant Research, 2014, three main application fields can be listed:

- Rural electrification
- Islands and remote communities
- Users with high reliability requests

2.1.1 Rural electrification

In 2011 the International Energy Agency (IEA) estimated that 1.3 billion people were living in small villages without grid connection. Figure 2.1 shows that this problem is mostly widespread in developing countries, especially in Sub Saharan Africa, Latin America and South-East Asia.

The lack of energy access does not allow to stock perishables, medicines and vaccines, to install a pump to draw water from a well or to purify water. The availability of electricity can dramatically increase the quality of life, allowing the reduction of the infant mortality and the transmission of diseases. Furthermore the lack of energy limits the opportunity for women and children who spend several hours daily harvesting wood or water for domestic purposes subtracting time to education or social and economic activities (Kanagawa and Nakata, 2007).

Grid extension has been the most common pathway for universal energy access in developed countries but it faces many difficulties in developing countries context (Mainali and Silveira, 2013). First, grid extension is capital intensive and the cost will only be recovered if the energy consumption volume is sufficiently high. In addition to this, the national grids

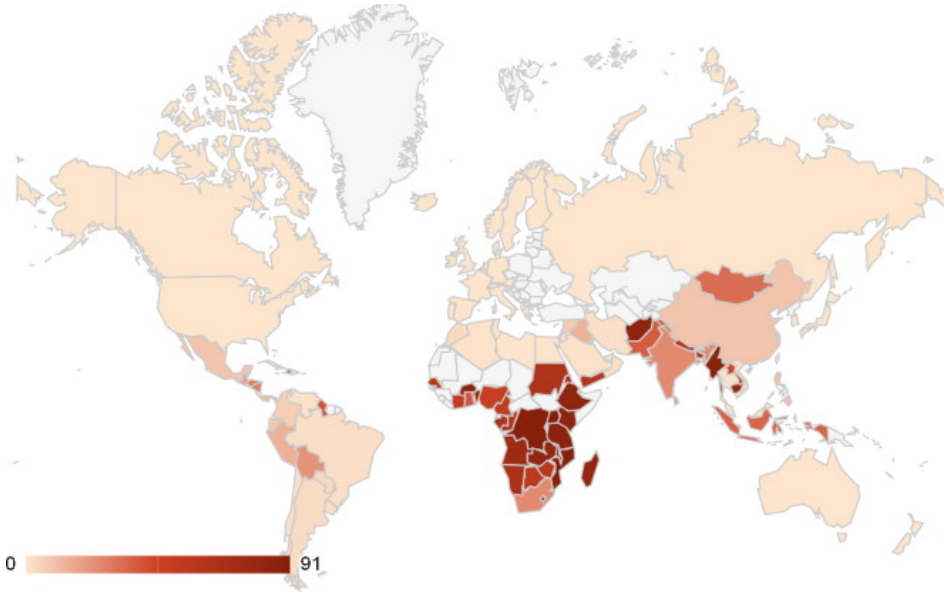

FIGURE 2.1: Share of population with no access to electricity (Javadi et al., 2013)

in developing countries are often weak and unreliable, suffering frequent outages during normal operation; in these cases the network reliability will simply worsen upon connection of additional rural consumers.

For this reason off-grid MGs are often the best solution for rural electrification, relying on local power generators and avoiding the need of the infrastructure to reach the existing grid and its associated energy losses. A study conducted to identify the best energy access pathways for Africa highlights that grid connection is the best option only for users close to existing grids while MGs based on diesel and PV are expected to cover the majority part of energy demand (Szabó et al., 2011).

The potential demand related to this segment is potentially very high. According to the 2016 World Energy Outlook (WEO) database[1], 1.2 billion people (17% of world population) lacks of energy access. The problem is more suffered in rural areas, which accounts for 80% of people without electricity. The WEO gives also an estimate of the minimum level of electricity consumption for rural households (250 kWh/year) and the number of people that will probably gain energy access from current situation to 2040 (2.7 billion). Even assuming that only 30% of this demand will be covered by off-grid MGs, we obtain that almost 200 TWh/year will be produced by MGs only for rural energy access.

The path is still very long, but there is a considerable amount of examples of successful MG installations around the world. A recent report from IRENA (IRENA, 2015b) shows that the market is growing worldwide, offering an overview of the situation for each single country. As stated in Schnitzer et al., 2014, the number of total installations will probably increase in the future, especially if main non-technical limits, including policy, regulation and social aspects to be considered in poor rural areas, will be overcome. Unfortunately, there is not a comprehensive database which can help determine exactly the overall development status and the data in literature come only from fragmentary sources.

2.1.2 Islands and remote communities

In the category of island and remote communities the cases where the energy access is already present are considered. The most common solution in these cases is power generation from diesel-fueled generators because the connection to an existing grid is practically unfeasible. In addition to contributing to CO_2 emissions and global warming, generation from fossil fuels comes with relevant drawbacks for the local communities: (i) the electricity price is considerably higher than mainland prices since diesel oil is generally more expensive in these contexts, (ii) the community is strongly dependent on resources coming from outside and (iii) generation from diesel brings local pollution, which can alter fragile ecosystems and have negative effects on tourism, which is often the first source of income.

Integrating RES in these contexts could be a potential solution for the drawbacks listed above and the increasing number of projects and installations of RES in islands seems to confirm it. IRENA estimates that there is currently a diesel generators total capacity of 12 GW, only considering islands (IRENA, 2015b), and so there is a large market potential

[1]Source: World Energy outlook;
Date of access: 28 Jun 2016;URL:`http://www.worldenergyoutlook.org/resources`

Table 2.1: Data for representative RES integration projects in islands. Data elaborated from Bunker et al., 2015a.

Island	**Peak**	**RES share**	**Diesel**	**Wind**	**PV**	**Hydro**	**Energy storage**
	MW	%	MW	MW	MW	MW	
Marble bar	0.82	30%	2.24	0	0.5	0	Flywheel
El Hierro	7.6	31%	12.7	11.5	0	11.3	Hydro
Falkland islands	3.2	33%	6.6	1.98	0	0	Flywheel
Bonaire	11	44%	14	11	0	0	Battery
Coral bay	0.6	45%	2.24	0.67	0	0	Flywheel
King island	2.5	65%	6	2.45	0.4	0	Battery+Flywheel
Isle of Eigg	0.065	87%	0.112	0.024	0.05	0.112	Lead-acid battery
Kodiak	27.8	97%	33	9	0	30	Battery+Flywheel

to replace the energy coming from diesel with RES. Numerous studies showing successful examples of RES integration in islands are available in literature (Neves, C. A. Silva, and Connors, 2014, IRENA-GREIN, 2014, Bunker et al., 2015a). A list of the most representative ones is reported in Table 2.1.

Looking at the whole table, it is evident that it is not trivial to reach high RES penetration, which would mean very high diesel oil savings. The three cases which exceed 50% of RES penetration rely massively on storage; in addition to this, in author's opinion, RES penetration given for the last two cases are not referred to yearly penetration, but, more probably, to the maximum penetration of RES during 1 hour or 1 day. Unfortunately only the report from Bunker et al., 2015a is available and there are not other resources about the two projects to confirm the data.

King Island is a great example of how a relevant share of RES can be reached using intermittent RES. In order to obtain this goal, a battery of 1.5 MWh battery (60% of hourly peak demand) and a flywheel helps stabilize the grid. Notice that, according to the data available from the King Island project[2], also a dynamic resistor, capable of absorbing and dumping up to 1.5 MW of power, is needed to operate the grid.

Another important case is the El Hierro island, which is expected to be the first 100% RES-based island. This will be possible thanks to the presence of a pumped hydro storage, with a nominal capacity exceeding the maximum peak demand. Even if there are many enthusiastic claims about the project, the data from Réd Electrica de España[3] say the opposite. Looking at the data from 2015, it is possible to note that we are far from 100% RES penetration and

[2]Source: The King Island Renewable Energy Integration Project (KIREIP); Date of access: 28 Jun 2016;URL:`http://www.kingislandrenewableenergy.com.au/project-information/overview`

[3]Source: Réd Electrica de España (REE); Date of access: 28 Jun 2016;URL:`https://demanda.ree.es/movil/canarias/el_hierro/total/2015-08-29`

only 33% of energy has been produced by RES. However this number is expected to increase together with the experience of the grid operator in managing such a system.

2.1.3 Users with high reliability request

A significant MGs growth is expected in the segment which include all the users which need a very high reliability of electricity supply. Energy security is the most important parameter for some applications, as remote industrial sites, telecommunication facilities and military infrastructures.

For the case of telecommunication towers, the proper trade-off between costs and reliability has to be found, considering that, if a fault occurs and the tower is located in a remote location, maintenance time and costs can be considerably high. All these aspects have to be taken into account during design, finding solutions with a certain degree of redundancy and acceptable costs (Kwasinski and Krein, 2006). Similar considerations apply to other industrial contexts (IRENA, 2015b).

Reliable power supply to military sites is another possible option for MGs. Considering the only US market, the market is growing very fast, going from an installed MG capacity of 5 MW in 2012 to more than 50 MW in 2018 (Navigant Research, 2014). Even in this case, the possibility to have an interruptible energy access is the main factor driving this growth, since military sites has a great importance for national security. In addition to this, the possibility to cogenerate heat and to increase the production by RES are other important factors, taken into account to reduce the energy costs and to mitigate CO_2 emissions. An example of great involvement is offered by the U.S. Navy, which is investing on MG technology performing technical and economic tests in different U.S. bases located in the South West (Maurer, 2013).

2.2 Architectures

Given the possible components of a MG, as generators, programmable loads and energy storages, there are different options to interconnect them. At the beginning, remote systems were made only by AC buses. In fact, both generation (Diesel engines) and consumption happened in AC, not requiring any conversion. Fixed the topology, the distribution network has to be designed, choosing the voltage level (one or more than one), the right components (i.e. distribution lines, transformers) and their location, taking into account the spatial distribution of the gen-set and the loads and the expected load consumption patterns. In that respect, different optimization tools have been proposed to tackle this task, finding the optimal network which minimize the sum of up-front and operation costs (Domingo et al., 2011). The introduction of other appliances working in AC does not generally make more complex the MG topology, as happened for Ramea wind-diesel power plant (Mariam, Basu, and Conlon, 2013).

The introduction of devices working in DC, as PV systems and batteries, changes the system architecture. There are different options, but the main point is to reduce the number of interface elements and therefore the energy losses during operation (Unamuno and Barrena, 2015). As shown in Figure 2.2, the AC bus and DC bus are coupled by a single converter and

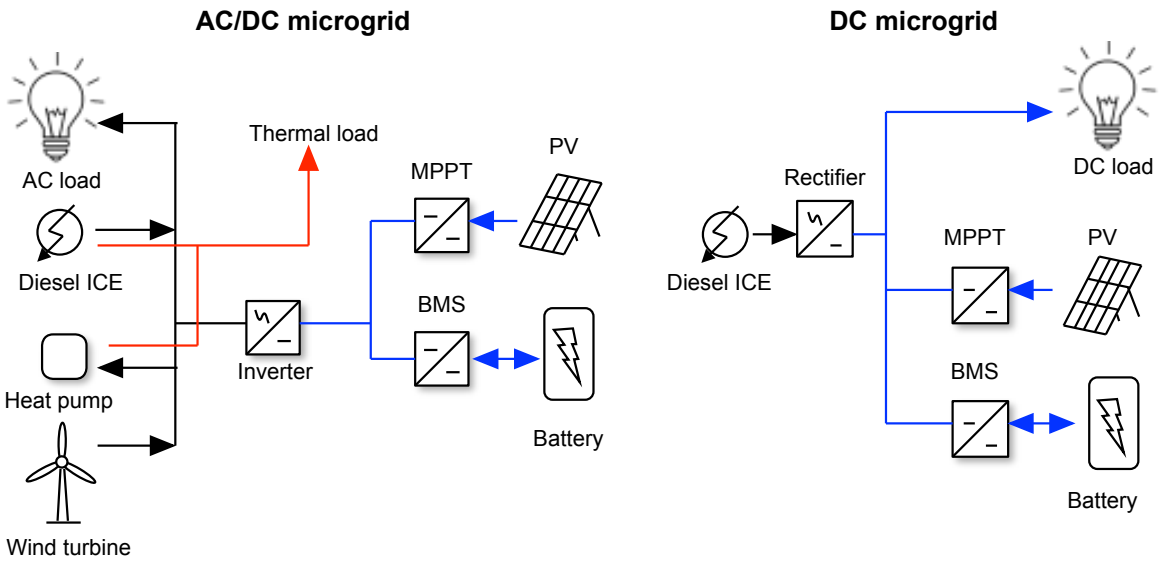

FIGURE 2.2: Schematics of AC/DC and DC microgrids

each device is connected to the most appropriate bus. Spatial restrictions or other limitations may lead to the use of multiple converters.

Recently another option is gaining attention. It is the case of DC microgrids, which have been proposed both for residential applications in developed countries and for rural electrification. Examples of real cases applications are present over the world, especially across Bihar (India) and Bangladesh, but the total number of installations is not comparable to AC microgrids. This solution has been developed to increase the penetration of energy produced by PV. In fact, considering that the most common residential loads are (or can be) powered in DC, the distribution network and the household electric systems can be made in DC. Eventually, a backup Diesel generator, which in these systems is expected to be in operation for few hours during the years, can be connected to the distribution network using a rectifier. This approach promises different benefits, as a reduction of conversion losses (from DC to AC for PV generation and from AC to DC in the loads) and a lower installation costs (Madduri et al., 2013). On the other hand, the lack of standardized design procedures and the limited maximum power capacity are the main limits (Groh et al., 2014).

Another possibility offered by MGs is the capability to use the waste heat produced by power generators. This capability, generally called cogeneration or combined heat and power (CHP), enables to reduce the overall fuel consumption in the system, limiting the use of other components, as boilers or heat pumps. Other possible synergies with programmable loads can be established, making the MG architecture more complex.

2.3 Power generation technologies

In this section an overview of some power generation technologies for MGs application is offered. First, internal combustion engines, which are the most traditional way to produce

energy in off-grid contexts, are analyzed. Then, a focus on energy systems fed by solar energy is given, considering PV (the most common) and CSP. Finally, small scale technologies for exploitation of wood biomass are presented. This section does not aim to be a comprehensive review of all possible technologies for power production in MGs (which should include at least mini-hydro and wind power), but it is a focus on the technologies that will be taken into account in the test-cases of this thesis, which investigate the value of generators dispatchability.

2.3.1 Internal combustion engines

An internal combustion engine is a heat engine able to convert in mechanical work part of the energy released during the combustion of a fuel. For microgrid applications, the mechanical energy is then converted in AC electricity thanks to an alternator. The working fluid (air before the combustion and flue gases after), thanks to expansion and compression, exchanges energy with the moving parts of the machine. Internal means that the combustion happens into the machine, without auxiliary external components as boilers. According to this definition, turbine gases should be considered in ICEs category, but usually this definition is only applied to volumetric ICEs.

ICEs are classified according to the fuel feed and the thermodynamic cycle. Natural gas and liquid products such as gasoline, diesel fuel and fuel oil are commonly used to feed ICEs. Recently, the interest in renewable fuels like biodiesel and biothenol is growing, as well as hydrogen, which can be produced starting from RES. Two main thermodynamic cycles options are available for ICEs. Otto cycle is the most typical cycle for gasoline based ones and it is characterized by spark ignition of fuel. On the other hand, in the Diesel cycle the fuel is ignited by compression. Even if, at the same maximum pressure, ideal Otto cycle has higher efficiency than Diesel cycle, Diesel ICEs are designed to reach higher pressure and practically they have better energy performance than Otto ICEs.

The most common fuel used in remote applications is diesel fuel. In fact, the transportation of a gaseous fuel for long distances is not economically feasible due to the low fuel density. Additionally, diesel is preferred to gasoline as well because of higher efficiency of conversion (resulting in a lower consumption) and the higher reliability of diesel engines. Diesel ICEs installed capacity in 2013 was 400 GW, considering all the remote applications as mining, industrial facilities and micro-grids energy supply (IRENA, 2015b). Regarding only diesel ICEs which supply power to rural communities with power less than 500 kW, Werner and Breyer, 2012 estimate a global cumulative installation of 1.26 GW.

Diesel ICEs technology electricity costs can be divided in three categories: investment, maintenance and fuel. Figure 2.3 shows the investment costs for different diesel ICEs manufacturers obtained from public websites of retailers in the US market[4]. It is possible to note that there are strong economies of scales below 100 kW; after this threshold the specific investment cost can be considered flat, around 120-150 USD/kW. The total investment cost can increase to values around 250-300 USD/kW if installation costs and other indirect costs are taken into account.

[4]Source: GeneratorSales; Date of access: 16 Apr 2016; URL:`www.generatorsales.com`

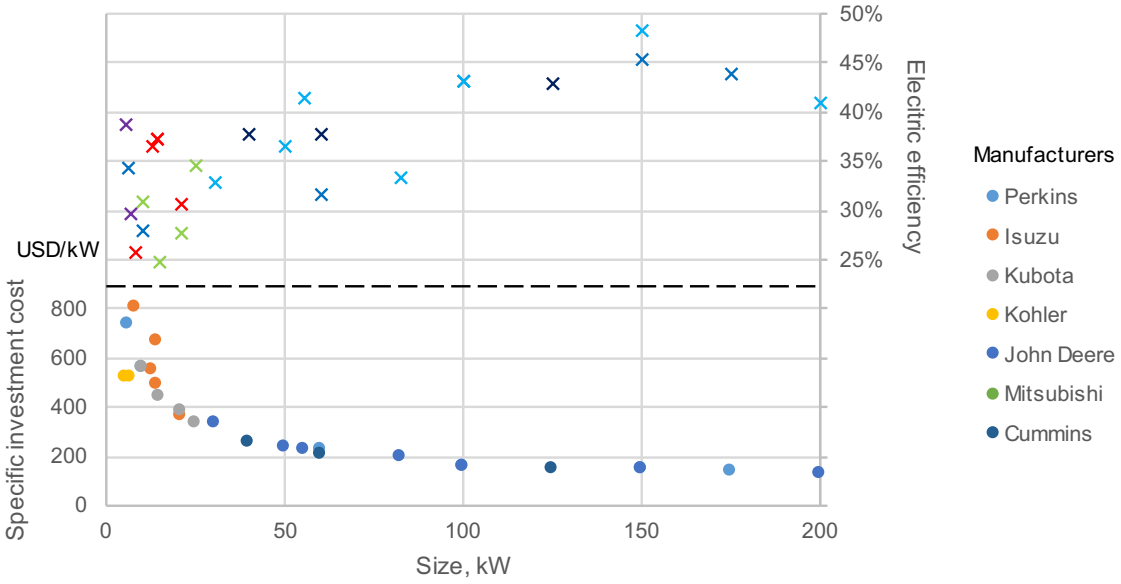

FIGURE 2.3: Specific investment cost and efficiency of diesel ICEs by size and manufacturers

Maintenance is a key factor to ensure reliability throughout the service life. Every manufacturer provides a maintenance schedule, which includes routine general inspections, lubricating oil change and other tasks. Cost of lubricants (which is the most relevant) is around 0.01 USD for each electric kWh produced and an additional yearly fixed cost equal to 10% of the investment can be considered for spare parts.

Finally, fuel consumption is the most important part in total costs, considering diesel ICEs which operate more than 1000 hours per year. It depends on generator efficiency and diesel fuel price. As for investment costs, the efficiency generally increases with higher sizes reaching values around 40-45%, equivalent to a fuel consumption of 0.24-0.20 l/kWh. Part load operation affects the fuel consumption: decreasing the load until 50% the specific fuel consumption decreases smoothly; for operation at very low load factor, the specific consumption is usually considerably higher. Another limitation is given by the minimum load factor: most of the generators manufacturers suggest to operate the generator below 10%-30% of the nominal load for limited periods in order to avoid excessive component wear[5].

The diesel fuel price is a crucial factor for remote applications. Wholesale price of diesel fuel have experience strong fluctuations in the last 20 years, ranging from 0.10 to 0.8 USD/l in the US market[6]. In addition to this, the presence of regional taxes or subsidies entails a great geographical variability. Finally, the other decisive factor which has to be taken into account is related to fuel transport. The lack of reliable transport infrastructure in rural areas has a sever impact which, in many rural areas of Africa, could double the diesel price (Szabó

[5]Source: Proper generator set sizing requires analysis of parameters and loads (Cummins Power Generation); Date of access: 30 September 2016; URL: `http://www.camelottech.com/CMFiles/Docs/PT-7007-SizingGensets.pdf`

[6]Source: U.S. Energy Information Administration (EIA); Date of access: 16 Apr 2016; URL:`https://www.eia.gov/dnav/pet/hist/LeafHandler.ashx?n=pet&s=ema_epd2d_pwg_nus_dpg&f=a`

et al., 2011). Reasonable values for remote location are around 0.8-1.2 USD/l, which lead to a variable cost of electricity in the range of 0.2-0.5 USD/kWh.

2.3.2 Solar energy systems

Photovoltaic

Photovoltaic (PV) technology is based on the direct conversion of global solar radiation into DC electricity using the photoelectric and Volta effects. When the PV module is hit by sunlight, the high energy photons[7] are absorbed and their energy is used to excite electrons, which can now participate in conduction moving from the bound state to the free state. The migration from one state to another is possible only in the semiconductors. The PV cell contains also additional materials which create an internal electric field. This electric field pulls electron toward one electrode, resulting in a dc electric current.

This process is valid for all the photovoltaic technologies, which differ in the semiconductor material. Three main families can be identified:

- First-generation (wafer-based crystalline silicon technologies)
- Second-generation (thin film technologies)
- Third-generation (innovative technologies as concentrated PV)

First-generation is the most developed and mature technology family. It is based on silicon, one of the most abundant elements in the earth's crust, and currently dominates the PV market with a cumulative capacity of 161 GW over the total cumulative of 177 GW (IEA PVPS, 2015; ISE, 2016). An additional classification is made according to the way the silicon wafers are produced((i) monocrystalline, (ii) polycristalline and (iii) EFG ribbon) which entails different production cost and cell efficiency (IRENA, 2014).

Second-generation technologies are now starting to have a significant role in PV market. This family is characterized by the use of thin-film cells in order to potentially ensure lower electricity cost than first-generation technologies. Thin-film cells are made by multiple thin layers (from 1 to 4 μm) deposited over a large substrate. The semiconductor material required is hence reduced, entailing a reduction in production and material costs. However, lower efficiency and reliability are still constraints for massive market growth.

Finally third-generation technologies are at development stage and need further research before entering the commercial stage. Four types are generally considered in this category: (i) concentrating PV; (ii) dye-sensitized solar cells; (iii) organic solar cells and (iv) other emerging concepts.

Regarding economic perspective, the electricity cost related to this technology is usually lower than the one related to diesel technology in remote locations. In fact, thanks to the great investments in developing countries (mainly in Europe), the last decade has seen a massive

[7] the minimum energy level required to consider a photon an *high energy* one is dependent from the material which constitutes the cell and its energy band-gap

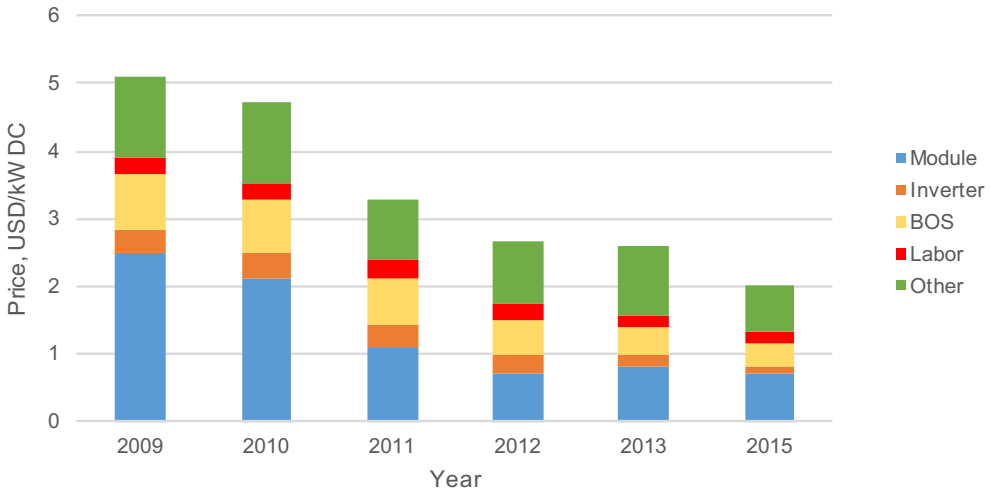

FIGURE 2.4: Price benchmark for commercial plant (200 kW) installation in the US. Data from Chung et al., 2015

decrease of the module costs, as shown in Figure 2.4. The price of PV modules is around 700-900 USD/kW_{peak} in 2015 and it is expected to decrease further. However, the cost of the PV system include also the so-called balance-of-system (BOS) costs, which include the inverters, wiring, the mounting system and the labor installation costs. Nowadays this accounts for 40-60% of the total PV system price, and, as suggested in the report by GTM-research, 2015, a consistent further reduction of PV systems will be strongly related to potential saving in the segment of BOS. Total system cost for sizes greater than 50 kW is nowadays around 1600-2200 USD/kW[8], depending on the location and the relative labour cost, and there are not strong economies of scale. In addition to this, thanks to the absence of moving parts, yearly O&M costs are limited to few percent of initial capital cost (1-2%).

Many studies in literature address the integration of PV systems in remote MGs. As reported in Table 2.2, it is very often convenient to add power from PV to reduce the fuel consumption and increase the share of energy coming from RES. However, the intermittent nature of the PV is a strong bottleneck to its integration and it is difficult to increase the share of PV over 30%. In fact, the power production has to match continuously the energy demand

[8]This value include also the inverter costs, whose value is around 200-400 USD/kW

TABLE 2.2: Examples of literature studies on hybrid Diesel/PV systems

	Location	**PV power**	**PV energy, %**	**LCOE, USD/kWh**
Bekele and Palm, 2010	Algeria	5 kW	16%	0.353
Rehman and Al-Hadhrami, 2010	Saudi Arabia	2000 kW	21%	0.219
Lau et al., 2010	Malaysia	60 kW	22%	0.309
Hrayshat, 2009	Jordan	2 kW	23%	0.238

and, when the sun is not shining, Diesel power is needed to run the MG. On the other hand, the PV size is usually limited to diurnal demand peak in order to avoid massive spillage. This is true when the system is not provided with an energy storage. In fact an energy storage is able to store the energy when the PV power exceeds the demand to give it back when it is needed, for example during night. However, as described in the subsection 2.4.1, energy storage adds an additional cost which can make it non-competitive with traditional power sources.

Concentrating solar power

Concentrating solar power technologies are based on the conversion of direct beam solar radiation in high temperature heat, then converted in electricity using a power cycle (Manzolini and P. Silva, 2013). Two main groups can be detected: linear focus collectors and point focus collectors. In the first group, which include parabolic troughs and linear Fresnel collectors, the solar radiation is focused on a focal line using single-axis tracking systems. In the second group, made by solar towers and solar dishes, the solar radiation is focused on a single point, using this case two-axis tracking systems.

Global installations survey shows that parabolic trough is the most deployed technology, representing 90% of total installed power of 5 GW in 2014 (IEA, 2014). Solar towers are expected to play a more important role in the next years thanks to the possibility to reach higher temperature and consequently higher conversion efficiencies. Both Fresnel collectors and solar dishes have a marginal role: Fresnel collectors have a lower specific cost per square meter of mirror compared to parabolic trough, but suffer of lower optical efficiency; solar dishes have the highest solar to power conversion efficiencies among CSP technologies, but they do not have the capability to store the heat, which is one of the most interesting advantages of CSP respect of PV technologies.

In Figure 2.5 the typical layout of a parabolic trough CSP plant is shown. The heat transfer fluid (HTF) flows through the solar field, where receives heat from the sun and increases its temperature. The heat is then released to the power block, where it is converted into electricity using a thermal cycle. In the hours when the heat produced by the solar field exceeds the heat consumed by the power block, the thermal power can be stored in thermal energy storage (TES). On the other hand, even when the sun is not shining, the power block can work using the thermal energy previously stored in the TES. For the same power block, the possibility to change the sizes of the solar field and the TES adds new degrees of freedom in the plant design. Two important parameters are commonly used: the solar multiple (SM) and TES hours. The solar multiple defines the size of the solar field and it is the ratio between the actual solar field area and the solar field area required to operate the power block at maximum load in nominal condition (i.e. at nominal DNI, generally 800 W/m^2). The hours of storage defines the size of the thermal storage and it is the maximum number of hours for which the plant can work at nominal conditions using only the heat in the TES.

Most of total CSP installed power is related to plants with a nominal power greater than 50 MW. This power range is not compatible with small-scale generation, needed for off-grid

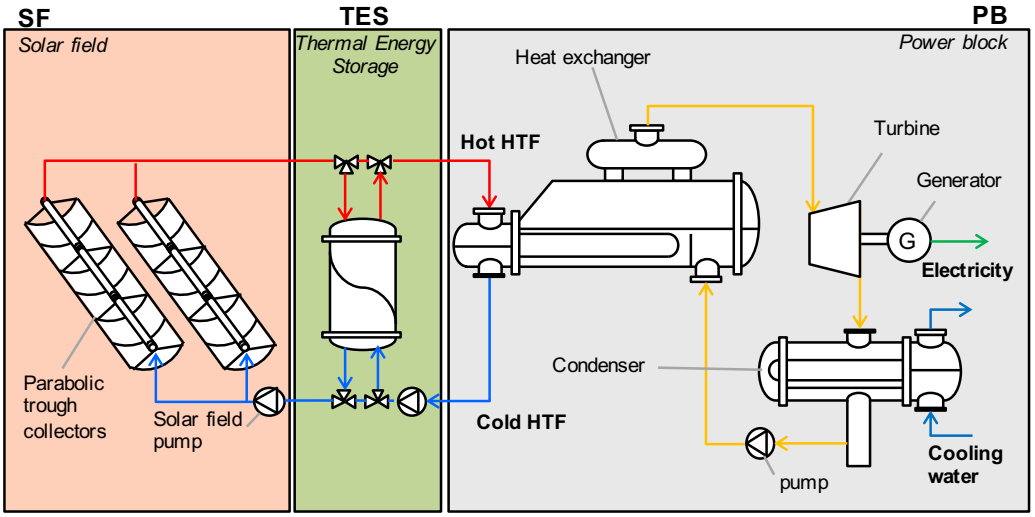

FIGURE 2.5: CSP plant with parabolic trough and thermocline TES layout

operation. However there are interesting examples of CSP plants with nominal power less than 5 MW, which could be used to power standalone grids.

With power less than 5 MW, parabolic trough is still the most common technology with 22 MW of the total 50 MW installed. All the details about the small-scale projects around the world are reported in Appendix A.1[9]. The power cycle commonly adopted for these applications is a Organic Rankine Cycle (ORC), which offers higher efficiency than traditional steam plants for the power and temperature range of interest (Marco Astolfi, 2014).

For very small-scale applications with an output of few kW, in Quoilin et al., 2011 the authors show the potential advantages related to use of small-scale CSP in rural areas, using ORC as power block. The system proposed, which has a nominal power output of 3 kW_{el} and works with low temperature heat (<200 C), was installed in 2007 in Lesotho. The simple layout proposed can be manufactured locally and, compared with PV systems, allows the production of hot water as additional product.

The costs associated to CSP are still very high. According to IRENA, 2015d, the installation costs of a CSP plant based on parabolic trough ranged from 3550 to 8760 USD/kW in 2013. The range is very wide because has been derived from different studies based on plants with different solar multiples and hours of storage. The installation costs are considerably higher than PV ones (from 2 to 5 times), but generally CSP plants have a higher capacity factor thanks to the TES.

Finally, CSP is still a young technology which is growing considerably in the last years, increasing its capacity of 286% from 2010 to 2014 (IRENA, 2015d). Compared with PV technology, CSP total installed power is still very low resulting in an high installation cost which makes this technology not fully competitive. The more complex system layout is another potential disadvantage. In addition to this, CSP productivity is related to direct normal irradiation which, differently from global, has stronger local variation.

[9]Source: CSP World; Date of access: 11 Jul 2016; URL:`http://www.cspworld.org/cspworldmap`

On the other hand, CSP has the possibility to efficiently produce low temperature heat during operation, which can be used to satisfy thermal loads or for other applications, as desalination, allowing to limit fossil fuel consumption. Thanks to the inertia of the rotating machine, the turbine of a CSP can give a relevant contribution to MG stability contributing to primary control (see Section 3.1.1). In addition to short-term stability, CSP has the capability to be dispatchable on longer time span: installing a relatively cheap thermal storage it is possible to shift in time the electricity production in periods of the day when the sun is not shining. This aspect will be further analyzed in Section 2.4.2, which focuses on the potential of thermal energy storages.

2.3.3 Biomass based systems

Biomass energy could play a relevant role in rural electrification in the next future. Considering only wood biomass and agricultural wastes, the worldwide potential is estimated to be $1.6 \cdot 10^4$ TWh/ year (Demirbas, M. Balat, and H. Balat, 2009). The wood biomass source is rather uniformly spread over the world and it is abundant in main developing areas, as Sub-Saharan Africa, Latin America and Asia. Nowadays biomass covers ca. 10% of worldwide primary energy consumption (BP, 2016); however, a relevant part is still used inefficiently in developing countries for cooking and heating. In most cases, an efficient usage of the biomass source could ensure clean energy access without increasing further exploitation. Furthermore, if compared with other RES technologies (i.e. PV, WT), biomass energy has a crucial property to offer in an off-grid system: the dispatchability. In fact, unlike solar and wind based power generators, the fuel can be stored and the generator produces electricity only when it is required. Due to the limited electricity demand in remote areas, it is not possible to install big size plants. Regarding small-scale application, two are the most suitable power generation technologies: gasification with internal combustion engine and solid biomass combustion with ORC (Dong, Liu, and Riffat, 2009).

Gasification

Gasification with internal combustion engine is nowadays the most common technology for rural electrification, in particular in India (Buragohain, Mahanta, and Moholkar, 2010). According to an IRENA report (IRENA, 2012a), 60 plants with downdraft gasifier (the most suitable configuration below 1 MW) have been installed around the country to power more than 250 rural communities. The working principle consists in two steps: (i) first in the gasifier a gaseous product (syngas) is formed by partial combustion of the biomass in a low oxygen environment, then (ii) the syngas feeds an ICE, which produces electricity and low temperature heat. Usually a syngas cleaning system, composed by a cyclone, scrubbers and/or fabric filters, is placed between the gasifier and the engine to keep under control the pollutants emission and the quality of the syngas (Dasappa et al., 2011).

The overall energy conversion performance (considering only electricity) is about 20% (Dong, Liu, and Riffat, 2009), assuming typical values of efficiency for each component (65% for gasifier, 32% for a Otto based ICE). On the other hand, some drawbacks are related to the

gasifier operations. In fact, the quality of the syngas produced can considerably change due to the feedstock composition and the operating condition, leading to frequent plant shutdowns, significant maintenance requirements and high wear of the ICE. For this reason, the generator will be affected by a reduced lifetime and higher O&M costs in comparison with fossil-fuel fed ones (Nouni, Mullick, and Kandpal, 2007).

Combustion

The ORC technology is the second option to exploit the biomass potential for the sustainable generation of electricity. The ORCs are based on a Rankine thermodynamic cycle where a suitable organic fluid (refrigerant fluids, hydrocarbons or siloxanes) is used instead of water. The possibility to select the best working fluid depending on the heat source characteristics is the key factor of the success of ORC since it allows exploiting low temperatures and/or small available energy sources with high efficiency cycles and to design efficient expanders. Nowadays, ORCs are the best technical solution to exploit a large variety of energy sources like geothermal hot brines, waste heat recovery from industrial processes, CSP and biomass combustion. The interest in this latter application has been noticeably grown in last decades in north Europe where the abundance of cheap biomass and feed-in tariff mechanism (promoted to reduce carbon dioxide emission) have favored the installation of these kind of plants. Today, specifically to biomass ORC systems, Turboden is the market leader with more than 260 plants installed in Europe while other companies like GMK, Exergy and Adoratech are gaining a large share in recent years. The total installed power worldwide overpasses 350 MW with plant sizes ranging from 200 kW_{el} to 6500 kW_{el} (Marco Astolfi, 2014). Medium size (above 1 MW_{el}) biomass ORC is a proven technology with less technical issues than a Gasifier+ICE system: ORCs have a long operative life (20 years), low maintenance costs and high off-design performances making them a promising solution for remote applications like rural electrification; in addition the biomass boiler is a component less critical than a gasifier without plugging issues and a more stable operation varying the biomass composition.

Three main components are present in a biomass ORC power plant: (i) the furnace where the biomass combustion takes place and heat is transferred to the heat transfer fluid, (ii) the heat transfer fluid loop which transfers heat from the furnace to the thermodynamic cycle and (iii) ORC engine. In spite of the increasing interest in biomass field, only few commercial ORC packages are available on the market for a power between of 25–100 kW_{el} mainly because of the difficulties in designing and producing small expanders while reaching high working temperatures.

2.4 Energy storages

The capability to store efficiently and economically energy from intermittent renewable sources and exploit it when it is needed is becoming more and more important in nowadays power sector. With the increasing share of intermittent RES, energy storages (ESs) are crucial to handle the natural variability of sun and wind. This challenge is even more severe in

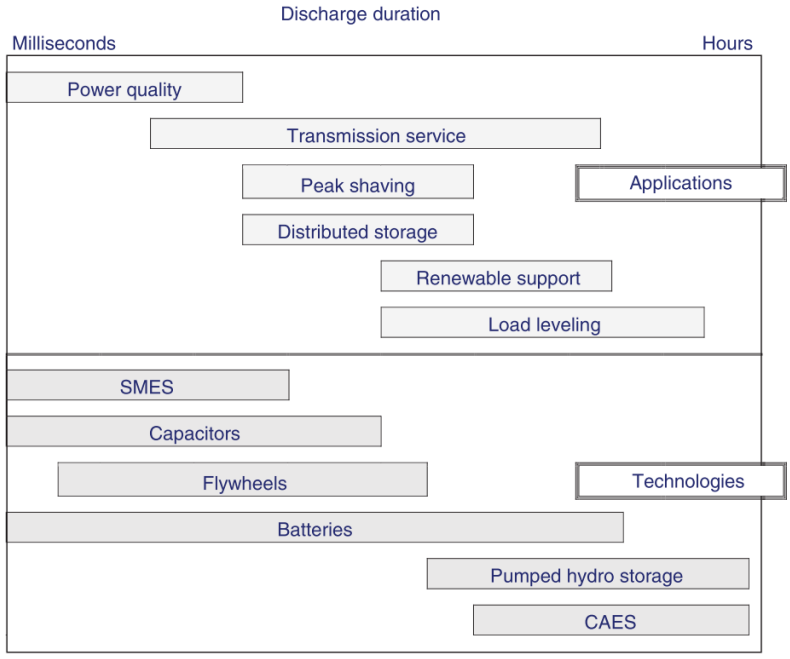

FIGURE 2.6: Energy storage technologies and application for different discharge time (Parker, 2009). The category "battery" includes all the electrochemical technologies

remote applications, where RES are already cheaper of fossil fuel solutions and the lack of dispatchability is the only barrier to the development of MGs with very high share of RES.

The market shows a huge variety of ES technologies, which can be classified according to their field of application and discharge time (see Figure 2.6). Two main categories can be identified: short-term and long-term ESs (Parker, 2009). Short-term ESs are capable of supplying high power for short-time and are hence used mainly for power quality enhancement. On the other hand, long-term ESs have longer discharge-time, suitable to cope with daily variation of RESs. Long-term ESs are the main focus of this thesis. In fact, even if the presence of short-term ES could be mandatory to have stable MG operation, the possibility to shift in time consistent amount of energy is more important to increase the share of renewable energy in off-grid systems. In addition to this, some of the technologies considered in this section (i.e. batteries) are capable to act in very short time-step and participate in frequency and voltage control.

Traditional large-scale power systems have been based mainly on pumped hydro-power storage, which consists in generating electricity from water flowing from an upper reservoir to a lower one, previously pumped on the opposite direction. A successful example of application of this technology in off-grid application is El Hierro. In this island, the presence of a pumped hydro storage promises to enable the integration of huge amount of wind energy, which should limit the fossil fuel energy share to less than 25% (Godina et al., 2015). However, even if this is usually the cheapest solution on the market, it can not be used everywhere due to the scarcity of available sites for two large reservoirs and the environmental issues related to plant construction (Kousksou et al., 2014). Similar problems affect the so-called CAES (compressed air energy storage).

In the following subsections, a review of energy storage technologies suitable for off-grid applications is reported. Even in this case, the aim is not to provide a comprehensive description of energy storages, but to give a brief description of the technologies that will be considered in final parts of the thesis. An overview of the economic and operational performance will be given, as well as the key parameters, as the investment cost, the life span and the charge/discharge efficiency.

The first subsection deals with battery storages, which are actually the most used and the most promising technologies for long-term storage applications in remote applications. This wide category includes multiple technologies, which differ for materials and chemistries. The last subsection is focused on thermal energy storage (TES), which could be used to store energy from renewable sources based on heat engines (CSP and biomass).

2.4.1 Battery systems

Batteries are electrochemical devices made of one or more electrochemical cells, embedded in a system (BESS) which ensures stable and safe operation. The working principle exploits chemical reactions, which involves the electrons transfer from one electrode to the other through an external circuit. The positive charges are transferred through a electrolyte, which separates the anode and the cathode and enables the ions transfer. During discharge, the chemical reactions create an electric potential between the two electrodes, which can be used to feed an external circuit. During charging process, the application of a higher external voltage makes the chemical reactions happen in the opposite direction. Battery systems differ for the materials used as electrodes and electrolyte, which determine properties and performances. The key parameters needed to define batteries economic and operation performance are:

- capital cost - amount of money requested to buy and install the BESS, generally referred to the BESS capacity (in $\frac{\text{USD}}{\text{kWh}}$)
- maximum depth of discharge (DoD) - share of battery capacity (in %) which can be fully utilized without incurring in massive degradation
- cycle life - number of charge/discharge cycles (at a certain temperature and DoD) a battery can complete before its capacity reaches 80% of nominal capacity
- charge/discharge efficiency - the ratio of the energy output after the charge/discharge process and the energy input (a part of the input energy is converted into heat and hence lost)
- operation constraints - temperature, maximum charge and discharge rate etc.

A valuable parameter which can be defined to assess approximately the life-cycle cost per unit of energy delivered is the levelized cost of storage (LCOS), firstly introduced by scientific community and now recently used even in financial reports (Lazard, 2015). Using some approximations, it is defined as:

$$\bar{c}^{\text{BESS}} = \frac{\text{capital} \quad \text{cost}}{\text{DoD} \cdot \text{Cycles}} \tag{2.1}$$

where the number of cycles are referred to the DoD used in the equation. Note that, even if the LCOS ($\bar{c}^{BESS}$) and the capital cost have the same unit of measure ($\frac{USD}{kWh}$), they have a completely different meaning: capital cost refers to the investment cost per unit of capacity while LCOS takes into account the entire lifetime and it is referred to the energy delivered[10].

While LCOS is a useful tool, detailed simulations are required to capture the real long-time performance of a battery storage. In fact, the life span of a battery is strongly affected by operating conditions. As highlighted by Sauer and Wenzl, 2008 in a literature review, many models have been proposed to effectively quantify the effect of temperature, full charges and low SoC (state of charge) operation. In the following subsections a description of battery technologies which can be used in MGs application is reported, focusing on lead-acid, lithium and sodium technologies. The most important data are summarized in Table 2.3. Note that high variability and uncertainty in expected number of cycles and cost leads to a wide range of possible LCOS ($\bar{c}^{BESS}$).

Table 2.3: Specifications and relevant data for battery technologies. Data elaborated from IRENA, 2015a

		Lead-acid	**Lithium**		**Sodium**	
			Li-ion	Polymer	NaS	ZEBRA
Charge/Discharge efficiency	%	85-90	90-100	90-100	75-92	high
Charge time	hours	8-16	1-4	1-4	8	1
Energy density	Wh/kg	30-50	80-200	100-150	150-240	100-130
Self discharge	-	5%/month	little	little	low	10%/day
Temperature	°C	-20/+50	-20/+60	-20/+50	+290/+360	+270/+350
Safety issues	-	no	high	high	-	low
Cycles	#	800-1800	1000-5000	1000-3000	2500	1000-3000
DoD	%	50-70	80-90		70-80	
Cost (2014)	USD/kWh	200-250	600-800		500-700	
$\bar{c}^{BESS}$	USD/kWh	0.15-0.625	0.17-0.56		0.21-0.67	

Lead-acid

Lead-acid technology has been the most commonly manufactured rechargeable battery technology, especially for off-grid applications. Considering the whole rechargeable battery market with its 380 GWh of total capacity in 2013, lead-acid has almost 90% of market share (Energy Avicenne, 2014). The name of the technology comes from its constituting materials. In fact negative electrode is made by a lead paste covered grid, while the positive electrode is usually a plate or grid made by lead dioxide. The electrolyte is usually a sulfuric acid solution.

[10]The value $\bar{c}^{BESS}$ is commonly used in operation optimization as a proxy for battery operation cost, as shown in Section 4.1.2

The two most common configurations are sealed valve-regulated (VRLA) and flooded. While the latter is usually cheaper, the VRLA technology has gained interest for its low maintenance requests. While lead-acid batteries have the lowest capital cost between the batteries (200-250 USD/kWh[11]), they are usually characterized by the shortest life span. The cycle life claimed by most manufacturers is around 800-1800 cycles with 50% DoD, which lead to 3-5 years of operation under massive usage conditions (1 full cycle per day). This results in an energy cost ($\bar{c}^{BESS}$) in the range of 0.16-0.62 USD/kWh.

The real lifetime can be even lower if higher DoD are considered (this aspect will be analyzed in Section 4.1.2). In addition to this, lead-acid batteries are usually characterized by low charge rate: 8-12 hours are usually required to charge completely the battery without incurring in relevant energy losses and battery degradation.

Lithium

Lithium based batteries are the most promising technology for BESS. Thanks to the huge implementation in the transport sector for the electric vehicle, lithium-ion batteries are experiencing the most relevant growth in the whole energy storage sector, increasing from almost 0 to 50 GWh in less than 10 years (Energy Avicenne, 2014).

All available configurations are based on the fact that when the battery is cycled, there is a transfer of lithium ions (Li^+) between the positive and the negative electrodes. There is a wide selection of anode and cathodes materials, resulting in more than 10 chemical configurations.

Lithium-ion batteries are characterized by a high efficiency (90-95%), power density (100-200 Wh/kg) and number of cycles (1000-3000). Unlike lead-acid batteries, the charge and discharge power are considerably higher, requiring around 1-4 hours for a full charge or discharge. Thanks to the great market growth, they are experiencing even a very strong reduction cost, going from around 2000 USD/kWh in 2009 to 600-800 USD/kWh in 2013 (IRENA, 2015a). The energy cost ($\bar{c}^{BESS}$) is in the range of 0.17-0.56 USD/kWh.

The most important drawback today is related to safety. In fact, lithium batteries suffer a very low overcharge tolerance which can results in cells overheating and damaging. The thermal management of the battery pack is a very important factor, which has to be fully investigated. Another aspect is that the frequent breakthroughs have not allowed the development of effective manufacturing process. Once one or few chemistries will become predominant, it is likely that a further reduction in manufacturing costs will happen, as already experienced with PV industry. An example of the movement of the industry in this direction is given by Tesla Gigafactory 1, which is a lithium-ion battery factory located in Nevada (USA) currently under construction which is expected to produce at full capacity 150 GWh/year of battery[12].

[11] Source: WholesaleSolar; Date of access: 16 Apr 2016; URL:`http://www.wholesalesolar.com`

[12] Source: Tesla website; Date of access: 30 September 2016; URL: `https://www.tesla.com/gigafactory?redirect=no`

Molten salts

This class of battery takes its name from material used as electrolyte (molten salts) which have to operate under high temperature. The most important technologies in this class are sodium-sulphur (NaS) batteries, sodium-nichel batteries (also called Zebra) and metal batteries.

Sodium-sulphur batteries are a relatively mature technology, commercialized since 2002 and demonstrated especially for grid application (as in Japan by utility Tokyo Electric Power Company and NGK Insulators in the late 1990s). Sodium-Nichel batteries was developed in the 1980 in South Africa and in Great Britain with the aim to obtain an high energy density battery with high performance. Nowadays, this technology is produced by Fiamm Sonick while General Electric (the other player in this market) moved its interests in lithium-ion batteries. Finally, liquid metal battery is the most recent technology, developed for the first time in 2009 at Massachusetts Institute of Technology (K. Wang et al., 2014). This technology promises longer lifetime than conventional batteries, but it is still at the early stages of development.

The main advantage related to molten salts batteries is the energy density, which can reach values 5 times higher than lead-acid, while life time is relatively low (1000-3000 cycles).

The disadvantages of NaS batteries are their high cost (around 350 USD/kWh), high self-discharge per day and high temperature requirements (300–350 °C) for operations (Kousksou et al., 2014).

2.4.2 Thermal energy storage

Thermal energy storage is a key components to improve the dispatchability of power plant based on a heat engine. Regarding renewable energy sources, it is applicable to both biomass systems based on combustion and CSP plants to enable one or more of the following capabilities (Kuravi et al., 2013):

- **Buffering** - fast fluctuations of the thermal power in input can entail transient operation conditions of the turbine, with consequent efficiency losses. For CSP systems, cloud cover can force the power block to off-design operation or unwanted shut-down if the TES does not act as a buffer. Similarly for biomass systems, it could be useful to have a TES to facilitate start-up and shut-down operations or to mitigate thermal power fluctuations induced by a change of feedstock quality.

- **Delivery displacement** - increasing the nominal capacity of the TES, it is possible to shift in time the thermal power production. In other words it is possible to decouple the thermal source contribution (the sun radiation or the biomass boiler) to the power production, adding new degrees of freedom in system operation and management. For CSP systems, the TES allows to produce electricity even during night with the thermal powered stored during the day.

- **Increasing capacity factor** - the TES allows in the case of CSP plants to increase the capacity factor of the power block, which is the ratio of energy delivered and the energy which could be delivered operating at nominal load for the whole year. Using

a TES, it is possible to install a solar field with a nominal thermal power greater than the one requested by the power block, increasing the number of hours of operation (SM>1). Increasing the capacity factor allows to reduce the LCOE, since the same power generator can produce a higher amount of energy.

TESs can be listed in three main groups: (i) sensible, (ii) latent and (iii) chemical heat storage (Tian and C. Y. Zhao, 2013). In sensible heat storage the heat is stored increasing the temperature of the storage media, which can be a liquid or a solid. A set of physical properties (i.e. density, specific heat, thermal conductivity) defines the amount of material required to store a unit of thermal energy and the volume occupancy, which changes for different kind of materials. Hybrid systems, made by more than storage media, are frequently proposed.

In the case of latent heat storage, the heat is stored in a medium which changes phase. These material allows to store large amount of heat per unit of mass, since generally the enthalpy variation related to phase change is sensibly higher than sensible one. It is preferable for applications when narrow working temperatures are required, since material store and release heat nearly isothermally. The most important drawback of this category is a low thermal conductivity, which requires the adoption of heat transfer enhancement techniques (C. Y. Zhao, Lu, and Tian, 2010).

Regarding chemical storage, they can store energy through the formation of chemical bonds in endothermic reactions. The process is reversible, and the chemical bounds are broken with exothermic reactions when the heat is released. The potentials related to this family of TES is very high, but further research and development are needed for its practical application.

Other important aspects, relevant for each kind of storage, is the working temperature range. In relation to the temperature range of the application purpose, material compatibility has to be check to ensure chemical and physical stability.

Nowadays the most common TES systems are based on sensible heat medium, while latent heat and thermo-chemical storage are restricted to niche applications (Yan, 2015). Focusing on latent heat systems, molten salts seem to be the most promising solutions for utility-scale CSP plants, thanks to their low costs and the capability to reach very high temperature with low pressure. In small-scale systems, where molten salts are not practically feasible due to system complexity, the use of packed bed with solid filling material is the most common choice.

The cost of the TES has a wide range of variability (30-90 USD/kWh_{th} according to Strasser and Selvam, 2014), depending on the material and the layout of the system. Similarly to what already done with battery systems, it is possible to evaluate the cost per delivered energy of this kind of storage in USD/kWh_{el}, i.e. the LCOS. This metric is very common for other form of energy storage, but, since TES is always embedded in more complex systems and can not act separately from the other components, there is not a clear definition. A possible approach follows.

The cost of the power block and of the thermal source are not considered, since the aim here is to assess the cost to store and deliver later 1 kWh_{el}. Contrary to BESS, we do not have a fixed number of cycles but an expected lifetime in years (20-30 years according to Kuravi et al., 2013). To evaluate the cost of delivered energy the efficiency of the power block (η_{PB})

has to be taken into account: in fact for the same electric output, more thermal energy (and hence a bigger storage) is needed if the efficiency of the power block is lower. The resulting cost of delivered electricity is evaluated using the following equation:

$$\bar{c}^{\mathrm{TES}} = \frac{\text{capital} \quad \text{cost}}{\text{Lifetime} \cdot \text{Cycles} \cdot \eta_{\mathrm{PB}}} \tag{2.2}$$

Assuming that the TES is fully cycled 100 times per year and the other values reported above, this results in $\bar{c}^{\mathrm{TES}}$ in the range of 0.03-0.14 USD/kWh$_{\mathrm{el}}$. This value is only a rough estimation, since it does not include any cash flow actualization[13] but it is evident that it is considerably lower of BESS systems LCOS (0.15-0.6 USD/kWh$_{\mathrm{el}}$). According to these results, it seems that it is more convenient to rely on TES instead of on battery systems to store and dispatch energy. However, we have to consider that, while BESS can be integrated everywhere in the grid, TES comes with an intrinsic higher complexity. In fact, the TES is a feasible option only when an heat engine is already installed and has to be associated with an existing plant. In addition to this, LCOS is only the additional cost we have to face to shift in time a certain amount of energy, but the system competitiveness depends also on the cost of energy production. The cost of production of thermal energy is hence important to perform a holistic assessment.

As for BESS systems, there is still room for improvements of TES technologies. Among all the possible options, the least mature technologies are expected to reduce the TES costs, decreasing the amount of material required for the storage (Kuravi et al., 2013). Finding and testing high energy density material with low costs are key aspects considered by research to develop new TES systems, together with the implementation and management in more complex systems.

[13] The actualization can change significantly the results because the expected lifetime is very long. Considering an interest rate of 6%, the LCOS is in the range of 0.06-0.23 USD/kWh$_{\mathrm{el}}$

Chapter 3

State of the art of microgrid management and design

Hybrid microgrids (MGs) are energy systems made by different units which have to be optimally coordinated to ensure reliable and cost-effective energy supply. Using properly the available units in the MG (i.e. generators, energy storages, schedulable loads) is not an easy task to be solved and has potential impacts on the competitiveness of this solution. In this chapter, two main topics will be addressed. First, current status of MG management and operation strategies will be described, focusing mostly on unit commitment based ones. In the second part, an overview of current methods used for long-term simulations and design optimization is given.

3.1 Microgrid management and operation

An operation strategy is required for both grid-connected and off-grid MGs. However, stand-alone operation (which is relevant for this thesis) is generally more challenging compared to grid-connected one. In fact, while in grid-connected operation the host grid ensures the MG voltage and frequency stability, in stand-alone operation the generators are responsible for reliable and stable MG activity. In particular, this aspect is even more relevant in MGs with a high share of intermittent renewable energy sources, where the units' schedule has to be frequently updated to cope with RES unpredictability and the power mismatches have to be immediately balanced by the operating units.

3.1.1 Microgrid control framework

According to Daniel E. Olivares et al., 2014 definition, two main categories of MG control can be defined: centralized and decentralized. In a fully centralized approach, a central controller is devoted to analyze the relevant data, perform the calculations and directly control the units. On the other hand, fully decentralized approach requires that each unit is provided with an internal controller, which takes decisions according to local information, without considering the condition of the other units or the whole system. The main drawback of a fully centralized approach is the need of an extensive communication infrastructure, which has to reach all the units in the MG; this can be challenging and expensive in the case of MGs which are spread over large areas.

Table 3.1: General information about microgrid control hierachy using Daniel E. Olivares et al., 2014 definition

	Primary	**Secondary**	**Tertiary**
Domain	single generator	whole MG	host grid and MGs
Time span	fast (seconds)	slow (minutes)	slow (minutes)
Type of control	decentralized	decentralized/centralized	centralized
Main functions	frequency and voltage stability	economic and secure operation	coordination among host grid and MGs

In real cases, the two approaches are both used, each for different purposes, in a hierarchical control scheme made by three different levels: primary, secondary and tertiary (see Table 3.1).

Primary control is responsible for the fastest response and can be listed as a decentralized control. Each unit is provided with a local controller which, fed by the set-points coming from the upper control levels, modifies the unit output with high speed according to measurements of local variables, as frequency and voltage. Synchronous generators primary control is performed by the voltage regulator, the speed limiter and the inertia of the rotating machine. Regarding inverters, different control design has been proposed to emulate the behavior of a synchronous generator (Faridaddin Katiraei, Iravani, and Lehn, 2005; Lopes, Moreira, and Madureira, 2006).

Secondary control, usually called Energy Management System (EMS), is responsible for the economic and reliable operation of the MG. A centralized approach is commonly used for the secondary level, but models which require that decisions are made locally have recently been proposed in literature (Farid Katiraei et al., 2008). The problem of the EMS is to determine the optimal (in terms of cost) schedule of the available units which would satisfy the expected demand, taking into account the non-dispatchable RES production. Compared with the primary control, the EMS is performed with a slower time rate, mainly related to forecast update frequency.

In the end, tertiary control is responsible for the coordination of a cluster of MGs with the host grid. According to this definition, it is needed only for grid-connected MGs. In this control level, specific requirements or needs can be communicated by the host grid to the connected MGs, which receive these data as an input for their own EMSs.

The control levels described above are referred to Daniel E. Olivares et al., 2014 definition. As highlighted in Meng et al., 2016, there is another possible definition more similar to the one used in conventional power systems. In this case primary level is responsible of the control of local power, voltage and current following the set-points given by upper level; secondary control is responsible of other functions of power quality control, as voltage/frequency restoration and harmonic compensation. These two control levels are equivalent to primary control in Daniel E. Olivares et al., 2014 definition. Finally the tertiary level has to coordinate the whole system and it is equivalent to the second level of the previous classification.The coordination of different microgrids is not considered in any level. The hierarchical structure

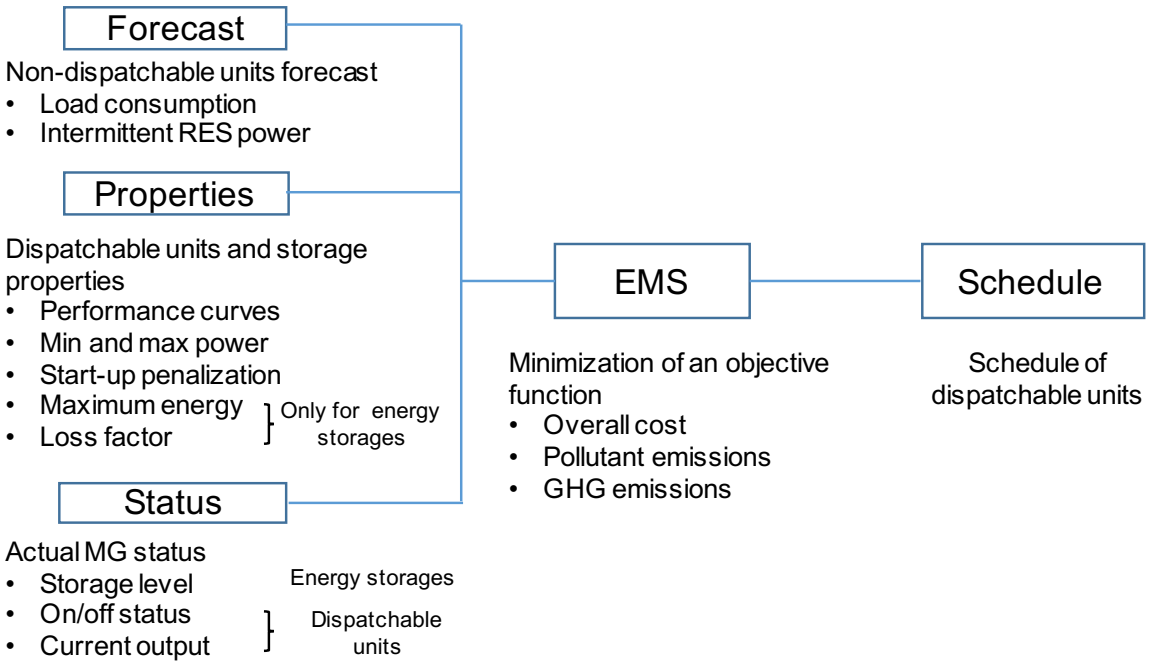

FIGURE 3.1: Schematic representation of EMS inputs and outputs for standard hybrid off-grid MG

proposed by Daniel E. Olivares et al., 2014 and synthetically shown in Table 3.1 is the only used for the rest of the thesis to avoid misunderstandings.

After the general description of the entire MGs control framework, a focus on centralized secondary controls models is proposed in the next sections. Even if primary control put several technical challenges in MG operation and demands for accurate design, overall economic performances are mainly related to how the MG is operated over long time horizons, and thus to the EMS definition. Moreover, the novelties proposed in this thesis are exclusively related to the EMS, and, for this reason, an accurate description of its state of the art is hereafter reported.

An EMS is a central controller which, using all the relevant data about the MG as input, finds the optimal unit commitment (UC), i.e the schedule of all dispatchable units. Total operation cost is the most common figure of merit of the minimization, but other objectives, as pollutants or green house gases emissions, or a proper combination of these can be taken into account. A schematic representation of the EMS framework is reported in Figure 3.1. EMS can be divided in two categories: non-predictive strategies (NPSs) and predictive strategies (PSs). For the first category, the EMS takes decisions only considering the units properties and the actual MG status. Regarding the PSs, the forecast of non-dispatchable units production or consumption is considered to find the optimal schedule.

3.1.2 Non-predictive strategies

Most of the studies on MG design rely on non-predictive dispatch strategies (NPSs) whereby the operation of programmable units is not defined according to the forecast of load and non-dispatchable RES power in the next hours. These studies are generally focused on the design

of standalone systems and calculations are carried out using HOMER (Hybrid Optimization Model for Electric Renewables), a commercial optimization software developed by NREL since 1995 (Lambert, 2006) and based on NPSs. It implements a large data bank of different components, i.e. wind turbines, photovoltaic panels, small hydro power, biomass fired engines, fuel cells and battery systems with referenced off-design performance maps. It works by simulating one year of operation for several combinations of generator sets and comparing them on the basis of the Levelized Cost of Electricity (LCOE). Each simulation is performed selecting a priori one of the two following NPSs: the load-following (LF) and the cycle-charging (CC) (Dennis Barley and Byron Winn, 1996). These strategies are simple and effective tools for the management of an off-grid power system but they present some limits in the simulation of complex systems.

In LF strategy, whenever a programmable generator is on, it produces only enough power to cover the electricity demand. This means that the generator operates at part load for most of the time, thus increasing its variable cost due to the lower off-design efficiency. On the other hand, the use of the energy storage is limited, thus entailing economic benefits related to a longer life of the batteries (Ruetschi, 2004). In the CC strategy, whenever a generator is on, it runs at its maximum rated capacity and charges the battery bank with the energy excess. The generator runs until the battery is charged up to a certain level, called set point. The main advantage is the more efficient use of the generators; on the other hand, the sequence of charging and discharging process may damage the energy storage leading to a higher replacement cost. In the case of multiple generators, for both LF and CC, the generators are switched on according to a priority list based on the marginal cost of operation.

In addition, HOMER can handle deferrable loads shifting in time a part of the electricity demand. This is an extremely relevant feature in systems with a high share of intermittent power sources as WT and PV plants. HOMER treats programmable loads as tanks gradually depleted proportionally to the load demand. The load is served when intermittent RES power is available and dispatchable power sources are used only if the tank is close to be empty. In this case the deferrable load is treated as a primary load. However, even in this case, the schedule of deferrable loads is not really optimized but it is the result of a greedy strategy, which may lead to non-optimal solutions.

More advanced models and different dispatch strategies have been proposed. For example, B. Zhao, X. Zhang, Jian Chen, et al., 2013 proposed an optimization model to define the input parameters of the NP dispatch strategy implement in a real off-grid MG. The model takes into account generators and battery operating cost (using a battery lifetime model) to obtain the set of optimal parameters for the operation strategy. The problem is solved using a nondominated sorting genetic algorithm. Similarly, Urtasun et al., 2014 proposed an energy management strategy for a hybrid PV-battery-diesel power system. In particular, three modes of operation and the conditions required to switch from one to another are investigated. Recently Hittinger et al., 2015 developed a new version of the standard dispatch strategies of HOMER which include a more detailed model for batteries; temperature effects, rate-based variable efficiency and capacity fade are the key factors introduced.

3.1.3 Predictive strategies

Predictive strategies (PS) have recently gained particular attention for isolated hybrid MGs. Even if many concepts have been recently introduced, the general structure of the EMS problem was firstly developed for large-scale systems, where a large number of units are considered in the UC.

In PSs, the EMS makes dispatch decision taking into account an estimate about future events, as load consumption and power generation from non-dispatchable RES. The time span covered with the forecasts is generally called **time horizon** (T_h) and generally ranges from 24 hours to few days in real applications. Starting from the forecasts and other information about current state of the MG (i.e. state of charge of ES, on/off status of generators), the optimal units' schedule is found solving the UC problem. Another important parameter is the **sliding time** (T_s), which is the time span between two consecutive calls of the UC solver. In this time span, the MG is operated following the set points obtained from the most recent UC solution and primary control is hence responsible to cope with power fluctuations and forecast errors. Additional auxiliary problems as the Economic Load Dispatch (ELD) or the Optimal Power flow (OPF)[1] can be solved to adjust the schedule taking into account a very short time-horizon. The general scheme of PSs (reported schematically in Figure 3.2) can be summarized as follows:

1. Obtain input data (forecast, actual state of units)
2. Solve the UC problem over a certain time horizon (T_h)
3. Use the setpoints obtained from UC solution for a certain time span (T_s)
4. Return to step 1

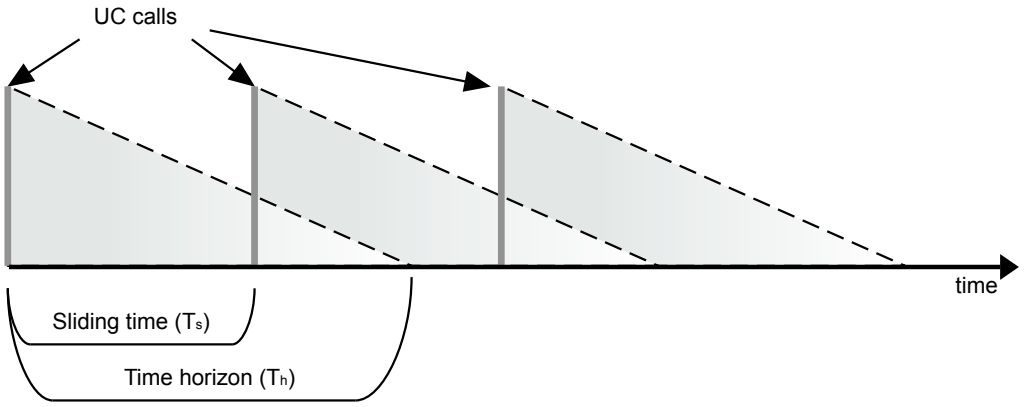

FIGURE 3.2: Schematic representation of application of a predictive strategy through a rolling horizon approach. The gray vertical lines represent the instants when the UC is solved while the dotted triangles represent the time span considered in the UC

[1]These two problems have the same structure of the UC, but are generally solved with only one time step as time horizon. OPF takes into account also network losses and nodes constraints, which can be relevant especially for large grids

This kind of approach is generally called rolling horizon (other recurrent denominations are receding horizon or sliding windows). The rolling horizon approach allows diminishing the effect of forecast uncertainties on the schedule errors (Sethi and Sorger, 1991). In fact, the optimization results are not followed over the entire time horizon but only over T_s, then the forecasts are updated and the inner problem is solved again. In this way the actual schedule of the MG is always based on more recent and reliable forecast and forecast error impact is reduced. The advantages related to a frequent update of the optimal solution make this kind of strategy very useful and commonly adopted in many fields, as operation of natural gas transmission networks and wind power balancing (Sethi and Sorger, 1991; Üster and Dilaveroğlu, 2014; Delarue and D'haeseleer, 2008). Regarding MG operation, Palma-Behnke et al., 2013 performed a simulation of a MG located in Huatacondo, applying a standard UC (only 1 forecast at the beginning of the day) and a rolling horizon approach with a T_s equal to 1 hour and showing that the application of a rolling horizon can lead to a cost saving in the range of 5-6%.

Performance of MGs are affected by the choice of T_h and T_s. Theoretically we would like to have an infinite T_h, to take into account all the future events, and an infinitesimal T_s to be sure that the schedules are always updated according to the last forecasts available. However both these two assumptions are not feasible and cost-effective in actual real implementation.

Regarding time horizon, its increase is generally related to a decrease in accuracy, especially in RES forecasts. The solution found by the UC is optimal considering the input data and when the forecasts used in the UC are not exact the resulting scheduling can entail an increase in operation costs. Another important aspect is computation time. When the T_h increases there is an increase of the time needed to find the optimal solution, which has to be compatible to the frequency at which the UC solver is calls (hence the T_s). Finally forecast service cost has to be considered, especially when the RES forecast are not generated inside the MG but are bought from outside. In fact, many forecast providers bill their service according to the time covered by each forecast (T_h) and to the frequency at which they are provided (T_s). In general all these considerations have to be addressed ad hoc for each single case, finding the best trade-off between the benefit and the cost related to more frequent UC calls and longer time horizon, as shown in the Section 4.2.3.

3.1.4 Unit commitment

After a description of PSs approach, a description of the UC problem, which is its core, is reported. The question solved by the UC can be formulated in the following way (Wood and Wollenberg, 1996):

Given a set of generating units, which subset should be used in order to provide minimum operating cost, satisfying the expected demand?

The general framework of the UC for off-grid MGs is reported in Figure 3.3; an overview of the most common solving methods and the detailed description of the objective function and the constraints is hereafter reported.

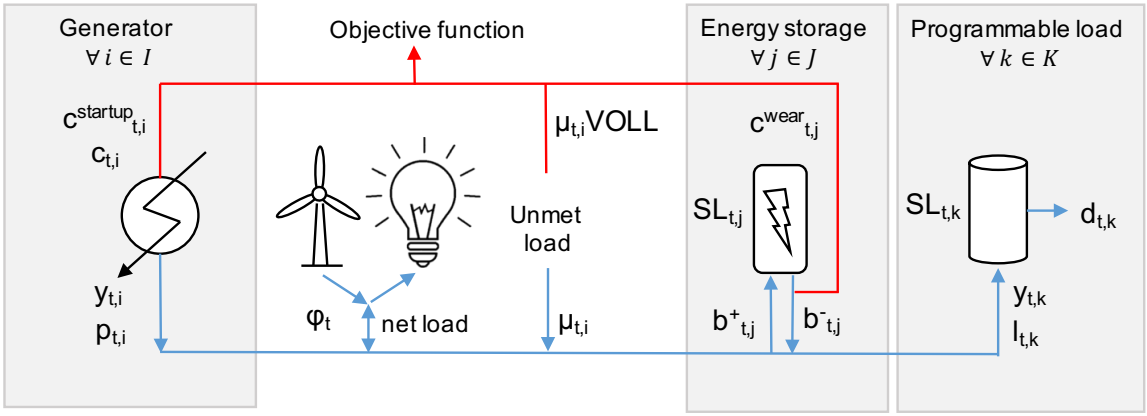

FIGURE 3.3: Schematic representation of UC problem for off-grid MGs according to the notation used in this chapter. Main variables for each set (generators, energy storages and programmable loads) are reported. Blue lines represent energy flows, red lines monetary costs

Resolution methods

In this subsection, a brief description of the most common methods for centralized EMS problem resolution is presented. Two main categories can be defined: (i) deterministic and (ii) soft computing algorithms (see Table 3.2).

The category of soft computing include a wide variety of methods as Genetic Algorithm (GA), Fuzzy Logic (FL) and Particle Swarm Optimization (PSO). They are commonly used to solve problems under circumstances of uncertainty and/or imprecision, which are inherent to the problem or added to overcome its complexity (Magdalena, 2010). Their capability to find one or more solution for very complex problems is their fundamental advantage. For this reason, they are massively used in fields where problems are practically intractable using conventional mathematical methods. However, as main drawback, these methods can not provide any proof of optimality.

On the other hand, deterministic algorithms are capable to model and precisely analyze relatively simple problems. They are very popular due to their commercial development and availability in software packages. The rigorous formulation of the EMS problem (which will be described in the following subsections) include both linear and integer variables and non-linear constraints and, for this reason, Mixed Integer Non-Linear Programming (MINLP) is requested to model accurately the problem. This approach has been widely used in literature for decades in various fields, especially for standard utility plants operation and design (Bruno et al., 1998). While MINLP continues to be used for CHP plants scheduling (Kim and Edgar, 2014), there are only few examples of application for MG scheduling, mainly focused on grid-connected applications (Shi, Luo, and Tu, 2014; Marzband et al., 2013). The advantages of MINLP are the high precision in components definition, which are not linearized or approximated as in other approaches. However, MINLP comes with two main drawbacks: (i) all MINLP methods can not guarantee that the solution is globally optimal, but only locally; (ii) increasing the number of units and/or time steps of the problem, the problem can become easily intractable.

In order to overcome these difficulty in treating non-linear integer problems, the original MINLP problem is usually converted into an approximated Mixed Integer Linear Programming (MILP) problem. As highlighted by Bischi et al., 2014, this conversion is usually advantageous for two reasons. First, switching to MILP it is possible to have the guarantee that solution found is a global optimum[2]. In addition to this, for practical cases, the time requested for the solution is very short and compatible with implementation in real operation.

Table 3.2: List of EMS problem resolution methods with references

Family	Algorithm		Literature examples
Deterministic	Mixed Integer Linear Programming	MILP	Morais et al., 2010 Palma-Behnke et al., 2013 Dai and Mesbahi, 2013
	Mixed Integer Non-Linear Programming	MINLP	Marzband et al., 2013 Bischi et al., 2014 Shi, Luo, and Tu, 2014
Soft computing	Genetic Alghoritm	GA	C. Chen et al., 2011 Elsied et al., 2014 Fossati et al., 2015
	Fuzzy logic	FL	Kyriakarakos et al., 2013 Chaouachi et al., 2013
	Particle Swarm Optimization	PSO	Ma et al., 2015

Objective function

The generalized formulation of the UC problem for large-scale systems is a mixed-integer non linear optimization problem (Baldick, 1995). The generalized form and the common expedients to express the problem with mixed-integer linear programming are reported. Given the set of generators I and the set of time steps $T = [1, 2...T_h]$, the objective function to be minimized is the following:

$$\min \sum_{t \in T} (\sum_{i \in I} (c_{t,i} + c_{t,i}^{startup}) + \mu_t \cdot VOLL) \tag{3.1}$$

where $c_{t,i}$ is the cost associated to generator i in time step t ($c_{t,i}^{startup}$ is its startup cost), μ_t is the unmet load in time step t and VOLL is the value of loss load. Using this notation, the option of load shedding is considered when the cost to serve a certain load exceeds its value (VOLL). As suggested by Parisio and Glielmo, 2012, multiple-objectives formulation can be efficiently implemented to find a trade-off between different objectives, as for example MG running cost and pollutants emissions.

[2]In order to reduce the computation time, a certain difference, called optimality gap, is allowed between the solution and the real optimum. However, theoretically, this gap can be set to zero to find the global optimum.

Balance constraints

The most simple balance equation of the grid is represented by the following set of constraints:

$$\sum_{i \in I} p_{t,i} + \mu_t = \varphi_t + \delta_t \quad \forall t \in T \tag{3.2}$$

where φ_t is the forecast demand in time step t and δ_t is a variable representing dump power in time step t. This set of constraints ensures that the total power coming from the generators exceeds the load, unless unmet load is admitted. In presence of intermittent RES, φ_t represents the net load, which is the difference between the load forecast and RES energy production forecast. This formulation is valid only assuming a one AC bus architecture; if multiple AC buses or DC buses are present, ad hoc formulation have been proposed for the specific case, adding power flow constraints and AC/DC conversion efficiency (Palma-Behnke et al., 2013).

Furthermore, this formulation does not enable to represent properly MG standard architecture. In fact, it is common that a MG is provided with an energy storage, especially when one or more intermittent RES are installed in the system. Frequently the contribution of the energy storage, which can act both as a load and a generator, is split in two positive variables, one responsible for charging (b^+) and the other for discharging (b^-) (Morais et al., 2010). Eq.s3.2 is accordingly substituted by the following set of constraints:

$$\sum_{j \in J} b^-_{t,j} + \sum_{i \in I} p_{t,i} + \mu_t = \sum_{j \in J} b^+_{t,j} + \varphi_t + \delta_t \quad \forall t \in T \tag{3.3}$$

where j is the generic energy storage in the set of all energy storages J. The level of each energy storage (SL) expressed in kWh is updated according to the following set of equations:

$$SL_{t+1,j} = SL_{t,j} \cdot (1 - \vartheta_j) + b^+_j \cdot \eta^+_j - b^-_j \cdot \frac{1}{\eta^-_j} \quad \forall t \in T, j \in J \tag{3.4}$$

$$SL^{min}_j \leq SL_{t,j} \leq SL^{max}_j \quad \forall t \in T, j \in J \tag{3.5}$$

where ϑ_j represents the loss factor related to storage j, η^-_j the discharge efficiency and η^+_j the charge efficiency. Eq.3.4 is valid only for hourly time steps; if time steps of different sizes are considered, the formulation has to be modified accordingly, as suggested by Palma-Behnke et al., 2013. To prevent simultaneous charge and discharge processes, a binary variable ($\alpha_{t,j}$) is usually added to the model. This variable is equal to 1 when the storage is charging, 0 otherwise. The two set of equations required are the following:

$$b^+_{t,j} \leq \alpha_{t,j} \cdot b^{max,+}_j \quad \forall t \in T, j \in J \tag{3.6}$$

$$b^-_{t,j} \leq (1 - \alpha_{t,j}) \cdot b^{max,-}_j \quad \forall t \in T, j \in J \tag{3.7}$$

where $b^{max,+}_j$ and $b^{max,-}_j$ represents respectively the maximum charge and discharge power of energy storage j.

Units operation limits and costs

Dispatchable units have always a feasible range of operation. In the cases with only a maximum power limit, only this set of constraints is required:

$$p_{t,i} \leq p_i^{max} \quad \forall t \in T, i \in I \tag{3.8}$$

where p_i^{max} represents the maximum power limit of unit i. When a unit has a minimum power limit, an additional binary variable is requested ($y_{t,i}$). This variable is equal to 1 if unit i is on in time step t and 0 otherwise. Then these two sets of inequalities are added to the problem:

$$y_{t,i} \cdot p_i^{min} \leq p_{t,i} \leq y_{t,i} \cdot p_i^{max} \quad \forall t \in T, i \in I \tag{3.9}$$

where p_i^{min} is the minimum operating power. Left-hand term of Eq.3.9 imposes that $y_{t,i}$ is equal to 1 if the power is greater than 0, while right-hand term of Eq.3.9 implies that, when $y_{t,i}$ is equal to 1, the power can not be less than the minimum power.

Operating costs The cost for unit operation considered in the objective function ($c_{t,i}$) has to be related to the output of the unit itself. The more generalized formulation is the following:

$$c_{t,i} = f(p_{t,i}) \quad \forall t \in T, i \in I \tag{3.10}$$

where f can be a function of any kind. The operation cost is expressed in USD and is the sum of two components: (i) fuel consumption, which has to be multiplied by the fuel price, and (ii) maintenance. The fuel consumption curve is related to the power output while the maintenance cost is usually a fixed cost per hour. This is a realistic assumption for diesel ICE generators because maintenance operations as the oil change are scheduled after a fixed number of hours, regardless of the average power factor.

When the function of interest (sum of both fuel and maintenance costs) is convex[3], the constraints represented in Eq.3.10 can be represented using a set of linear constraints and hence solved using linear programming (LP). In this particular case, Eq.3.10 can be expressed as:

$$c_{t,i} \geq m_{pw} \cdot p_{t,i} + q_{pw} \cdot y_{t,i} \quad \forall t \in T, i \in I, pw \in PW_i \tag{3.11}$$

where m_{pw} and q_{pw} are respectively the slope and the intercept of pw line, and PW_i is the set containing all the lines describing the behavior of unit i. The higher is the number of lines considered to describe one single unit, the better is the representation of the original function. On the other hand, an increase of the lines entails an increase of the computational costs, which are related to the number of variables and constraints.

[3] A function $f : \mathbf{R}^n \to \mathbf{R}$ is *convex* if **dom** f is a convex set when $\forall x_1, x_2, \forall t \in [0,1] : f(tx_1 + (1-t)x_2) \leq f(x_1) + (1-t)f(x_2)$. In other words f is convex if the line segment between any two points on the graph function lies above or on the graph

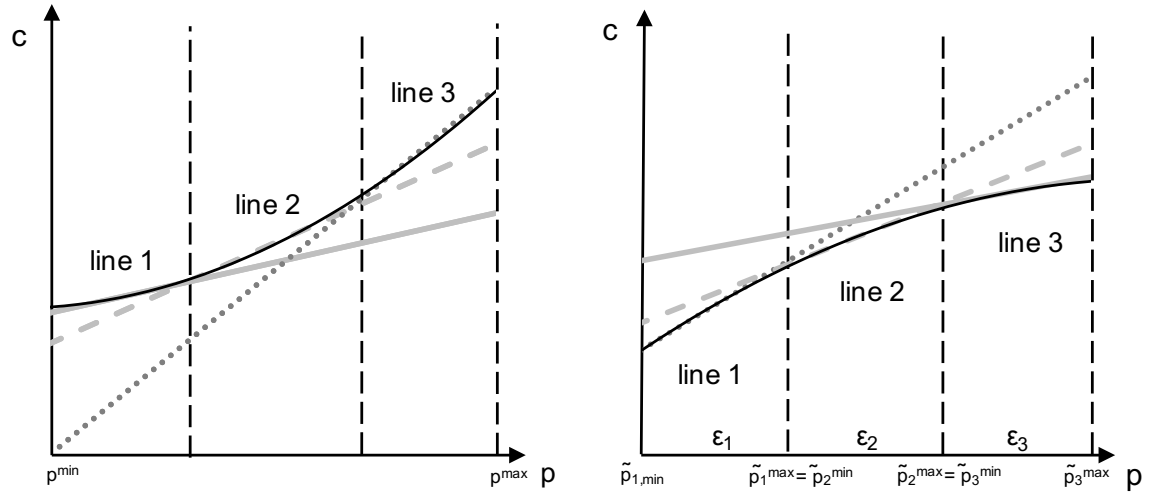

FIGURE 3.4: Two examples of cost curves: (left) convex curve with only inequalities constraints and (right) non-convex curve, with the need of additional binary (ε_{pw}) and continuous ($\widetilde{p}_{pw}$) variables

When the function is not convex, Eq3.11 is not valid and has not to be used. In these cases, the function is generally approximated by piecewise linear segments and, for each one (pw), a new binary variable ($\varepsilon_{t,i,pw}$) and a new continuous variable ($\widetilde{p}_{t,i,pw}$) are introduced. Eq.3.10 are then modified into:

$$p_{t,i} = \sum_{pw \in PW_i} \widetilde{p}_{t,i,pw} \quad \forall t \in T, i \in I \tag{3.12}$$

$$\varepsilon_{t,i,pw} \cdot \widetilde{p}^{min}_{i,pw} \leq \widetilde{p}_{t,i,pw} \leq \varepsilon_{t,i,pw} \cdot \widetilde{p}^{max}_{i,pw} \quad \forall t \in T, i \in I, pw \in PW_i \tag{3.13}$$

$$c_{t,i} = \sum_{pw \in PW_i} (m_{pw} \cdot \widetilde{p}_{t,i,pw} + \varepsilon_{t,i,pw} \cdot q_{pw}) \quad \forall t \in T, i \in I \tag{3.14}$$

$$\sum_{pw \in PW_i} \varepsilon_{t,i,pw} = y_{t,i} \quad \forall t \in T, i \in I \tag{3.15}$$

where $\widetilde{p}^{min}_{i,pw}$ and $\widetilde{p}^{max}_{i,pw}$ are respectively the low and upper bounds of the range related to pw segment. Note that this formulation entails an increase of binary variables in the problem, with a consequent increase in computational time. This aspect has been well described by Bischi et al., 2014, which show the trade-off between representation accuracy (with a high number of piecewise segments) and computational costs. Figure 3.4 shows two examples of cost functions and their approximation with 3 lines.

Startup costs Startup costs play an important role on the management of big size plants since a relevant amount of time (up to several hours in certain cases) is required to prepare and heat up the plant (Wood and Wollenberg, 1996). In small-size hybrid MGs, the most common units are diesel ICEs, which are flexible and require few minutes for startup. Dennis Barley and Byron Winn, 1996 suggest that startup cost is equivalent to 1-4 minutes of nominal rate

operation, this contribution can be taken into account in the objective function, as shown in Eq.3.1. Furthermore, other technologies which could play a relevant role in MGs in the next future as biomass-based systems and CSP are usually less flexible and have more consuming startups, which have to be properly considered by the EMS. Startup costs in MILP formulation are usually described by the following equations:

$$c_{t,i}^{startup} \geq 0 \quad \forall t \in T, i \in I \tag{3.16}$$

$$c_{t,i}^{startup} \geq \bar{c}_{i}^{startup} \cdot (y_{t,i} - y_{t-1,i}) \quad \forall t \in T, i \in I \tag{3.17}$$

where $\bar{c}_{i}^{startup}$ is the cost per single startup of unit i. Note that, thanks to Eq.3.17, $c_{t,i}^{startup}$ is equal to $\bar{c}_{i}^{startup}$ only when the units is on in the time step t and was off in the previous time step $t-1$ ($y_{t,i} = 1$ and $y_{t-1,i} = 0$). In the other cases, $c_{t,i}^{startup}$ will be equal to zero.

Battery wear cost In standard UC formulation, the cost considered in the objective function are only related to the generating units. Even if hydro storage are present in some formulations (Baldick, 1995), usually there is no cost associated to the hydro storage usage. This is not true for battery energy storage systems (BESS), whose cost and lifespan are strongly related to the frequency of charge and discharge. When a battery is present, Eq.3.1 has to be updated adding the battery wear cost ($c_{t,j}^{wear}$) which is defined by the following constraint:

$$c_{t,j}^{wear} = \bar{c}_{j}^{wear} \cdot b_{t,j}^{-} \quad \forall t \in T, j \in J \tag{3.18}$$

where $\bar{c}_{j}^{wear}$ is the wear cost per unit of energy delivered. Note that the battery wear is only related to the BESS discharge, and not to the charge; in this way, the battery is always charged when "free" power is available and the monetary penalization is reserved only to the discharge step, which is comparable to power generation from a standard unit.

According to Eq.3.18, the battery wear cost is constant. However, experimental results have shown that the BESS deterioration is strongly related to its operating condition; in particular it has been found that the state of charge plays an important role, with the battery degradation that is greater the emptier is the BESS. Very detailed highly non-linear models have been proposed to better describe the behavior of the BESS wear (Sauer and Wenzl, 2008) but their application in MILP models is not practical. Only few examples in literature propose a detailed description of battery degradation in MILP models. It is the case of Palma-Behnke et al., 2013, who proposed a UC model in which the battery degradation is described with state of health of BESS, determined its temperature and its state of charge. Three possible working zones (with one binary variable for each one) are defined, resulting in a better description of BESS behavior but with a more difficult problem to be solved.

Reserve constraints and solution robustness

The EMS has to ensure stable and proper operation of the MG even in the case of an error in forecast of load or non-dispatchable units. The interest in this topic is rapidly increasing, especially to deal with the massive integration of wind energy which, for its nature, is highly intermittent and very often not easily predictable (Lowery and O'Malley, 2012). In traditional electric systems, MG stability is obtaining ensuring that the spinning reserve exceeds the power requested by loads in the worst-case scenario. The spinning reserve is the total generating capacity available in a short interval of time in case of a sudden increase of the load (Wood and Wollenberg, 1996) and it is ensured by all spinning machines and the extra generating capacity which is not switched on but can be available in a short interval of time. In a MG, other appliances such BESS can provide the same service, having the capability to supply power very quickly if needed. In this case, since the reserve is not given only by "spinning" generators, it is usually called operating reserve.

Dividing the set I of generating units in two subsets (I^{slow} for slow generators, I^{fast} for fast generators) the operating reserve constraints are described by the two following sets of equations:

$$\sum_{i_1 \in I^{fast}} p_{i_1}^{max} + \sum_{i_2 \in I^{slow}} y_{t,i_2} \cdot p_{i_2}^{max} + \sum_{j \in J} b_j^{-,max} \geq \widetilde{\varphi}_t \tag{3.19}$$

$$\sum_{i_1 \in I^{fast}} p_{i_1}^{max} + \sum_{i_2 \in I^{slow}} y_{t,i_2} \cdot p_{i_2}^{max} + \sum_{j \in J} (SL_{t,j} - SL_j^{min}) \geq \widetilde{\varphi}_t \tag{3.20}$$

where $\widetilde{\varphi}_t$ is the worst-case net load during time step t. This value is higher than the value considered in the balance constraints (φ_t), because it takes into account that the load may higher than expected and that RES production may be overestimated.

Differently from standard generators, BESS contribution is limited not only by the maximum power rate, but even by the energy available in the storage itself. This is the reason why two different sets of equations are required, one for power limit (Eq.3.19) and one for energy limit (Eq.3.20). A more detailed formulation should take into account even the kinetic behavior of the battery, which could described accurately using battery models as the KiBAM, developed by Manwell and McGowan, 1993. This model is widely used for simulations based on non-predictive strategy as HOMER (Lambert, 2006), but it is not a common practice to embed it in predictive UC models for MGs.

For sake of completeness, the other approaches used to tackle uncertainties are hereafter reported. The formulation proposed above, generally called deterministic UC, considers only one single net load forecast and handles the uncertainties using the operating reserve constraints reported in Eq. 3.19 and 3.20. Two other families of approaches have been developed, mainly for big-size grid management: stochastic and robust UC.

In stochastic UC a set of net load forecasts is considered, each one with its probability. The objective function to be minimized is hence the sum of the total cost for each scenario, weighted on its probability of realization. Stochastic UC has the potential to reduce operation

cost compared with deterministic UC, but the computation cost may become very high when the number of scenarios considered increases (Ruiz et al., 2009).

The other family of models are based on robust UC. In the standard formulation (Bertsimas et al., 2013), the input data is a central forecast and two bounds; the scheduling takes into account all possible realizations of uncertainty in that given range and it minimizes the overall cost under the worst realization. More advanced models, which are the hybrid combination of the ones described above, show promising results (Ruiz et al., 2009; Dvorkin et al., 2015). The same concepts and models can be applied successfully to MGs instead of large scale grids, as shown by the works of Daniel E Olivares et al., 2015 and R. Gupta and N. K. Gupta, 2015.

Programmable loads and CHP systems

The possibility to shift in time particular loads in the MG is a very promising feature to reduce the overall operation costs. In practice programmable loads can act exactly as a storage, shifting in time the consumption and reducing the load peak during critical hours.

As already underlined above, the first step could be to admit the possibility to have unmet loads. This concept is already currently applied by distribution system operators in weak grids during peak hours to reduce the operation costs and can be successfully applied to MGs. This is the case of the model proposed by Parisio, Rikos, and Glielmo, 2014, in which a part of non-critical loads can be curtailed admitting a profit loss as already described in Eq.3.1.

The possibility to curtail part of the load is a valuable option, but the possibility to schedule programmable loads is something more, because it does not affect the user comfort. This solution has been proposed especially for Home management system, in which a certain set of appliances can be scheduled during the day to match the production of PV panels (Barbato et al., 2014). For the same application (Home management system) Kriett and Salani, 2012 developed a MILP model differentiating the loads in more complex categories. Extending the field of application, programmable loads have been considered also in distribution systems. M. Zhang and Jie Chen, 2014 showed that, using a proper MILP model, the charging of an high number of electric vehicles can be coordinated. In a scenario where electric vehicles are a commonly adopted solution, a EMS may reduce the grid operation costs, reducing power consumption peak and increasing the load during non-critical hours.

Regarding off-grid MGs, the same concept can be effectively applied with even better results. In fact, in off-grid systems the operation may be more challenging due to the need to balance continuously power and load. When a great amount of energy is coming from intermittent RES, the problem is even more difficult and programmable loads are a key factor to match the intermittent power production.

One of the most common and flexible way to model programmable loads is the lumped tank model, described in Figure 3.5 and currently used in HOMER (Lambert, 2006). This model is very useful to model loads in which the useful effect can be decoupled from the energy consumption. A typical example is a vessel of water pumped from a well, already applied in a EMS model for an off-grid MG by Palma-Behnke et al., 2013: the tank is filled when the pump uses power and it is discharged by the use for irrigation or for domestic purposes.

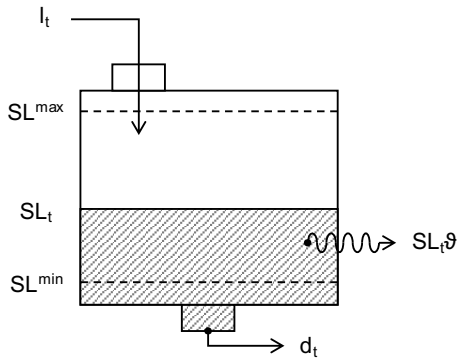

FIGURE 3.5: Schematic representation of a programmable load

For each programmable load k in the set K containing all the schedulable loads, a maximum (SL_k^{max}) and a minimum level (SL_k^{min}) can be imposed in order to limit dissipations of energy or an excessive depletion of the reservoir. The presence of a minimum energy level entails the possibility for a schedulable load to become non-schedulable. An example is a refrigeration cell where an unexpected amount of perishables is stored in a certain time step requiring a certain amount of energy ($d_{t,k}$). The cell temperature rises and it reaches a temperature close to the maximum allowable for proper food conservation (minimum energy level): in the further time step this load shifts in the non-schedulable loads category since it must be cooled down. When the temperature is reported again below a threshold the load becomes a schedulable load again and the EMS can plan its operation without this constraint. On the contrary, if the temperature into the cell is very low (maximum energy level) a further operation of the cell is detrimental since it results in a dissipation of energy: the load cannot take in more power and it is automatically switched off with a limitation of its availability.

This model can be implemented in MILP language, adding the following constraints, similar to the ones related to energy storages:

$$SL_{t+1,k} = SL_{t,k} \cdot (1 - \vartheta_k) + l_{t,k} - d_{t,k} \quad t \in T, k \in K \tag{3.21}$$

$$SL_k^{min} \leq SL_{t,k} \leq SL_k^{max} \quad t \in T, k \in K \tag{3.22}$$

where $l_{t,k}$ is the power consumed by the load and ϑ_k is the loss factor related to the storage of load k. Note that, with this formulation, all the variables related to the programmable loads are converted in electric variables (in kW and kWh). For example, the volume of a water tank, expressed in m^3, has to be converted in the equivalent kWh. The balance equation (Eq.3.3 has to be updated to take into account the programmable load consumption:

$$\sum_{j \in J} b_{t,j}^{-} + \sum_{i \in I} p_{t,i} + \mu_t = \sum_{j \in J} b_{t,j}^{+} + \varphi_t + \delta_t + \sum_{k \in K} l_{t,k} \quad \forall t \in T \tag{3.23}$$

Additional constraints are needed to model the operating constraints of the programmable loads:

$$y_{t,k} \cdot l_{ki}^{min} \leq l_{t,k} \leq y_{t,k} \cdot l_{k}^{max} \quad \forall t \in T, k \in K \tag{3.24}$$

where $y_{t,k}$ is the on/off variable analogous to the ones related to generators (see Eq.3.9). The details of representation of programmable loads can be increased, including startup costs (similarly to Eq.3.17) or admitting discrete levels of power. This solution, already implemented in Dai and Mesbahi, 2013, allows to simulate loads which has for example two discrete power levels, including in the MILP formulation integer variables.

Including programmable electric loads is only one of the possible ways to obtain flexible operations of a MG. Additional degrees of freedom can be added considering in the optimization not only electricity, but also other valuable goods as heating and cooling. This concept has been deeply and widely studied for grid-connected MG (Gu et al., 2014) that, in this case, are usually called combined heat and power (CHP) systems; when the cooling demand is taken into account the term trigeneration systems is usually adopted. CHP units, which are the core of these systems, are able to produce simultaneously both heat and power and their proper schedule has to take into account the demand of both heat and power. Other kind of synergies are explicitly taken into account: for example, cooling by heat pumps require a certain amount of electricity and, using properly the UC framework, heat pumps can be switched on during those parts of the days when the intermittent RES production is high or the non-schedulable load consumption is low. The problem framework is similar to what have been proposed above, but additional variables and constraints are needed to describe the balance of the other goods (heating, cooling) and CHP units (Bischi et al., 2014; Bracco, Dentici, and Siri, 2013).

3.2 Design optimization

The definition of an efficient operation strategy is important not only for its practical implementation in running a MG, but also during the MG design step. In fact, to find the optimal mix and size of technologies, different configurations are generally tested over a long time span to assess the operation cost; the tests should be performed considering for each case the optimal management because the operational cost obtained without the definition of a suitable logic for the scheduling of both the loads and the generators may lead to misleading results. Solutions which are more conservative could be favored, as well as combinations of generators which would be able to take advantage from a more flexible MG management could be unfairly penalized.

MG design is a challenging task which has been deeply studied in literature. In the classification hereafter proposed power control analyses tool which aim to represent the MG behaviour and reactions in small time-steps (less than seconds) are excluded. All the design methods based on MG long-term operation can be classified in three different areas:

1. **Average** methods
2. **Simulation** methods

3. **Capacity planning** methods

The definition and the analysis of each category is reported in the following subsections.

3.2.1 Average methods

Average methods make use of simple algebraic relationships to evaluate the performance (energetic and economic) of different MG configurations. All the calculations are made using average values, as average daily load consumption and average monthly energy production by RES. An example of well known and popular software based on a average method is RETScreen. RETscreen is a feasibility study tool developed by Ministry of Natural Resources of Canada and its scope is to evaluate the financial and the environmental costs and the benefits of different Renewable Energy Sources (RES) in different locations of the world using a monthly time scale (Lee et al., 2012). Other examples of this kind of approach are available in literature (Elhadidy and Shaahid, 2000; Bhuiyan and Ali Asgar, 2003).

The main advantage of this kind of approach is the very high speed in computation time. Because of the very small number of variables, it is possible to evaluate a huge number of different configurations in a short period of time, making possible to perform extensive sensitivity analyses on the input data. In addition to this, these methods can be very useful in the first part of the design procedure, when accurate data (hourly or sub-hourly time series over one year) are not available and accuracy is not the primary objective.

In fact, the high computation speed is paid with an imperfect representation of reality. Using only hourly, daily or monthly averages does not allow to have a proper insight on the real working condition of the MG and the averages could lead to an underestimation of real costs. Although there is a good representation of long-term dynamics, these methods have not the capability to describe efficiently sub-daily dynamics, that, especially in off-grid environments, have generally a great impact.

3.2.2 Simulation methods

Realistic simulation methods are based on the simulation of the real working conditions of the MG. Given a MG configuration, the aim is to evaluate the main operation costs, as fuel consumption and battery degradation, performing a simulation of the operation of the MG with relatively small time steps (i.e. 15 minutes, 1 hour). Performing the simulations for different configurations is then possible to compare them and to find the best one according to a certain objective (i.e. lifetime cost, RES penetration, pollutant emissions).

The most popular software which rely on a simulation method is HOMER (Lambert, 2006). Given a set o MG configurations that the user want to test, HOMER performs for each one a long-term simulation (usually one year) using one of the two available non-predictive strategies (LF or CC). HOMER is largely used both for grid connected and off-grid MGs and there is a huge number of publications using it to find the optimal design of a MG (Hafez and Bhattacharya, 2012; Montuori et al., 2014).

The main problem related to the use of HOMER is that it relies on non-predictive strategies (NPSs). The quality of the results obtained with LF or CC depends on the value of

input parameters assumed for the simulation, such as the storage set point or the battery minimum state of charge (Dufo-López and Bernal-Agustín, 2005). A first improvement to the standard NPSs is obtained with the optimization of these parameters which allows obtaining a consistent decreasing of the operation costs. This approach is implemented in HOGA software, introduced for first time by Dufo-López, Bernal-Agustín, et al., 2011. It is based on traditional NPSs but each user-defined parameter is chosen solving an auxiliary problem with a genetic algorithm. The same genetic algorithm is even responsible to find the optimal sizes of each generator (PV, WT and others).

A similar approach has been used by B. Zhao, X. Zhang, Li, et al., 2014 to find the optimal design of a MG located in Dongfushan Island (China). In this case, the input parameters of the NPSs used to simulate the MG are considered constant and hence, once fixed the MG configuration, the operation cost are determined simulating one year of operations. The optimal sizes of generators and battery are obtained using a genetic algorithm which aims to minimize the life-cycle MG cost, the RES penetration and the pollutant emissions.

Another example of software is W-ECoMP which is a tool developed by Thermochemical Power Group of University of Genova[4]. The software can be used to simulate and design a wide variety of energy systems, a shown in various publications (Rivarolo and Massardo, 2013; Rivarolo, Greco, and Massardo, 2013; Rivarolo, Magistri, and Massardo, 2014). The approach is divided in two different hierarchy levels: the inner level, once fixed the sizes of the components, simulates system operation over one year; the outer level has to find the optimal design, taking into account total annual cost, made by variable cost (found at the inner level) and capital cost. The inner level has the possibility to handle very complex systems, made by different goods (e.g. hydrogen, heat, electricity), offering new degrees of freedom compared with HOMER. In addition to this, operation strategy definition is based on an optimization algorithm which finds the contribution by each single component leading to the least costly solution. However, even in this case, operation decisions do not rely on forecasts but only on present values and this could result in a overestimation of operation costs, as demonstrated in Chapter 5.

In general, compared to average methods, simulation methods can offer a better representation of reality, especially if hourly or sub-hourly time steps are used. The computation time requested to find an optimal solution is strongly related to the optimization algorithm used and it is greater compared to average methods. Additional time consumption has to be considered if the input parameters of the dispatch strategy have to be tuned through optimization.

Even if MG behavior is well described using standard simulation methods, there is room for further improvement. In fact, as already described in the previous section, predictive strategies are gaining more and more interest and they are expected to allow consistent money savings compared to NPSs. However, only one study in literature have proposed a long-term simulation using a PS and the simulation is only used to test and find the operating cost of a fixed MG configuration (Palma-Behnke et al., 2013).

[4]W-EComP - URL:`http://www.tpg.unige.it/TPG/portfolio-item/w-ecomp/`; Date of access: 28/06/16

3.2.3 Capacity planning methods

This category includes all the optimization models which simultaneously find the optimal operation and the optimal design of a MG. The general class of capacity planning problems have been defined to find the optimal capacity in supply chains of different fields and it has been commonly adopted for large grids generation planning, especially in the case of a centrally coordinated monopoly (Kagiannas, Askounis, and Psarras, 2004). The generating planning problem for large grids consists in finding the optimal combination of power generation technologies (i.e. coal, natural gas, nuclear, hydro) which entails the minimum cost of electricity, considering both operation and up-front costs.

The same concept applies to smaller grids, both connected or not to the grid. The most popular commercial software in this field is DER-CAM (Distributed Energy Resources Customer Adoption Model) which is a decision support tool for the introduction of distributed energy sources in MGs and buildings[5]. Focusing on few representative weeks of the year, DER-CAM solves a capacity planning problem minimizing total energy costs, including up-front and running costs, and/or CO_2 emissions.

Other models have been developed in literature. Wouters, Fraga, and James, 2015 proposed a capacity planning model for residential CHP, including the pipelines installation for district heating as investment variable and using a representative time interval made by 4 days (one for each season). Regarding off-grid MG, Ho, Hashim, and Lim, 2014 developed an optimization model to design a cost-effective MG based on solar and biomass. Even in this case the operation costs estimation over the year are obtained applying the model to 5 representative days which differ for solar intensity during the day. In Malheiro et al., 2015 the optimal sizes of different conversion systems (solar, wind) and energy storage (battery) are obtained using the same concept taking into account 365 days in the optimization problem.

The capacity planning problem formulation is similar to the UC one with few major changes. First, a new set of variables is needed to represent the investment decisions. Continuous, binary or integer variables can be used to represent the set of sizes we want to optimize. Consequently, the objective function has to be modified to include capital costs along with operation costs, as shown in the following equation:

$$\min \quad w \cdot OPEX + \sum_{i \in I} z_i \cdot C_i^{inv} \cdot CRF_i + C_i^{O\&M} \tag{3.25}$$

where w is the weighting factor for the operating costs, OPEX represents the operation costs as for UC with a 1-year time horizon (see 3.1), z_i is the binary variable representing the investment decision for unit i, C_i^{inv} is the up-front cost related to unit i, CRF_i is its capital recovery factor[6] and $C_i^{O\&M}$ are its fixed O&M cost. The term w is needed when the time horizon considered in the optimization problem is less than one year in order to normalize the

[5] DER-CAM - URL:`https://building-microgrid.lbl.gov/projects/der-cam`; Date of access: 28/06/16

[6] Capital recovery factor (CRF) is a parameter which allows to determine the impact of a multi-year investment on a single year. It is a function of the lifetime of the investment (LT) and of the interest rate (i) ($CRF = \frac{i(1+i)^n}{(1+i)^n-1}$)

value. For example, if the time horizon used is 5 days, the weighting factor w will be $\frac{365}{5}$ in order to extend those operating costs over one entire year.

This objective function formulation proposed implies that only "yes" or "no" decisions are available for units installation. Continuous or integer variables can be eventually included in the formulation using the same rationale. The constraints of the problem are the same as UC, but some of them (especially the ones related to operation limits and costs in 3.1.4) have to be modified to take into account the new investment variables. The resulting formulation is considerably heavier and for this reason one-piece linear functions are adopted to represent units part-load operations (Malheiro et al., 2015) or start-up penalizations are omitted (Ho, Hashim, and Lim, 2014).

The main advantage related to this kind of approach is its capability to find the optimal sizes ensuring optimal operation at the same time. With only one-shot is possible solve the sizing problems, without the need of iterating and simulating different configurations (as requested by simulation methods).

However, this important feature comes with significant disadvantages. The time horizon is usually limited to few days, and as for intuitive methods, some dynamics could be lost especially if energy sources with high seasonality as wind or solar are considered. However, problems with time horizon covering the entire year (8760 hours) overcome this problem and have already been demonstrated feasible in literature (Malheiro et al., 2015).

However, the problem will become completely intractable when more complex systems are considered, including more dispatchable generators (i.e. biomass, CSP) or adding other valuable goods in the optimization (as heat for CHP systems). Another important point is that, using as reference to evaluate the operating costs a UC over 1 year, could lead to misleading results. In fact assuming the perfect knowledge of future events for 365 days will not be realistic in real life operation and the resulting operation cost could be too optimistic.

Chapter 4

Methodology

In this chapter the description of the models developed during the thesis is reported, highlighting the originality and novelty in relation with the current state of the art in MG operation and design. Two different contributions can be highlighted: (i) the development of a model for the optimal management of a microgrid and (ii) the application of the model for long-term simulation aimed at supporting the MG design.

4.1 Multi-good model

The first objective of the thesis was to propose a new and more general approach to the solution of the Energy Management System (EMS) problem starting from the state of the art methodologies in literature and adding new features.

In the proposed approach, the MG operation is defined through an EMS model able to determine the schedule of each programmable unit to fulfill the most important needs of the users served by the MG at the lowest operation cost. Unlike the current approaches, described in detail in the previous section, the problem formulation developed allows considering different goods in the MG and multi-input and multi-output units.

In literature there are different works in which the optimal planning of a MG takes into account the heat and cooling demand, as well as the electricity consumption (Bischi et al., 2014; Bracco, Delfino, et al., 2014). However, the possibility to include in the optimal planning each valuable asset requested by the users served by the MG has not been investigated. The possibility to consider explicitly goods easily storable (i.e. wood chips, potable water, heat) can play a relevant role in operating cost reduction and adds new degrees of freedom in MG scheduling. Formulating the problem with different goods, instead of considering them only as deferrable electric loads (a solution already adopted in other publications as Faxas-Guzmán et al., 2014; Dai and Mesbahi, 2013; Palma-Behnke et al., 2013), allows modeling units requiring more than one good during operation and taking into account their off-design performance, as well as technical operation constraints and start-up penalties.

The management of complex systems including multi-input and multi-output units can be really optimized only when the goods are considered as separated entities, as shown by the test-case reported at the end of this section (see 4.1.3). In addition to this, a more accurate description of battery behavior is proposed and implemented in the model. A description of the additional constraints and variables needed in the formulation to include kinetic constraint and the aging process models is reported.

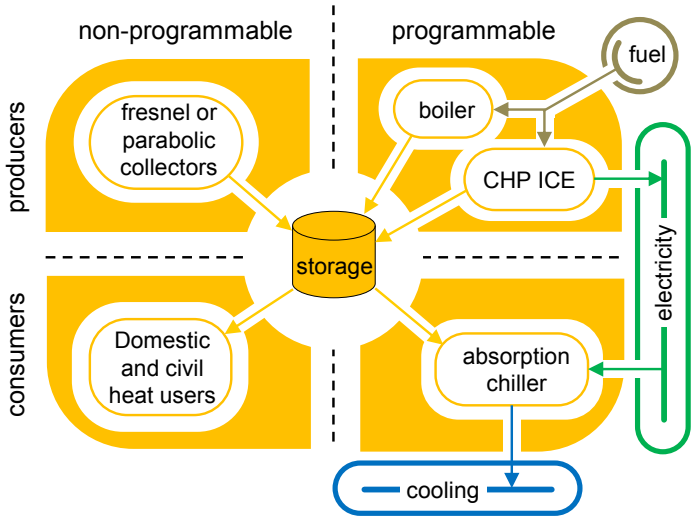

FIGURE 4.1: Example of the subsystem framework for the good "Heat", including storage, producers and consumers (both programmable and not). (Mazzola, Marco Astolfi, and Ennio Macchi, 2015a)

4.1.1 Problem statement

The solving of the EMS problem determines for each time step t in the whole time horizon T_h the schedule of each programmable unit and the storage level of each storable good, minimizing the overall operation cost and respecting all the operation constrains. The information required are:

1. the initial condition of storages and programmable units
2. the production and consumption of each good by non-programmable units for each time step
3. the performance curves, the start-up penalties and operations constrains of each programmable unit
4. the penalty for the unmet demand and the storage properties of each good

Each good in the MG represents a subsystem. Each subsystem is composed by a storage (if present for that kind of good) and a set of units that produce or consume the good. In Figure 4.1 the subsystem "Heat" is represented as example. The units which interact with this good are listed in two categories.

First we have non-programmable units, whose production and operation cannot be modified by the EMS. Concentrating solar thermal collectors, as Fresnel or parabolic trough, are an example of non-programmable producers while the use of the heat by domestic and civil users can be considered a non-programmable load. The difference between production and consumption by non-programmable units is the gross aggregate balance of the good, a useful information to assess properly the programmable units schedule.

On the other hand, there are programmable units whose operation is defined by the EMS. For goods without storage, the EMS ensures the balance of production and consumption

in each time step using the programmable units. If the storage is available, the excess of production in a certain time step can be stored and used in the future; otherwise the storage can be discharged to satisfy the good demand. In Figure 4.1 two programmable producers are shown: a boiler which uses fuel to produce heat and a cogenerator that produces both heat and AC power. An example of a programmable consumer of the good "Heat" is the absorption chiller. The cogenerator and the absorption chiller are two examples of multi-input and multi-output programmable units respectively; these units can be simulated by the definition of a specific performance curve for each good consumed or produced.

The penalty term is a function of the unmet demand of each good: depending on the penalty value, the EMS could decide to meet only partially the demand, if this avoids a huge increase of operation costs. In general, a high penalty term is related to a very high priority load, as for example health care appliances, and a low penalty term is related to interruptible load, as part of the public lighting.

4.1.2 Mathematical model

The core of the methodology proposed is the MILP problem that allows the definition of the most cost effective schedule of each programmable unit over a certain time horizon. The rigorous formulation of the scheduling problem is a Mixed Integer Non-Linear Problem, but a conversion in MILP is obtained using linearization techniques. Hence, near-optimality and fast convergence is ensured thanks to current MILP solvers. The problem is implemented in AMPL[1] and the algebraic formulation is hereafter presented. Note that mist of the set of constraints and variables used in the multigood model are similar to the one already described in the Section 3.1.4 of the previous chapter for the generic UC model. Even if the concept is the same, they have to be changed to take into account that more than one good is considered in the formulation.

Sets

First of all, the sets are introduced. They allow describing the problem in a concise and clear formulation. The time steps considered in optimization model are defined with the set $T = \{1, 2, .., T_h\}$ where T_h is the time horizon, the number of hours which are taken into account in the schedule defining.

The set G includes each good present in the MG. It contains a subset which contains all the goods which have a storage ($G^{storage} \subseteq G$). The set U includes each programmable unit present in the MG. The following subsets are defined:

- $U^{minload} \subseteq U$: set of units which have a minimum production rate once they are on.
- $U^{startup} \subseteq U^{minload}$: set of units which have start-up penalization.on.
- $U^{minN} \subseteq U^{startup}$: set of units which have constraints on minimum running hours once they are switched on.

[1] AMPL (A Mathematical Programming Language) is a an algebraic modeling language used to solve large-scale mathemetical optimization problem

The following subsets describe relations between goods and units in terms of production and consumption:

- G_i^p: set of goods that can be produced by the unit i, with $i \in U$
- G_i^c: set of goods that can be consumed by the unit i, with $i \in U$
- U_g^p: set of units that produce the good g, with $g \in G$
- U_g^c: set of goods that consume the good g, with $g \in G$
- PW_{i,g_1,g_2}: set of linear inequalities that relate the production of good g1 by unit i and the consumption of good g2, with $i \in U, g1 \in G_i^p, g2 \in G_i^c$.

Parameters

The parameters are constant values representing the inputs of the problem and they can have different values for each time step. The parameters used to goods properties definition are hereafter reported:

The parameters used to goods properties definition are hereafter reported:

- $\varphi_{t,g}$: production and consumption by non-programmable units of the good g during the time step t, $\forall t \in T, g \in G$
- $\varphi_{t,g}^{reserve}$: production and consumption by non-programmable units of the good g during the time step t in the worst-case scenario, $\forall t \in T, g \in G$
- π_g: penalty related to the unmet demand of the good g
- SL_g^{min}: minimum level of good g that can be stored in the related storage, $\forall g \in G^{storage}$
- SL_g^{max}: maximum level of good g that can be stored in the related storage, $\forall g \in G^{storage}$
- SL_g^0: amount of the good g stored in the related storage in the first time step, $\forall g \in G^{storage}$
- ϑ_g: self discharge factor of the good g in the related storage, $\forall g \in G^{storage}$

The parameters used to units properties definition are hereafter reported:

- $P_{i,g}^{rate}$: maximum production rate of the unit i of each good g that can be produced by unit i, $\forall i \in U, g \in G_i^p$
- $P_{i,g}^{min}$: maximum production rate of the unit i of each good g that can be produced by unit i, $\forall i \in U^{minload}, g \in G_i^p$
- $c_{i,g}^{startup}$: start-up additional consumption of good g by the unit i, $\forall i \in U^{startup}, ginG_i^p$
- N_i: number of minimum running hours of the unit i, $\forall i \in U^{minN}$
- N_i^0 : number of residual minimum running hours of the unit i, $\forall i \in U^{minN}$

- on_i^0 : state of operation of the unit i at the beginning of time horizon, $\forall i \in U^{startup}$
- $m_{i,g1,g2,pw}$: slope of the pw line that relates production of good g_1 by unit i and the consumption of good g_2, with $i \in U, g_1 \in G_i^p, g_2 \in G_i^c; pw \in PW_{i.g_1,g_2}$
- $q_{i,g1,g2,pw}$: intercept of the pw line that relates production of good g_1 by unit i and the consumption of good g_2, with $i \in U, g_1 \in G_i^p, g_2 \in G_i^c; pw \in PW_{i.g_1,g_2}$

Variables

Variables are the quantities that are varied by the solver in order to reach the minimum of the objective function while respecting all the constraints of the problem. They are divided in real continuous variables and Boolean variables.

Continuous variables

- $SL_{t,g}$: storage level of the good g in the time step t, $\forall t \in T \cup (T_h + 1), g \in G^{storage}$ and $SL_g^{min} \leq SL_{t,g} \leq SL_g^{max}$
- $\delta_{t,g}$: amount of the good g dumped in time step t, $\forall t \in T, g \in G$
- $\mu_{t,g}$: unmet demand of the good g in time step t, $\forall t \in T, g \in G$
- $p_{t,i,g}$: production of the good g by unit i in the time step t, $\forall t \in T, i \in U, g \in G_i^p$ and $p_{t,i,g} \geq 0$
- $c_{t,i,g}$:consumption of the good g by unit i in the time step t, $\forall t \in T, i \in U, g \in G_i^c$ and $c_{t,i,g} \geq 0$
- $p_{t,i,g}^{reserve}$: production of the good g by unit i in the time step t in the worst-case scenario, $\forall t \in T, i \in U, g \in G_i^p$ and $p_{t,i,g} \geq 0$
- $c_{t,i,g}^{reserve}$: consumption of the good g by unit i in the time step t in the worst-case scenario, $\forall t \in T, i \in U, g \in G_i^c$ and $c_{t,i,g} \geq 0$

Boolean variables

- $y_{t,i}$: binary variable related to on/off status of unit i in the time step t, $\forall t \in T, i \in U^{minload}$
- $on_{t,i}$: binary variable related to the startup of unit i in the time step t, $\forall t \in T, i \in U^{startup}$
- $\alpha_{t,i,g}$: binary variable that avoid simultaneous production and consumption of the same good by one unit, $\forall t \in T, i \in U^{startup}$

Objective function

The objective function is to minimize the operative costs and the penalties related to unmet goods demand:

$$\sum_{t\in T} C_{t,money} + \sum_{t\in T} C^{startup}_{t,money} + \sum_{t\in T} P_{t,money} + \sum_{t\in T}\sum_{g\in G} \mu_{t,g}\pi_g - \sum_{g\in G^{storage}} SL_{T_h,g}\frac{\pi_g}{M} \quad (4.1)$$

where $C_{t,money}$ denotes the operation cost of all the units in time step t, $C^{startup}_{t,money}$ denotes the monetary start-up cost of all units in time step t, $P_{t,money}$ denotes the total revenue in time step t (only if a unit in the MG can produce the good 'Money'). They are defined similarly for each generic good:

$$C_{t,g} = \sum_{i\in U^c_g} c_{t,i,g} \quad \forall t \in T, g \in G \quad (4.2)$$

$$C^{startup}_{t,g} = \sum_{i\in U^{startup}\cap U^c_g} c_{t,i,g} \quad \forall t \in T, g \in G \quad (4.3)$$

$$P_{t,g} = \sum_{i\in U^c_g} c_{t,i,g} \quad \forall t \in T, g \in G \quad (4.4)$$

The second to last term of Eq. 4.1 is the penalization related to the unmet demand of each single good over the whole time horizon. In this case we consider only money as good whose consumption has to be minimized, but, if requested, other goods (as for example pollutants or CO_2 emission) can be considered similarly. The last term takes into account that time horizon is limited. If we do not include this term, from a mathematical point of view, there would not be any difference between solutions with different storage level at the end of the time horizon. Giving a value to the amount of good stored in the last time step, the solution which entails the maximum storage level is preferred between the other solutions with the same costs. In this way, the dissipation of energy or other goods is implicitly avoided. Furthermore, using a value which is proportional to the unmet term, we are even giving a priority order to store different goods.

Constraints

The goods without storage must respect the balance between consumption and production in each time step as shown in Eq. 4.5. Note that the parameter φ is positive if the difference between non-programmable units production and consumption is positive and negative is the consumption exceeds the production.

$$\varphi_{t,g} + P_{t,g} + \mu_{t,g} = C_{t,g} + C^{startup}_{t,g} + \delta_{t,g} \quad \forall t \in T, g \in G \setminus G^{storage} \quad (4.5)$$

Goods with storage can be stored if there is excess of production to be exploited when there is an excess of consumption, as shown in the following equation.

$$SL_{t+1,g} = SL_{t,g}(1-\vartheta_g) + \varphi_{t,g} + \mu_{t,g} - \delta_{t,g} + P_{t,g} - C_{t,g} - C^{startup}_{t,g} \quad \forall t \in T, g \in G^{storage} \tag{4.6}$$

Relation between consumption and production of good by each unit are expressed through a set of linear inequalities:

$$c_{t,i,g2} \geq m_{i,g1,g2,pw} \cdot p_{t,i,g1} + q_{i,g1,g2,pw} \cdot y_{t,i} \quad \forall t \in T, i \in U, g1 \in G^p_i, g2 \in G^c_i, pw \in PW_{i,g1,g2} \tag{4.7}$$

The last term, present only for units with on/off binary variable, disables the constraint when the unit is switched off. This formulation requires that performance curve to be linearized has to be convex; if it is not, piecewise linearization techniques can be used accepting the introduction of new binary variables, and hence higher computational time (D'Ambrosio, Lodi, and Martello, 2010). The approach that has to be implemented in this case has already been described with Eq.3.12-3.15 in chapter 3. In the configurations studied in this thesis, only the battery life loss is modeled with a non-convex relation and this will be discussed in detail in 4.1.2. Maximum production by a unit is expressed with Eq. 4.8. For units that have minimum load constrains, two additional constraints have to be considered:

$$p_{t,i,g} \leq P^{rate}_{i,g} \quad \forall t \in T, i \in U \tag{4.8}$$

$$p_{t,i,g} \leq y_{t,i} P^{rate}_{i,g} \quad \forall t \in T, i \in U^{loadmin} \tag{4.9}$$

$$p_{t,i,g} \geq y_{t,i} P^{min}_{i,g} \quad \forall t \in T, i \in U^{loadmin} \tag{4.10}$$

The variable related to the start-up of a unit is defined through the following constraint:

$$on_{t,i} \geq y_{t,i} - y_{t-1,i} \forall t \in T, i \in U^{startup} \tag{4.11}$$

Note that this constraint allows to consider $on_{t,i}$ as a continuous variable because $y_{t,i}$ is boolean. Some units can be affected by technical limit as minimum running hours once the unit is switched on. This is taken in to account through the following constraints:

$$y_{t,i} \geq on_{t,i} \qquad \forall i \in U^{minN}, \tilde{t} \in T : t \leq \tilde{t} \leq t + N_i \tag{4.12}$$

$$y_{\tilde{t},i} = 1 \qquad \forall i \in U^{minN}, \tilde{t} \in T : \tilde{t} \leq t + N^0_i \tag{4.13}$$

Eq. 4.13 takes into account the minimum number of residual hours of operation if the unit is already operative at the beginning of the time horizon. Some auxiliary constraints are added for those units that can produce and consume the same good. This is the case of a bidirectional inverter than can produce and consume both DC and AC power depending on

the way it is working. In order to avoid a simultaneous production and consumption of the same good the two following constraints are considered:

$$p_{t,i,g} \leq \alpha_{t,i,g} \cdot M_{1,i} \qquad \forall t \in T, i \in U, g \in G_i^p \cup G_i^c \tag{4.14}$$

$$c_{t,i,g} \leq (1 - \alpha_{t,i,g}) \cdot M_{2,i} \qquad \forall t \in T, i \in U, g \in G_i^p \cup G_i^c \tag{4.15}$$

where the parameters $M_{1,i}$ and $M_{2,i}$ are large enough to enable or disable the respective constraint. In off-grid systems, where a significant amount of power is supplied by intermittent RES, the operating reserve is needed to guarantee system stability even if forecasts are inexact. The EMS has to ensure that the running units can cover the goods demand if the supply by intermittent RES is not available and the real load consumption is higher than the forecast one. The parameter $\widetilde{\varphi}$ is similar to φ but it describes the worst-case scenario, where intermittent RES supply is underestimated and highest feasible good consumption is considered.

$$\widetilde{p}_{t,i,g} \leq P_{i,g}^{rate} \qquad \forall t \in T, i \in U, g \in G_i^p \tag{4.16}$$

$$\widetilde{p}_{t,i,g} \leq y_{t,i} P_{i,g}^{rate} \qquad \forall t \in T, i \in U^{loadmin}, g \in G_i^p \tag{4.17}$$

$$\widetilde{c}_{t,i,g2} \geq m_{i,g1,g2,pw} \cdot \widetilde{p}_{t,i,g1} + q_{i,g1,g2,pw} \cdot y_{t,i} \quad \forall t \in T, i \in U, g1 \in G_i^p, g2 \in G_i^c, pw \in PW_{i,g1,g2} \tag{4.18}$$

$$\widetilde{\varphi}_{t,g} + \widetilde{P}_{t,g} + \mu_{t,g} \geq \widetilde{C}_{t,g} \quad \forall t \in T, g \in G \setminus G^{storage} \tag{4.19}$$

$$\widetilde{\varphi}_{t,g} + (SL_{t,g} - SL_{t,g}^{min}) + \widetilde{P}_{t,g} + \mu_{t,g} \geq \widetilde{C}_{t,g} \quad \forall t \in T, g \in G^{storage} \tag{4.20}$$

Eq.s 4.16-4.18 define the production and consumption by programmable units in the scenario with $\widetilde{\varphi}$ in place of φ. The constraints defined by Eq.s 4.19-4.20 have the same structure of Eq.s 4.5-4.6 and guarantee that the available units, modulating the production and consumption, can face the worst case scenario. In addition to the units production, goods provided with a storage can use an amount of previously stored good to meet the operating reserve constraint.

Battery modelling

Another key aspect of the proposed approach is the battery behavior description. In optimization problems the battery is usually considered in a simplistic manner, neglecting its properties and limits. The three areas which would need more attention are:

- efficiency in different conditions
- kinetic constraints

- aging description

In the model, standard battery systems are represented as units which put in communication the goods DC and $DC_{storage}$, as shown in Figure 4.2. The good DC is not storable and includes other appliances working in DC, as PV systems, while good $DC_{storage}$ is storable with a maximum storage level equal to the battery capacity.

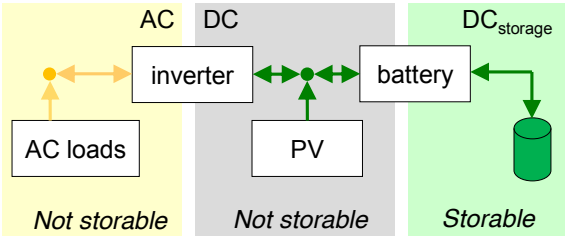

FIGURE 4.2: Battery modelling in multi-good model

The multigood model enables to describe the battery as a standard unit and hence a piecewise linear function can be implemented without further complications. In order to not increase the computation time, the efficiency has been formulated as a function of the only discharge or charge power, neglecting the effect of the temperature and the SOC.

Practically, during discharge, the battery consumes energy from $DC_{storage}$ to produce power in DC and the opposite happens when the battery is charged. The value of energy consumed is higher than the value produced to take into account of energy losses. An example of how the efficiency curve looks like is reported in Figure 4.3. Notice that, in the chart, the efficiency in a certain point is proportional to the inverse of the slope connecting that point to origin of the two axes. Looking at the original function, we have that the efficiency from the value of 95% for low discharge power decreases up to 85% for maximum discharge power (100 kW in the example). This behavior can be represented in the MILP model using a limited number of lines (two in this case). Note that, since charge/discharge losses increase more than proportionally respect of charge/discharge power (Vergara, 2015), the efficiency curves are generally convex and they can represented without the need of binary variables.

Regarding the second point, we can not omit to model the kinetic constraints. In fact, if we do not consider them, solutions which are practically unfeasible could be found through the optimization. For this reason, the kinetic battery model (KiBaM) by Manwell and McGowan, 1993, which is also used in HOMER, has been implemented in the model. The main advantage of the model is that it can be implemented through linear equations, and thus it is not responsible for a relevant increase of computation time. This model splits the battery stored energy in two parts, one promptly available (SL^1) and one bound (SL^2), introducing an analogy with two fluid tanks separated by a conductance. The capacity ratio (c) is the ratio of the available energy tank volume respect to the total volume while the rate constant (k) is the conductance of the valve between the tanks. The values of the two constants are available for an extensive set of commercial batteries consulting HOMER libraries. According to the model, the dynamics of the two tanks are described by the following equations:

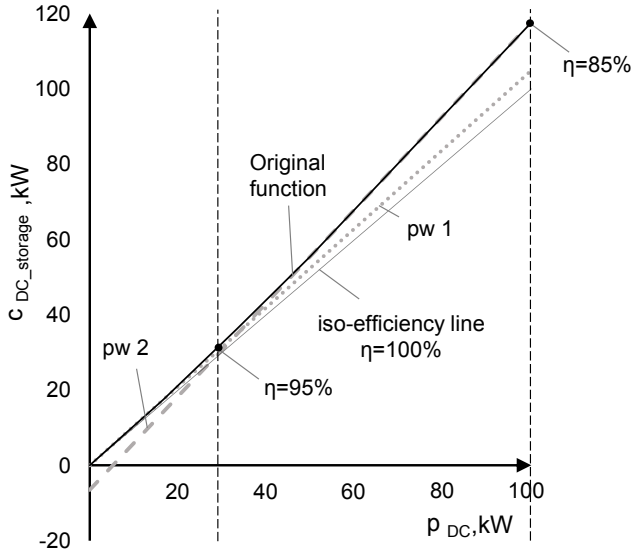

FIGURE 4.3: Discharge efficiency representation in the multi-good model with 2 lines.

$$SL^1_{t+1} = \beta_1 SL^1_t + \beta_2 SL_t + \beta_3 SL_{t+1} \quad \forall t \in T \tag{4.21}$$

$$SL^2_{t+1} = SL_{t+1} - SL^1_{t+1} \quad \forall t \in T \tag{4.22}$$

where

$$\beta_1 = e^{-k} \tag{4.23}$$

$$\beta_2 = c(1 - e^{-k}) \tag{4.24}$$

$$\beta_3 = \frac{1}{k}(1 - e^{-k} + c(k + e^{-k} - 1)) \tag{4.25}$$

The laws governing the battery kinetics impose an upper bound to the maximum charge ($p_{t,DC_{storage}}$) and discharge ($p_{t,DC}$) power, as described by Eq. 4.26 and 4.27 :

$$p_{t,DC_{storage}} + \leq \gamma_1 + \gamma_2 E^1_t + \gamma_3 E_t \quad \forall t \in T \tag{4.26}$$

$$p_{t,DC} \leq \gamma_2 E^1_t + \gamma_3 E_t \quad \forall t \in T \tag{4.27}$$

where

$$\gamma_1 = -\frac{cE^{max}}{\beta_3} \tag{4.28}$$

$$\gamma_2 = \frac{E^{-k}}{\beta_3} \tag{4.29}$$

$$\gamma_3 = -\frac{c(1 - e^{-k})}{\beta_3} \tag{4.30}$$

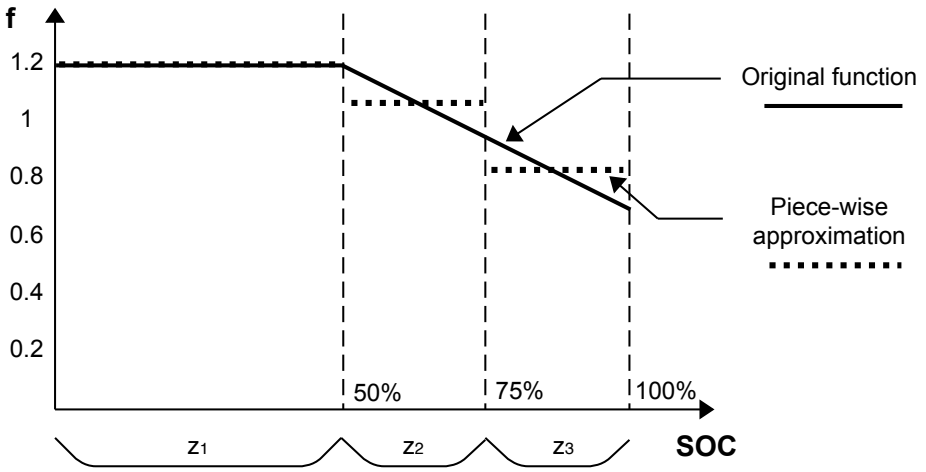

FIGURE 4.4: Aging factor (f) changing the SOC: original function (from Jenkins, Fletcher, and Kane, 2008) and piecewise approximation

Regarding the final point (aging process description), the weighted-Ah model proposed by Drouilhet et al., 1997 has been implemented in the model and successfully applied in the test-cases of this thesis to model the battery wear. The model concept is the following (B. Zhao, X. Zhang, Jian Chen, et al., 2013): one battery has a total energy throughput which can deliver until the end of its useful time. Some factors, as the cell temperature and the state of charge, can affect the total energy throughput. Considering only the effect of the SOC, we have that operations at low SOC accelerates the battery depletion and the same energy discharge affects more the total energy throughput if happened when the battery is almost empty. This is taken into account through a factor (f), which is function of the SOC and it is shown in Figure 4.4. The wear of the generic battery j can be hence described with the following equation:

$$c_{t,j,money} = p_{t,j,DC} \cdot \bar{c}^{wear} \cdot f(SL_{t,DC_j}) \quad \forall t \in T \tag{4.31}$$

where $\bar{c}^{wear}$ is the energy cost, calculated with Eq.2.1 and related to the reference conditions given by manufacturers. However, the function f is not convex and thus a piecewise approach is needed. Using a PW discrete steps (an example with 3 pieces is shown in Figure 4.4), the formulation is the following:

$$c_{t,j,money} \geq \bar{c}_j^{wear} \cdot f(j,pw) \cdot p_{t,j,DC} - M_j \cdot (1 - z_{t,j,pw}) \quad \forall t \in T, pw \in PW \tag{4.32}$$

This constraint is strict only when $z_{t,j,pw}$ is equal to one, otherwise the big-M value disables the constraint. The binary variable $z_{t,j,pw}$ is equal to 1 if the SOC is in the related interval. This is modeled with the following equations:

$$z_{t,j,pw} \leq 1 + (SL_{j,pw}^{ub} - SL_{t,DC_j}) \quad \forall t \in T, pw \in PW \tag{4.33}$$

$$z_{t,j,pw} \leq 1 + (SL_{t,DC_j} - SL^{lb}_{j,pw}) \quad \forall t \in T, pw \in PW \tag{4.34}$$

$$\sum_{pw \in PW} z_{t,j,pw} = 1 \quad \forall t \in T, pw \in PW \tag{4.35}$$

where $SL^{ub}_{j,pw}$ and $SL^{lb}_{j,pw}$ are respectively the upper and lower bound values which describes the pw-th interval.

4.1.3 Test-case example

In this section an example of how the multigood model works is reported, applying it to the configuration described in Figure 4.5.

The power supply is provided by a WT, a PV plant and an ORC which produces AC power consuming medium temperature heat. The thermal power can be produced by both Fresnel collectors and a biomass boiler: the Fresnel collectors produce heat when direct solar radiation is available while the biomass boiler is a programmable unit and the only constraint is the availability of a sufficient amount of woodchips. Woodchips can be previously produced by the chipper and stored in a dedicated tank. The ORC is the only controllable unit producing AC power and it guarantees in each time step the grid power balance with the assistance of a lead-acid battery, connected to the DC bus. A thermal storage allows decoupling heat and AC power production increasing the flexibility of the EMS. The community requires water and ice blocks which are produced by an icemaker, consuming water and AC power during its operation. The goods properties are reported in Table 4.1.

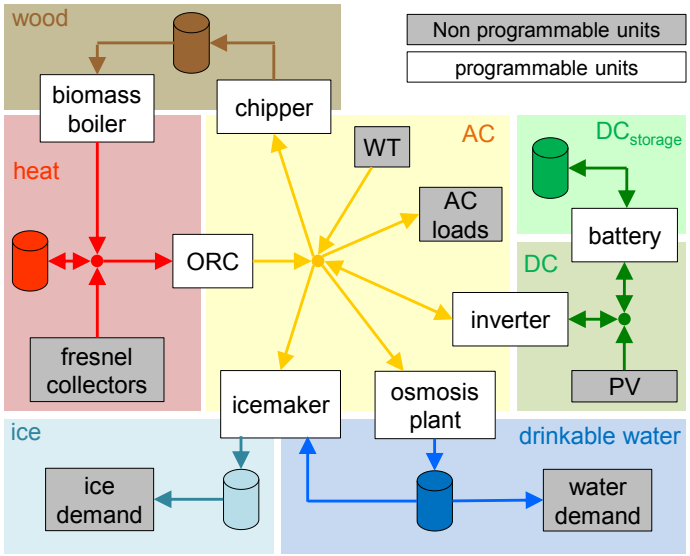

FIGURE 4.5: MG framework of the test-case (Mazzola, Marco Astolfi, and Ennio Macchi, 2015a)

In this case, differently from the other cases reported in Chapter 5 is not possible to make a comparison with other approaches since none of the strategies proposed in literature is able to manage a grid with several goods, a variety of programmable units and multi input/output

TABLE 4.1: Test-case goods properties (Mazzola, Marco Astolfi, and Ennio Macchi, 2015a)

Good		**Storage**	**SL (t=0)**	$\mathbf{SL^{min}}$	$\mathbf{SL^{max}}$	$\boldsymbol{\vartheta}$
AC	kWh	No	-	-	-	-
DC	kWh	No	-	-	-	-
$DC_{storage}$	kWh	Yes	300	35	350	0%
Water	m^3	Yes	14	0	25	0%
Heat	kWh	Yes	1500	0	3000	1%
Ice	kg	Yes	150	0	1000	2%
Woodchips	kg	Yes	1800	0	3000	0%

components. Hence, the analysis is limited to the optimal operation of the whole system obtained using the multigood model. The time horizon is equal to 24 hours and the forecasts are exact. The optimal operation of all the units over two-days is reported in Figure 4.6.

The first day is sunny and windy and the PV plant, the WT and the Fresnel collector supply a large amount of power, while in the second day most of the power is provided by the biomass combustion.In the first day, the ORC is immediately switched on because of the fixed AC consumption for public and domestic uses. The battery is slightly discharged during the following hours but the SL level remains above the minimum threshold (35 kWh) avoiding excessive storage depletion. Forecast information about the Fresnel contribution during the day and the trend of fixed AC loads are available and the EMS runs the ORC only for two hours exploiting the available stored heat without switching on the biomass boiler. During the central hours of the day the Fresnel collector produces a large amount of thermal power and the ORC is switched on again to avoid heat storage saturation and energy dumping. The programmable AC loads are scheduled in those hours to shave the energy flux to the battery. The battery is filled by intermittent generators PV and WT production up to 80%. At this point the EMS discharges the heat storage to operate the ORC with the aim to minimize the energy fluxes through the battery and to limit its wearing. The heat stored during the day is not sufficient to fuel the ORC during the nocturnal hours and the biomass boiler is switched on the 21^{st} hour. This unit runs almost until the end of the two days, minimizing the number of start-ups and working, when it is possible, at partial load with a higher efficiency. During the biomass operation the woodchips are gradually consumed and the chipper is switched on to fill the tank again.

In the second day the energy supplied by intermittent energy sources is not relevant and the biomass boiler runs the whole day to provide heat to the ORC. Both the biomass boiler and the ORC modulate their power to follow the load, limiting the use of the battery. Consequently, the heat storage remains almost empty until the 14^{th} hour when the EMS starts to increase the boiler load because it is aware of the future forecast. The small contribution of WT in the nocturnal hours of the second day results in the necessity of filling both the heat storage and the battery. In this manner, the EMS is able to guarantee a sufficient available

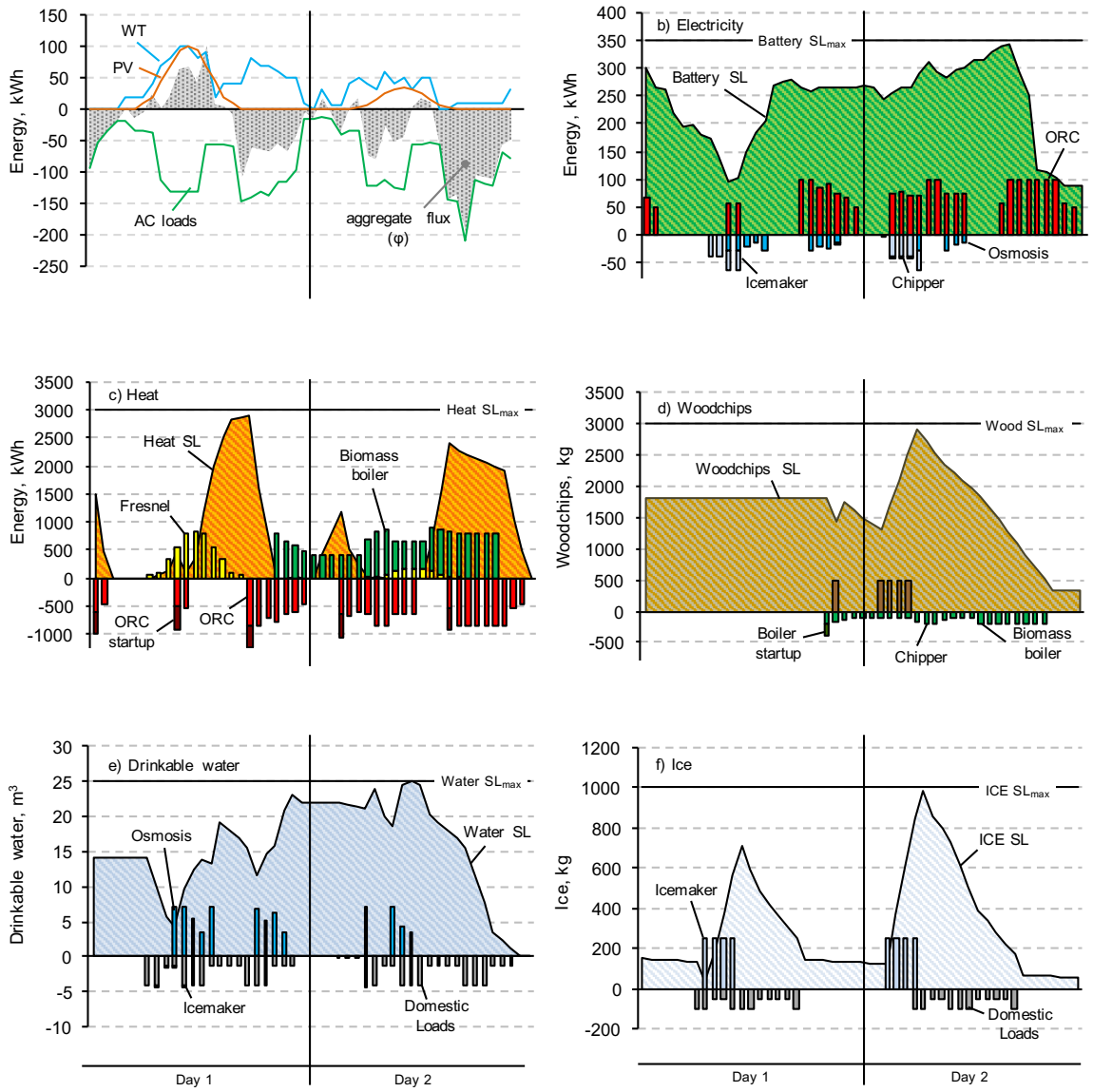

FIGURE 4.6: Hourly trend of the SL for each storable good in addition with the production and consumption by all units related to that good. Electricity diagram includes AC, DC and $DC_{storage}$ goods. (Mazzola, Marco Astolfi, and Ennio Macchi, 2015a)

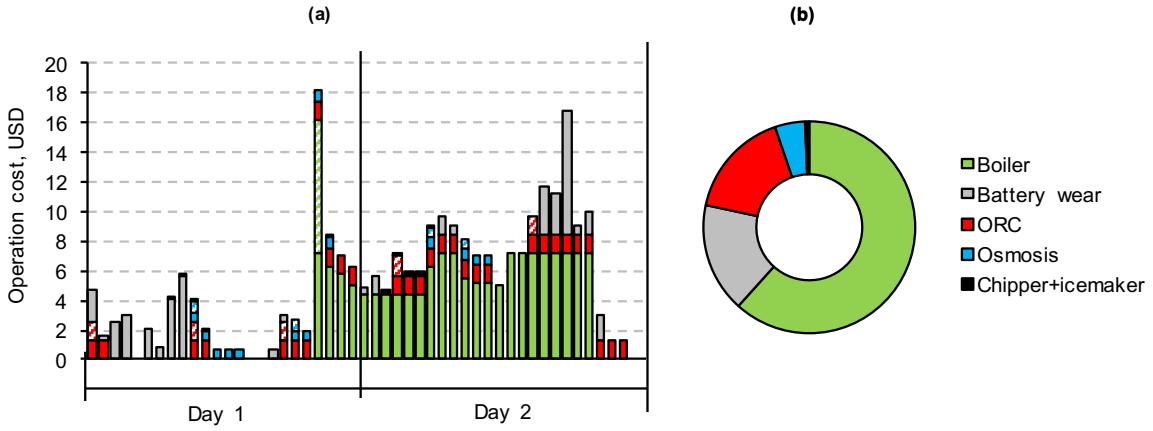

FIGURE 4.7: (a) Hourly trend of monetary cost related to operation (solid fill) and start- up (pattern shaded) of each programmable unit. (b) Cost share over the whole timespan. (Mazzola, Marco Astolfi, and Ennio Macchi, 2015a)

energy in the following hours when the AC loads are higher and the biomass boiler is not enough to satisfy the thermal load of the ORC.

The scheduling of the reverse osmosis plant and the icemaker highlights the advantages related to the multigood approach. In fact, considering the two goods separately and not as a singular deferrable electric consumption, allows decoupling the icemaker and osmosis plant operation. The EMS exploits this possibility, scheduling these two units in different hours in the central hours of day in order to shave diurnal power peaks and to obtain an operational cost reduction.

The operating costs resulting from the optimized management of the MG are reported in Figure 4.7 (a-hourly data and b-aggregate cost over two days). Pattern shaded and solid fill data refer to start-up and operation costs respectively. More than 60% of the total cost is related to the boiler operation because the wood consumption cost is allocated to the biomass boiler instead of the chipper. This assumption is due to numerical reasons and it allows finding the solution with a reduced computational time and without any effect on the veracity of the results. Finally, Figure 4.7.a highlights as the battery wear cost is extremely low for many hours during the two-days simulation proving the capability of the proposed approach in limiting the fluxes through this component.

To summarize, this test-case shows that complex MG configurations can be handled by the multigood model. Synergies between different components can be highlighted and this will be shown in the last two chapters, where the multigood model is used to perform long-term simulation of advanced configurations.

4.2 Long-term simulation and design optimization

The multi-good model described in the previous section is expected to be used in real operation to manage a MG, promising to achieve sensible cost saving compared to non-predictive strategies. However, if properly included in a simulation framework, it can be used to determine a priori the performance of a certain MG over a long-term horizon and to compare options with different technologies and components sizes.

4.2.1 Simulation framework

The simulation framework proposed is shown in Figure 4.8. Three main steps are defined:

- Input data definition
- Rolling-horizon simulation
- Output calculation

In input data definition step all the data needed for the long-term simulation are gathered. First, the goods considered in the MG simulation have to be defined. For the goods which have a contribution by non-programmable units, the yearly profile has to be evaluated starting from historical data or location info. In the same way the forecast pattern have to be defined: real forecast datasets are the best option, but, if not available, forecast pattern can be obtained starting from the actual data and applying an error. Finally, for each unit making part of the MG, all the relevant properties (both technical and economic) have to be defined.

When all these data are finally available, the simulation can start. It is based on multiple calls of the multi-good model according to the rolling horizon approach. If the forecasts are perfect, the actual MG operation corresponds to the UC output. When the forecasts are not perfect, an auxiliary routine which adjusts the initial schedule is needed. Fractions of year (as representative weeks) can be considered to reduce the computation time.

Once the simulation is performed, its output can be managed to evaluate indexes which represent the MG overall performance. These can include economic parameters (as the net present value (NPV) or the levelized cost of electricity (LCOE)) and others indexes which capture other aspects, as the renewable penetration and carbon dioxed emissions.

The whole process is used to assess the performance of a single MG configuration. However, when the final objective is to find the best MG configuration among all the possible options, the simulation framework has to be called several times (one for each option). For this purpose, we can proceed in two different ways. The first and more intuitive approach (which is part of the family of the enumeration methods) is to select a limited pool of configurations to be tested and perform the simulation for each one of them. In the end, it is possible to select the most promising one respect of a certain global objective function, which is the output of the simulation (e.g. the net present value).

The other possibility is to use a black-box algorithm which, looking at the output of the simulation, changes the design variables in order to reduce the global objective function. Even

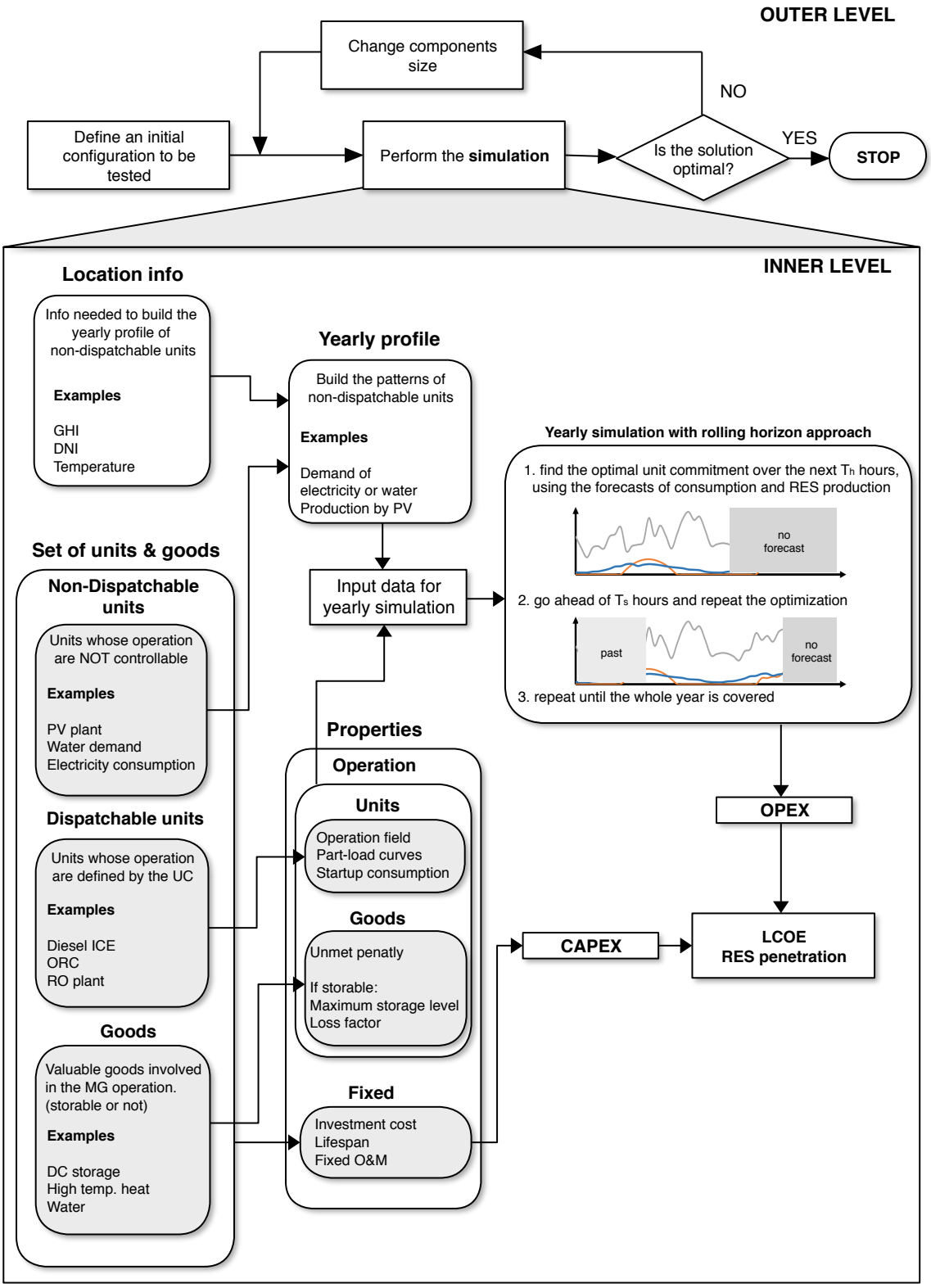

FIGURE 4.8: Overview of the hierarchical design optimization approach

in this case, we have an iterative approach but the configurations to be tested are chosen by an algorithm.

Thanks to its nature, the second approach is expected to find an optimal solution in a shorter time span, because it is not going to explore all the possible combinations. On the other hand, there is always the possibility that the optimizer gets stuck in a local optimum, which is a point that is optimal compared to the neighboring solutions but it is not the global optimum looking at the whole variables space. For the test-cases presented in the last chapters an enumerative approach has been used to find the optimal design. The final objective in those cases was not to find the optimal solution as quick as possible, but to obtain a good description of the objective function trend changing the design variables to highlight useful insights about MG design in general.

In the following sections a focus on the input data definition methodologies and the output indexes is presented. Finally, a comparison with other approaches finalized to MG design and simulation is reported.

4.2.2 Input data

Consumption patterns

Consumption time series are a key input to perform the yearly simulation. For simulations based on the multi-good model, a consumption pattern for each good is needed. Two options are available: (i) historical data and (ii) synthetic data.

Historical data are, without any doubt, the best option in terms of reliability. Using real data, collected during previous measurements, ensures that all the simulation are based on the best available representation of the reality and thus the resulting insights in terms of system design are more valuable. However, historical data are not always available. For example, in rural areas which are not electrified, we do not have the possibility to obtain any previous measurements. Even in cases where electricity is already there, hourly or sub-hourly time series could not be available for the lack of proper measurement procedures. In other cases, such as space heating or irrigation, only rough estimation data (for example average monthly demand) are often accessible.

In these cases, models able to generate synthetic consumption patterns are the only option. For the electricity demand, we have the possibility to start from some assumptions about the single device or class of device to build the daily pattern using models available in literature. In the work proposed by Mandelli, Merlo, and Colombo, 2016, different models able to generate a daily profile are shown. Using a set of input data (type of electrical appliances or user class, number of users, nominal power rate, functioning time and functioning windows), the models build a realistic daily profile, which is the sum of the consumption for each single appliance or user class. Water daily consumption for agriculture is another important consumption value which has to be considered, especially in the case of rural areas. In this case the Braney-Criddle equation, described in detail in Allen et al., 1998, is a very valuable tool: it allows to evaluate the water daily requirement for each crop, starting from some general info, as average temperature, monthly precipitation, wind speed and solar radiation. Finally for other goods

demand, as potable water or sanitized heat water, there is the possibility to derive the pattern from similar ones in other locations. For example, for potable water consumption, one option is to consider the water consumption in a certain area coming from other detailed studies [2] and resize it in order to be coherent for the case in study.

RES production profiles

The model needs weather forecast depending on the type of generators installed on the MG. These are needed to evaluate the contribution of non-programmable units, i.e. the units whose output is not controllable by the EMS as PV and the CSP solar field[3]. Usually data are required for wind speed, solar irradiation, ambient temperature and rivers flow rate if hydro power systems are installed. These data can be obtained from different sources in literature like NREL, Energy plus weather and PVGIS databases[4] which provide, for each location, a representative year considering historical data collected in several years. Usually, data are available with a hourly discretization and they are obtained with different techniques like time series analysis with the aim at obtaining a realistic year able to catch the peculiarities of the site.

Unfortunately, for many sites hourly data are not available, in particular in those contexts which can be interested by the installation of a standalone grid. In rural regions of developing countries only average monthly data are available. A lack of data is noticed for wind speed (often the height of the probe is not declared) and for water flow rate of river which often have a seasonal or ephemeral behavior. In these cases different strategies can be adopted with the goal to define synthetic weather data. These methodologies have to respect not only the global quantities for each period but they must guarantee a sufficient variability of the energy sources profiles from one day to another (but even in the same day) in order to test the system flexibility and stability on extreme conditions. In fact, the use of average smooth profiles is not of interest for the operation, the stability and the reliability of a MG which must be able to face random sources. Different approaches for the generation of reliable synthetic weather data are available in literature for solar radiation (Graham and Hollands, 1990, Aguiar and Collares-Pereira, 1992) and wind velocity (Carapellucci and Giordano, 2013).

Once the weather data are available, the production yearly profile can be built considering the properties of the RES-based system. The best option in this case is to use a simulation tool, as SAM [5], able to evaluate the yearly time series. Once the weather data is loaded in the software, SAM is able to produce the energy yield for most of RES technology, starting from an extensive library of commercial models. For CSP solar field, SAM gives even the

[2] From the report Funk and DeOreo, 2011 is possible to derive hourly trend of water consumption of a developed country divided by sector (households, industry, public)

[3] CSP systems are modeled with 3 components: (i) the solar field (which is not controllable) which produces heat in relation to the weather data, (ii) the power block (which is controllable) and (iii) the thermal energy storage

[4] NREL - data available on SAM
Energy plus weather - Date of access: 23 June 2016 - URL `https://energyplus.net/weather`
PVGIS - Date of access: 23 June 2016 - URL `http://re.jrc.ec.europa.eu/pvgis/`

[5] SAM (System advisory model) is a free software developed by the NREL (National Renewable Energy Laboratory)
Date of access: 23 June 2016 - URL: `https://sam.nrel.gov`

auxiliaries consumption related to the circulation pump; in this cases this contribution has to be added to the electricity base load for a better representation of the case.

4.2.3 Rolling horizon

The yearly simulation is conducted using the rolling horizon approach, already described in detail in 3.1.3. The most important steps are:

1. obtain the forecast of consumption and RES production for the next T_h hours
2. evaluate the optimal unit commitment
3. follow the UC schedule for T_s hours
4. go back to point 1, until the whole year is covered

In real operation, it is very likely to perform the unit commitment using all the available forecast range, usually between one to few days. In addition to this, optimization can be repeated very frequently, following the frequency at which the forecasts are updated.

In the simulation, this is not always the best approach. In fact, simulating one entire year using long T_h and short T_s could result in computational times not suitable for design scope. The time horizon T_h increases the complexity of single UC call, which has to solve a problem with a higher amount of variables and constraints; the T_s increases the frequency at which the single UC is solved, resulting in a higher number of optimization problems to be solved. On the other hand, limited T_h and large T_s are expected to entail an increase of the objective function and, hence, of the operation costs.

This aspect is clearly shown from the results reported in Table 4.2. This reports the effect of different T_h and T_s on the computational time and the operation costs. The data have been obtained from different simulations of the test case described in Chapter 7, made by a huge number of goods (7) and programmable units (9) (see Figure 7.4 for the detailed system description).

The results confirm the expected trends. The total computation time is strongly related to the T_h and T_s of the simulation. The most accurate simulation, performed with $T_h = 30$ hours and $T_s = 2$ hours, has a computation time which is compatible with real operation (less than 1 minute per UC call) but not appropriate for simulation (more than 3 days). A decrease of T_h and an increase of T_s lead to considerable decrease in computation time. On the other hand there is an increase of the operation costs found in the simulation, which are usually limited to few percents compared to the reference case. Only when the time horizon is limited to 12 hours, there is a strong increase of the operation costs obtained during the simulation due to the high presence of unmet demand.

Another possible option to be considered to reduce computation time is the use of variable time-steps. This means that the whole time horizon is not covered with time step of the same length (1 hour usually), but time steps with variable length can be used. In particular, the time-step can be progressively increased (for example from 1 hour to 6 hours) to cover the same time horizon with a reduced number of time steps (see example in Figure 4.9). As a

TABLE 4.2: Computation time and operation costs obtained for the same configuration simulated with different T_h and T_s. In bold the reference case

T_s	**T_h**	**UC calls**	**Single UC complexity**	**Computation time**	**OPEX**	**ΔOPEX**
hours	hours	number	# variables × # constraints	minutes	kUSD	%
2	12	4380	1032 × 1321	94	1004	3.79%
6	12	1460	1032 × 1321	34	19574	>100%
12	12	730	1032 × 1321	16	266706	>100%
2	18	4380	1548 × 1971	336	986	1.91%
6	18	1460	1548 × 1971	133	988	2.17%
12	18	730	1548 × 1971	64	1005	3.88%
2	24	4380	2064 × 2631	1428	974	0.67%
6	24	1460	2064 × 2631	510	979	1.17%
12	24	730	2064 × 2631	287	984	1.72%
2	**30**	**4380**	**2580 × 3281**	**3915**	**967**	-
6	30	1460	2580 × 3281	1345	972	0.5%
12	30	730	2580 × 3281	675	978	1.06%

result, the near future is described with high accuracy while the farthest forecasts, which affect less the present, are taken into account in an aggregate form. In order to do this, problem formulation has to be rearranged to consider time steps with different lengths.

In Table 4.3 the results coming from simulations with different variable time steps patterns are reported. The simulation are performed with the same configuration and test case already used for Table 4.2, with a $T_h = 24$ hours and $T_s = 12$ hours.

The results coming from Tables 4.2 and 4.3 suggest that there is the possibility to reduce considerably the total computation time accepting a lower accuracy in the final results. Even if the qualitative trends are expected to be similar for different cases, the error in the OPEX evaluation can be considerably different changing the case in study. For example, if storages which act on a weekly base are considered it is likely that time horizon higher than few days could be required. For this reason, an analysis of the problem and a sensitivity analysis is required at the beginning of test case study to understand which is the combination of T_h,T_s and variable time-step pattern entailing the best trade-off between computation time and accuracy in cost estimation. In the example, accepting an operation cost increase of around 3%, it is possible to reduce the computation time from 3915 minutes to 49 minutes., using $T_h = 24$ hours, $T_s = 12$ and the variable time-step pattern reported in the last row of Table 4.3.

TABLE 4.3: Computation time and operation costs obtained for the same configuration simulated with different variable-time step patterns (with T_h=24 hours and T_s=12 hours)

Time steps per class			**Total time-steps**	**Computation time**	**OPEX**	**ΔOPEX**
1 hour	4 hours	6 hours	#	minutes	kUSD	%
24	0	0	24	287	984	-
20	1	0	21	164	990	0.62%
16	2	0	18	95	994	1.04%
12	3	0	15	56	1001	1.72%
18	0	1	19	110	996	1.23%
12	0	2	13	49	1007	2.32%

4.2.4 Output indexes

At the end of the simulation, the results obtained are elaborated to obtain indexes which summarize the techno-economic performance of a particular configuration. The cost of a configuration has two components: the up-front costs (CAPEX), the fixed operation and maintenance costs ($O\&M^{fixed}$) and the operation costs (OPEX).

The CAPEX is the sum of all components investment costs (see 4.36). In order to compare investment with different lifespans, the investment cost of each component is annualized using the Capital Recovery Factor (CRF), a function of the interest rate and of the expected lifespan of the component. The resulting equation is:

$$CAPEX = \sum_{j \in J} C_j^{inv} \cdot CRF_j = \sum_{j \in J} C_j^{inv} \cdot \frac{i(1+i)^{LS_j}}{(1+i)^{LS_j} - 1} \tag{4.36}$$

where j is the generic component, C_j^{inv} is its investment cost and LS_j is its expected lifespan.

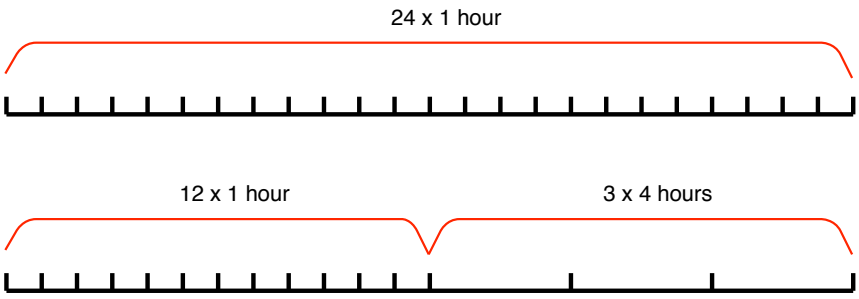

FIGURE 4.9: Standard hourly pattern (24 time steps) and example of variable time steps pattern (15 time steps) covering a 24 hours time horizon

Since the terms in Eq. 4.36 do not depend on the simulation results, CAPEX is not a function of the simulation. The only exception is the battery: as already mentioned previously, the battery lifespan is strongly related to how it is operated, being a function of the power discharge and the SOC (see 4.1.2). The amount of annual life loss (LL) related to the battery can be evaluated using the following equation:

$$\mathrm{LL_{batt}} = \frac{\sum_{\mathrm{t\in Y}} \mathrm{c_{t,batt,money}}}{\mathrm{C_{batt}^{inv}}} \tag{4.37}$$

where the numerator represents the yearly wear cost, made by the sum of the hourly wear cost ($\mathrm{c_{t,batt,money}}$) over the year (Y is the set containing all steps in the yearly simulation). The ratio of yearly wear cost over the whole investment costs gives a proxy of the life loss per year, from which the lifespan is evaluated:

$$\mathrm{LS_{batt}} = \frac{1}{\mathrm{LL_{batt}}} \tag{4.38}$$

Together with the installation cost, fixed operation and maintenance costs ($\mathrm{O\&M^{fixed}}$) have to be considered. These represent the annual expense to maintain a certain component, regardless of how much time the component is operated during the year.

$$\mathrm{O\&M^{fixed}} = \sum_{\mathrm{j\in J}} \mathrm{C_j^{O\&M}} \tag{4.39}$$

where $\mathrm{C_j^{O\&M}}$ is the annual O&M expense for the component j.

Finally we have annual operation cost, which is the output of the simulation. According to the nomenclature introduced in 4.1.2, it is defined by the following equation:

$$\mathrm{OPEX} = (\sum_{\mathrm{t\in Y}} \mathrm{C_{t,money}} + \sum_{\mathrm{t\in Y}} \mathrm{C_{t,money}^{startup}}) \tag{4.40}$$

which is the difference between total monetary cost and battery wear cost, already taken into account in the CAPEX. Note that the term OPEX takes into account variable O&M, start-up costs and the monetary expenses for fuel provision (diesel oil for standard off-grid microgrids and biomass, if a biomass-based system is present).

The total yearly expense (also called ANPC [6]) is hence defined using the following equation:

$$\mathrm{ANPC} = \mathrm{CAPEX} + \mathrm{OPEX} + \mathrm{O\&M^{fixed}} \tag{4.41}$$

The configuration with the lowest ANPC is the one which entails the minimum overall cost, taking into account operation, maintenance and initial investments. The ANPC can be normalized dividing by the total energy delivered by the system. The resulting index, the levelized cost of electricity (LCOE), is a measure of the average total cost of a unit of delivered energy:

[6] Annualized Net Present Cost

$$\text{LCOE} = \frac{\text{ANPC}}{\text{Yearly} \quad \text{energy} \quad \text{demand}} \tag{4.42}$$

Note that the denominator represents the total energy demand, and not the energy produced by the generators. This term is equal for all configurations referring to the same test case, allowing a fair comparison between different configurations. The production term can be considerably different from the demand, especially when intermittent RES are present. In fact, part of the energy produced can be wasted in curtailment and battery charging/discharging losses.

Finally, other indexes can be useful to assess how a certain MG configuration perform. An index frequently evaluated in the test cases of this thesis is the RES penetration, which is the share of energy coming fron renewable energy sources. Even in this case, we want to evaluate only the net contribution, neglecting the part of energy lost. The RES penetration is defined using the following equation:

$$\text{RESpenetration}_{\text{j}} = \frac{\text{Energy}_{\text{ref}}^{\text{diesel}} - \text{Energy}_{\text{j}}^{\text{diesel}}}{\text{Yearly} \quad \text{energy} \quad \text{demand}} \tag{4.43}$$

where the RES penetration for the configuration j is defined comparing the energy produced by diesel with configuration j ($\text{Energy}_{\text{j}}^{\text{diesel}}$) with the energy produced by diesel in the reference case, with only diesel generators ($\text{Energy}_{\text{ref}}^{\text{diesel}}$). Even in this case, the denominator contains the yearly energy demand.

4.3 Comparison with other approaches

The most common approaches defined in literature have been already described in Sec.3.2 of the previous chapter. The approach developed in this study can be included in the **simulation methods**: in these methods some important indexes depending on MG operation (i.e. operation costs, renewable penetration) are evaluated simulating its operation over time. Despite of other simulation methods proposed in literature, in this case the operation are not based on non-predictive strategies, but on the predictive one proposed in the previous section.

The main advantages are:

- **Optimal operation** - operation is based on the output of multiple UC calls instead of simple rules which do not look at the future. This leads to relevant cost savings, as shown in the next chapter (5).
- **Complex systems** - as shown in the test-case, the multi-good model allows to manage and test complex MG configurations, adding new degrees of freedom in the management. Relevant examples are shown in the two last chapters 6-7.
- **Realistic operation** - operations obtained are more realistic than the ones obtained by capacity planning methods. In fact, these ones assume that perfect forecast over a very long time span are available. The issue of cost underestimation in capacity planning methods is addressed in chapter (5).

- **Problem tractability** - when the number of goods and components increases the problem could become intractable using capacity planning methods. The proposed approach branches the main problem in multiple UC calls, easily solvable thanks to the use of variable time steps.

The main drawbacks related to this approach is the long computation time. Compared with other simulation methods, the computation time is considerably higher because of the multiple UC calls in the framework. The comparison with capacity planning methods has to consider two aspects: (i) the single instance (one year with a fixed MG design) is usually solved more quickly using the proposed approach, because many small problems are usually easier to be solved compared to a big one (the computation time is not linear); (ii) however, while in the proposed approach the yearly simulation have to be carried out for different MG configurations, for capacity planning methods only one call is needed to find simultaneously the optimal operation and the optimal MG configuration. A proper choice of parameters as T_h, T_s and the variable time-step pattern can help reduce the computation time. However, it is reasonable to use the proposed approach only after a limited pool of possible solutions have been found using average methods or simulation methods based on NP strategies.

Another possible application is the evaluation of the impact of forecast error on the MG operation. Capacity planning methods find the optimal configuration assuming that perfect forecasts are available over the entire year. This is not true in real applications and the proposed approach allows to estimate the cost increase related to different forecast accuracy. This feature will be further analyzed in the next chapter.

Chapter 5

The value of predictive strategies

In this chapter, the potential benefits related to the use of a predictive strategy are investigated. Applying the methodology described in the previous chapter, a comparative analysis between predictive strategies (PSs) and standard non-predictive ones (NPSs) is conducted, quantifying the potential cost saving related to the use of forecasts and optimization.

As reported in the chapter about the state of the art, in literature there are different models which apply the unit commitment to the management of a MG, but in any of them the cost savings attainable in comparison with standard strategies which do not rely on forecast are evaluated. Another important point is the effect of forecast error: all the studies about MG operation rely on the assumption that perfect forecasts are available, but what happens in real cases where the forecast are not perfectly accurate has not been studied yet. The problem has been studied for large grids: errors in generation and load forecast lead to pre-dispatch decisions which require real-time corrections, and it has been widely shown that the impact of forecast errors on total operation cost could be relevant (Valencia et al., 2015; Delarue and D'haeseleer, 2008; Ruiz et al., 2009; J. Wang et al., 2011). In the case of off-grid MG, where the forecast accuracy is expected to be lower, this effect could even be greater, having implications on both operation and design.

This chapter aims to investigate the previous mentioned factors. In this first section, PS and NPSs will be tested on a 2-day test-case to show how differently they perform under the assumption of perfect forecasts. In the second section, the PS and NPS are applied in a different test-case in which the impact of forecast errors is considered.

5.1 Performance of predictive strategies

In this section the main differences between operations based on PS and NPSs will be shown, showing how differently they perform in a 2 days test-case.

5.1.1 Test-case overview

The MG configuration used in the test-case is characterized by the presence of non-programmable RES producers, namely a PV plant and a WT (both of them have a nominal power of 100 kWel), the AC loads for domestic consumption and a small reverse osmosis plant which satisfy the potable water demand and can be used as programmable load (Figure 5.1(A)). The trends

of the electricity generated and consumed by non-programmable units is reported in Figure 5.1(B).

Simulations are carried out on a 48 hours timespan and it is possible to notice that the first day is characterized by a large production by RES, in fact the PV plant reaches its nominal power output and the WT operates with a high average power. On the other hand, the second day is representative of a cloudy day with a low wind speed. The AC loads are higher in the morning and during the night because of public lighting and domestic appliances use. The grey shaded area represents the resulting aggregate energy flux through the battery (φ) if programmable units are not used. Minimizing the extent of these fluxes allows reducing the battery wear and the energy losses in charging/discharging process and it is implicitly accounted for by the objective function of the EMS problem.

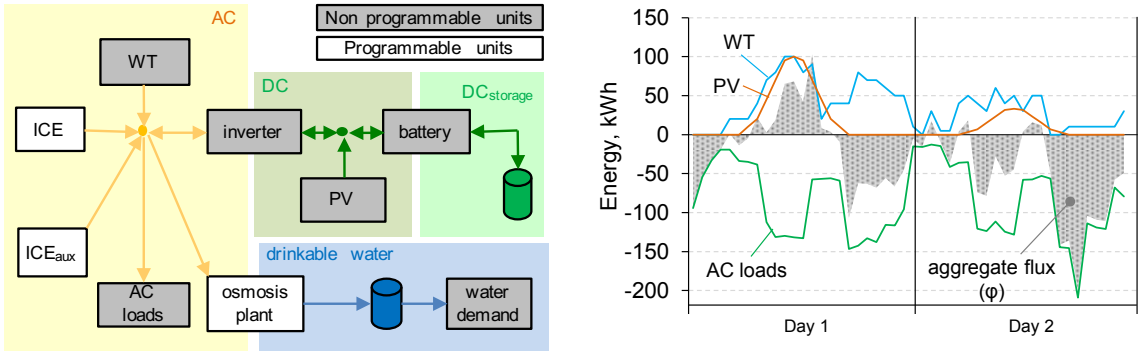

(A) MG configuration (B) Hourly pattern

FIGURE 5.1: (A) MG configuration according to the multigood model and (B) hourly contribution of non-programmable units (PV, WT, AC loads) and the resulting aggregate net flux. (Mazzola, Marco Astolfi, and Ennio Macchi, 2015a)

Two identical programmable generators are available: the first one (ICE) is used as primary generator while the auxiliary one (ICE_{aux}) is switched on only to avoid battery depletion or power shortages. The rolling horizon strategy is based on a 24-hour time horizon updated every hour (T_h =24 hours and T_s =1 hour according to the notation used in Figure 3.2).

The operation cost to be minimized by the EMS problem is formed mainly by two terms: (i) ICE operation cost due to O&M the fuel and (ii) the battery wear due to discharge. In addition, a penalty term proportional to the difference between a reference storage level (SL) and the actual SL at the end of day has been added.The reference SL is equal to the maximum one among the different strategies. The monetary value of the energy stored in the battery is set equal to 0.2 \$/kWh, which is the price of a kWh of electricity generated by Diesel ICE working in nominal condition and stored in the battery. This additional term allows a proper comparison between dispatch strategies having different SL at the end of the simulation and it is required only for short-term simulations. In fact, if a whole year is considered the effect of different final battery levels on the overall solution is negligible. Finally, the comparison between the different dispatch strategies have been carried out under two different assumptions: (i) neglecting the start-up penalizations and (ii) considering them

as an additional cost for the first hour of operation. In the start-up cost two terms are considered: (i) a consumption of the input goods without any useful effect and (ii) a monetary cost due to component wear and O&M (see Appendix A.3 for all the details).

The PS has been investigated under two different assumptions: the first one can use the two generators, while in the second one, only the primary ICE is available. This approach is compared with the five different heuristic dispatch strategies considered: the LF and four CC strategies with different battery Set Point levels. The minimum SOC level of the battery is a parameter of great influence since the same battery operation at a lower storage levels results in higher wear cost. On the other hand, working at high SOC may lead to battery saturation and energy dumping. For each heuristic strategy, the minimum SOC is optimized with a relevant operational cost decrease, especially for the LF approach, which tends to manage the battery close to the minimum SOC level.

5.1.2 Results

The operative costs for all the investigated strategies are reported in Figure 5.2 where it is possible to appreciate the cost reduction attainable with the PS. Without considering start-up penalization of the components, the PS reaches a cost reduction of 9.61% in comparison with the most cost effective NPS (LF strategy). Considering start-up penalizations, the cost saving of PS increases to 13.09% in comparison with the CC-SP=50% strategy which becomes the most cost effective among the NPSs. In fact, the start-up impact is higher in LF because of the high frequency of start/stop affecting ICE schedule.

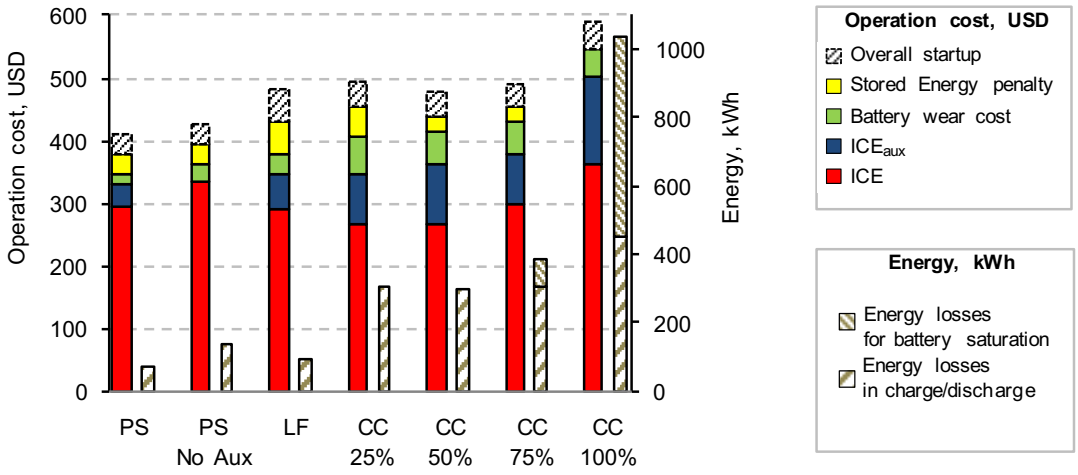

FIGURE 5.2: Comparison of cost and energy losses over the two-day simulation between the dispatch strategies under consideration. (Mazzola, Marco Astolfi, and Ennio Macchi, 2015a)

These results can be explained considering the differences of unit scheduling and battery use for the different strategies. Results are reported in Figure 5.3 for the PS with one or two ICEs, for the LF and for the best CC among those investigated.

The following observations can be addressed:

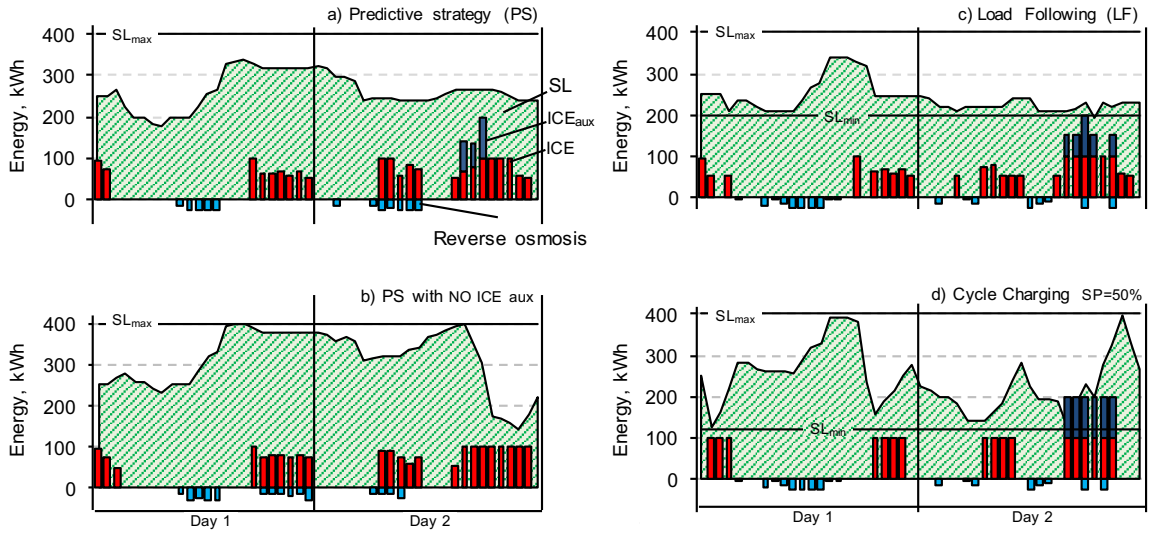

FIGURE 5.3: Hourly contribution of programmable units (ICE, ICE_{aux}, reverse osmosis plant) and battery SL for the dispatch strategies under consideration. (Mazzola, Marco Astolfi, and Ennio Macchi, 2015a)

- Both the PS (with and without auxiliary ICE respectively) and the CC approach limit the number of start-ups and shutdowns for the ICE generator. The LF approach requires seven start-ups instead of four and three times the generator is operated for just one hour leading to high overall start-up costs.

- The PS is the only one able to fulfill the electricity demand without using the auxiliary ICE. In this case, the EMS is able to modify the schedule to cover the demand with a slight cost increasing (3.2% addressable to a higher wear of the battery the second day). The battery is charged to a higher SL since the first hours of the days to satisfy the operating reserve. During the last hours of the second day the ICE is switched on and it runs close to its nominal load even if the battery SOC is about 100%. This allows storing energy in the battery during the evening to be released during the nocturnal hours when the ICE generator is not able to cover the whole demand. This farsighted operation cannot be scheduled by any of the heuristic dispatch strategies, because it requires the use of forecasts of future power production and consumption. For this reason, besides obtaining a not negligible cost saving during operation, the PS leads to investment cost reduction during the design and the sizing of MG. In fact a better use of the available units avoids the need to oversize the power generation set or the battery system.

- CC strategies work always at full load and the average ICE efficiency is equal to 34.2% (the nominal one). In load following the average efficiency is lower (30%) because of the frequent part load operation of the generator. In the PS, instead, where the ICE load in each hour is the result of an optimization process, the average efficiency is equal to 32.3%. A value slightly higher is attainable if no auxiliary ICE is available because the generator is operated at full load for a longer number of hours.

- The auxiliary ICE (if available) is used by all the strategies at the end of the second day to avoid the total discharge of the battery. The CC strategy since it cannot control the generators power output operates the generator at its nominal load for six hours until the battery is full. LF is able to reduce the number of hours of operation but it entails two start-ups. Finally, the PS based configuration runs the ICE_{aux} for only three hours at reduced loads with evident economic benefits.

- Battery state of charge trend changes appreciably from one case to the others. The trend of the energy fluxes trough the battery is reported in Figure 5.4 for the three different strategies with the respective curves of cumulative absolute energy handled by the battery. In CC strategies, the battery wear cost is on average higher than in all the other cases because it is frequently used with a total processed energy three times higher than in the other cases leading to a relevant loss in charging/discharging process. Furthermore, the average hourly absolute flux is close to 35 kWh entailing a high wear of the battery compared to LF and PS showing an average value of 11 and 9 kWh respectively. This problem is reduced in both the PS and the LF strategies where the usage of the battery is reduced and a small part of energy is lost in the charging/discharging process

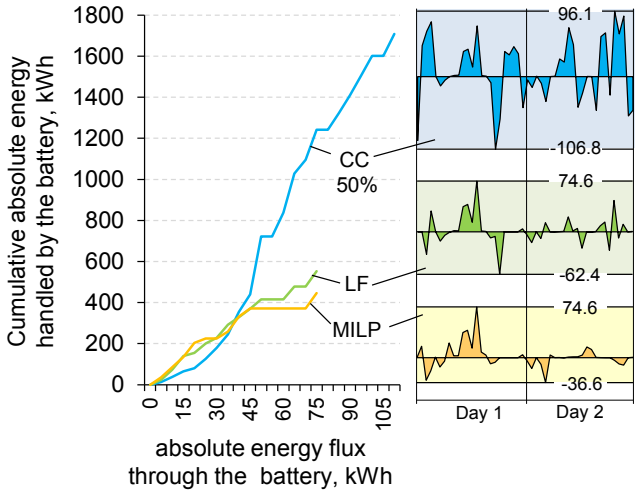

FIGURE 5.4: Cumulated energy processed by the battery under a certain energy rate. (Mazzola, Marco Astolfi, and Ennio Macchi, 2015a)

As a conclusion, the farsighted operation of programmable units allows a better exploitation of the RES and a limited wear of the battery. The advantage is greater if start-up penalties are considered because, in this test-case, partial load operation of programmable units is more advantageous than their intermittent use.

5.2 The effect of forecast error

The potential benefits of the PS have been highlighted in the previous section, showing that relevant cost savings can be achieved using forecast and optimization. However, the previous test-case is focused on the operation related to a single configuration during only two days and it is not representative of the MG behavior over an entire year. In addition to this, the forecast of loads and RES production are assumed to be perfect, giving a great advantage to the PS. In this section, the impact of error in forecast is investigated, showing how the cost savings changes according to forecast accuracy.

A meaningful comparison between operation strategies has to be grounded on a reasonable estimation of how the system would operate in reality when the strategy is followed. For this reason, the performance of the dispatch strategies considered in this test-case are evaluated with reference to the same test-case, consisting on a yearly simulation with 1-minute time step of an off-grid MG provided with a battery energy storage system (BESS), two internal combustion engines (ICEs) and a photovoltaic generator (PV). The chosen time step enables an adequate representation of the short-term power fluctuations from the PV generator, while at the same time prevents an explicit representation of frequency and voltage dynamics, with the consequent savings in computational burden.

5.2.1 Analysis framework

Regarding NPSs, the most used dispatch strategies (Load following (LF) and cycle charging (CC)) are considered. Since a very small time-step is used in the simulation, a 15 minutes minimum running time for each generator start-up is imposed in order to avoid very frequent start-ups. Under the assumption that the MG control system can make dispatch decisions every minute based on knowledge about the present state of the system, the benchmark simulation of these two strategies is straightforward.

Regarding the PS, contrary to the NPSs, it is not realistic to assume that the optimization problem is solved minute by minute during operation for two different reasons:

1. the computation time could not be compatible with this kind of application, especially for multigood MGs with a high number of units

2. PV and load forecasts may not be available or be too expensive at this update frequency

For these reasons, in real applications, the unit commitment (UC) is called with a certain frequency (e.g. 15 minutes or 1 hour) to obtain the schedules of the generators, the battery and the schedulable loads (if available). In this work, the operation strategy of the PS are simulated using a rolling-horizon strategy with T_h =24 hours, T_s =15 minutes and a variable time steps pattern (8 of 15 minutes, 22 of 1 hour) to reduce the computation time. The PV forecasts are updated every 3 hours (a reasonable value for real applications) whilst load forecasts are updated every 15 minutes.

After each execution of the UC, the real MG operation is simulated starting from the set-points obtained from it, until the next UC call. If forecasts are exact, the working condition of each component in the MG will be exactly the same as the schedule. When the forecast

are not perfectly accurate, starting from the optimization output, another algorithm, called Real Operation (RO), adjusts the operation on 1-minute step basis to cope with deviations from the data in the forecast (see Figure 5.5 for an outline of the analysis framework). The RO algorithm follows these rules:

- If at least one ICE generator is on, it will balance the net load variation adjusting the power in the feasible operation range (minimum and maximum power).
- If no ICE generator is on or the available power variation is not sufficient due to the power limits, the battery will balance the remaining net load
- In the end if not even the battery is able to balance the fluctuation due to feasible operation constraints (kinetic constraints, maximum charge/discharge power or empty/full energy capacity) the remaining variation is dumped or accounted as unmet load.

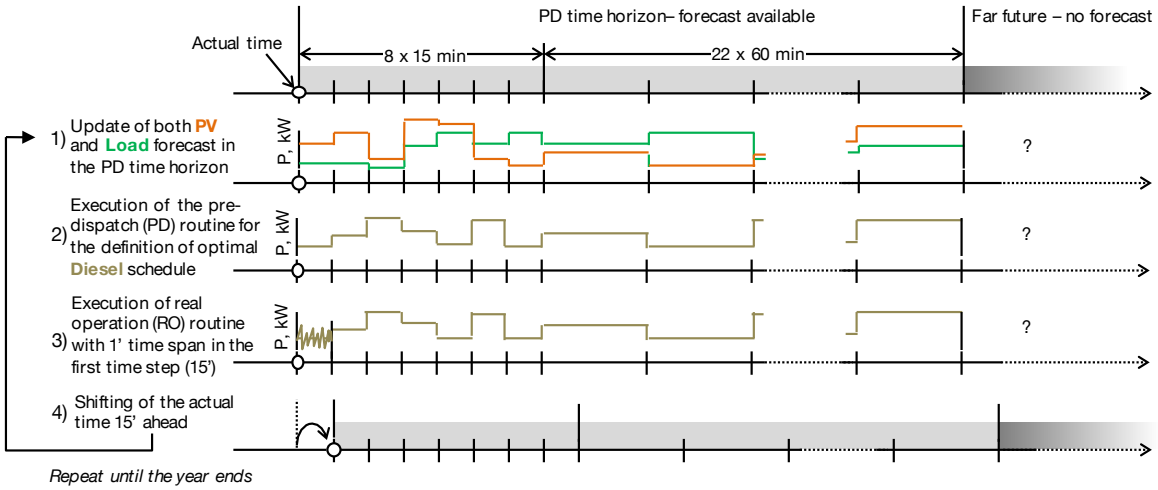

FIGURE 5.5: Predictive strategy (PS) simulation scheme, including RO algorithm. (Mazzola, Vergara, et al., 2017)

5.2.2 Test-case overview

For the purpose of this study, we consider a village of 600 households. Electricity is provided by two differently sized ICE generators, PV panels and a battery energy storage system (BESS). These elements connect to AC and DC buses, which exchange power by means of a bidirectional inverter. The relevant parameters of these equipment are listed in Table 5.1, and are representative of lead-acid batteries and bidirectional inverters technologies used for off-grid applications. Regarding the parameters of ICEs (see Table 5.2), we rely on public data sheets of commercial diesel models. Start-up costs, which are usually not provided by manufacturers, are assumed to be equivalent in terms of consumption to 2.5 minutes of rated power operation, as suggested by Barley and Winn Dennis Barley and Byron Winn, 1996.

[1]The capacity ratio and the rate constant describe the kinetic behavior of a battery according to the kinetic battery model developed by Manwell and Gowan Manwell and McGowan, 1993. See 4.1.2 for further details

Properties	Symbol	UM	Value
Charge/discharge efficiency	η^+/η^-	%	85
Capacity ratio[1]	c	-	0.28
Rate constant	k	1/h	1.85
Battery wear	$\bar{c}^{wear}$	USD/kWh	0.23
Inverter efficiency	η^{inv}	%	95
Rectifier efficiency	η^{rect}	%	90

TABLE 5.1: BESS and inverter properties. (Mazzola, Vergara, et al., 2017)

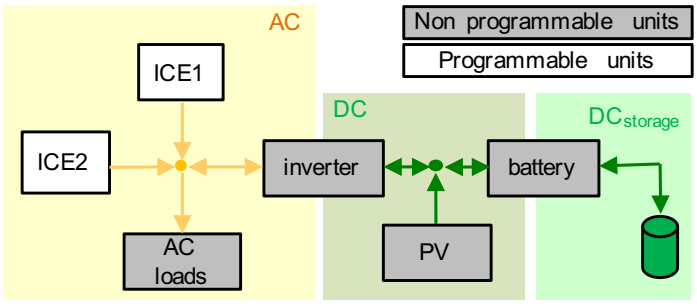

FIGURE 5.6: MG configuration according to the multigood model

PV resource estimation

To obtain a realistic time-series for the electricity produced by the PV panels, one year of data from a PV facility, located at the Instituto de Investigación Tecnológica in Madrid, are used, scaling it to match the size of the PV array in the village. This choice allows to use for the simulations very detailed data, with a 1-minute sampling time, which are generally not available in rural areas.

	Power		Fuel consumption		
	kW		l/h		l
	Rate	Min	Rate	Min	Start-up
ICE1	13.5	1.35	4.24	1.00	0.18
ICE2	20.6	2.06	6.10	1.42	0.25

TABLE 5.2: Internal combustion engines properties. (Mazzola, Vergara, et al., 2017)

Load estimation

Load trends definition relies on Universal Energy Access Research Group experience in rural electrification. The electric load of the village are synthetically generated by means of a probabilistic appliance ownership and utilization model, which results in an individual load profile for each building with one minute time resolution and for an entire calendar year.

The eligible appliances are LED lights, television, phone charger, and fans. This set of appliances is commonly found in low-income rural villages with some level of electricity access electricity access. In terms of their operation, there are time restrictions in accordance to the expected pattern of use for each appliance, except for the fans, whose operation is linked to the ambient temperature. Also, the lights are enabled when the total solar irradiance is below a certain threshold. Within these restrictions the model then chooses randomly, with prescribed variability, the actual times when the appliance is turned on. These individual load profiles are then aggregated into a single one and used for the simulations. In Figure 5.7(A) the synthetic power consumption patterns for the days of the year with minimum and maximum energy consumption are shown.

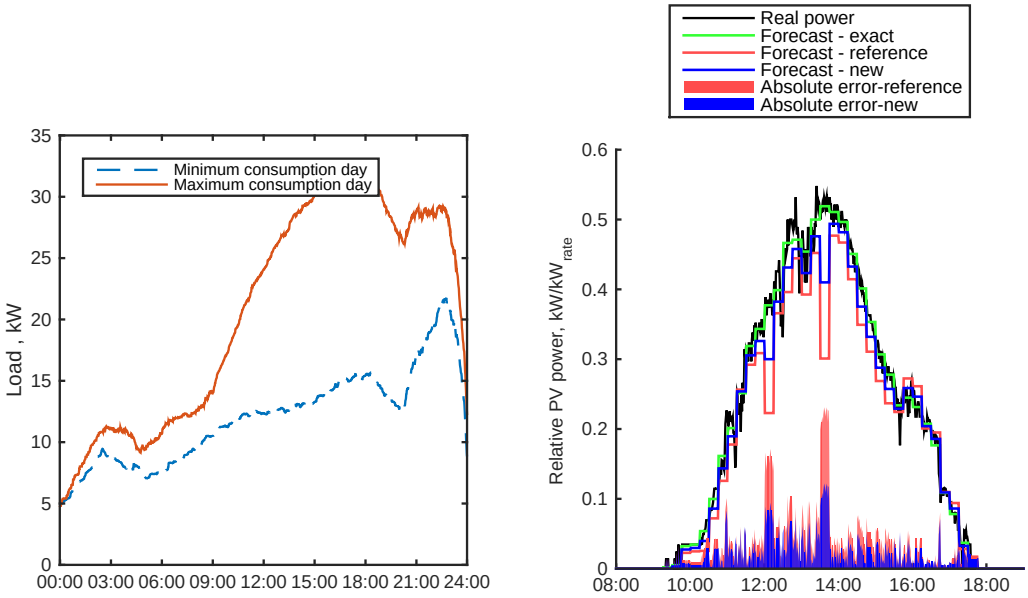

(A) Daily power consumption (B) Forecast generation example

FIGURE 5.7: (A) Power consumption patterns for two representative days of the year, the hottest and the coldest and (B) generation of new (worse) forecast for a day using 2 as correction coefficient. (Mazzola, Vergara, et al., 2017)

5.2.3 Forecast characterization

Since the objective of the study is to relate the value of forward-looking optimization to forecast accuracy, in this section the methodology to represent forecasts of different accuracies is described. The accuracy of the forecast is represented using the Normalized Root Mean

Square Error (NRMSE), which is one of the most common metrics to assess PV forecasts accuracy IEA-PVPS, 2013. It is defined as:

$$\mathrm{NRMSE} = \frac{\sqrt{\frac{1}{n}\sum_{i=1}^{n}(\widetilde{x}_i - x_i)^2}}{x_{max}} \tag{5.1}$$

Where x_i and $\widetilde{x}_i$ are the measured and the predicted values for sample i, and n is the total number of samples.

Reference data sets

The reference data set of PV forecast is a set of real forecasts obtained from a commercial provider for a facility in IIT Comillas, Madrid. The original data set consists of 35040 different forecast time series (each one was made available on the provider's server every 15 minutes) each covering a time horizon of 24 hours with 96 forecast values, each corresponding to 15 minutes. Regarding loads, and in the absence of available house-level representative time series, a data set of load forecasts has been evaluated starting from the load time series generated with the process described in 5.2.2. The prediction for each time step corresponds the average of the past year's power consumption at similar times. More specifically, the load forecast at hour h of a certain day is set equal to the the average of the power consumption at the same hour h of the other days of the year with similar temperature and irradiation.

Generation of forecast time series of various accuracies

In this section the method to generate synthetic load and PV generation forecasts of different accuracies starting from the reference ones is described. First, for each single forecast value the error with respect to the perfect forecast is evaluated; then, this error is multiplied by a correction coefficient (see Figure 5.7(B)) and a new forecast time series is created adding the new error time series to the real data one. By choosing a value greater than 1 for this coefficient, the error will increase, leading to a worse forecast. The opposite happens for values under 1, reaching the perfect forecast for 0. The final result is a new data set that preserves the error pattern but has a different NRMSE.

5.2.4 Application of the simulation framework

In Figure 5.8 an example of how the PS is simulated is reported, considering both EMS and RO routines. In both cases the colored areas represent the dispatch calculated by the EMS using the unit commitment, and the lines are the results of the corrections by the RO algorithm. The two cases differ in forecast qualities: on the left the case with exact forecast, on the right one case with erroneous forecasts for both loads and PV power. Note that, in the latter, the predictions underestimate PV production and slightly overestimate the load during the middle of the day and underestimate it during the night.

During the first part of the day (until 9:00) the MG operation is similar for both cases: the small size ICE (ICE1) modulates its power to ensure the energy balance while ICE2 is off, presumably as a consequence of the lower efficiency it would have at low power output.

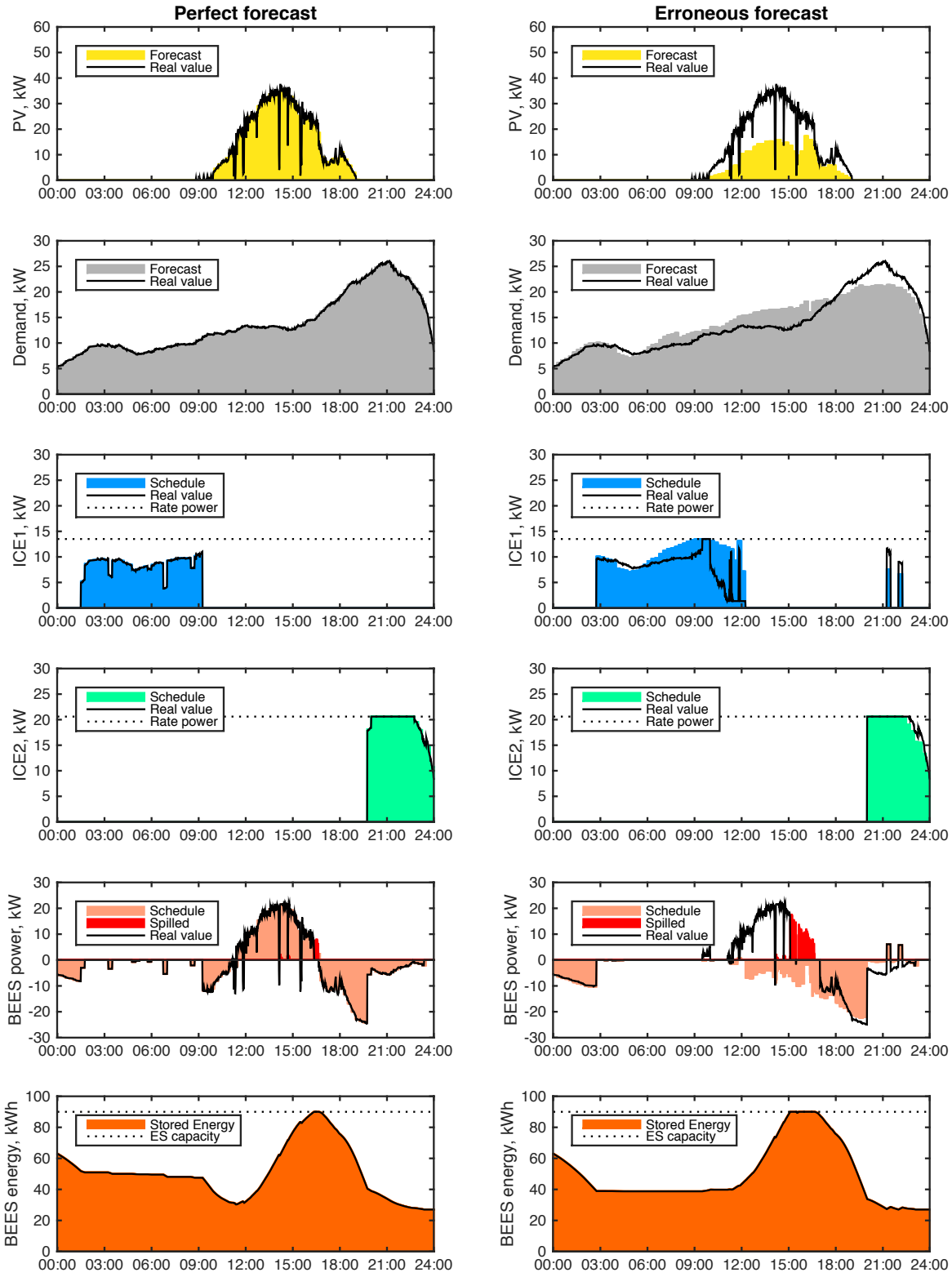

FIGURE 5.8: Real operation during one example day. (Mazzola, Vergara, et al., 2017)

Starting at 9:00, there are two different behaviors: in the case with exact forecast, ICE1 is switched off and the battery is partially depleted, hence with capacity to absorb the PV energy production in the midday. In the case with erroneous forecast, the underestimation of the PV power leads the EMS to keep ICE1 on for other 3 hours (until 12:00) with the two following consequences: (i) the battery is not sufficiently depleted and a considerable amount of "free" PV energy is spilled (14.6 kWh, which is 8.6% of the total PV energy production of the day); (ii) ICE1 is forced to follow the load, but, because of the overestimation of loads, this entails part load operation (<25% of rate power) with related lower efficiency.

During nocturnal hours, the ICE2 generator is switched on to cover the peak. In the case with perfect forecast, this is sufficient to match the load until the end of the day, in combination with a small depletion of the BESS. In the case with erroneous forecast, ICE2 is switched on later (30 minutes) and ICE1 is forced to two additional start-ups (with related start-up costs) in order to prevent unmet load.

5.2.5 Results

In previous sections, the methodology used to simulate the MG operations with erroneous forecast has been defined, together with the data sets that will be used. Now, the annual operational costs obtained by simulating the hybrid MG described in 5.2.2 are obtained with four approaches:

- non-predictive strategies (NPS)
  - load following (LF)
  - cycle charging (CC)
- predictive strategy (PS) with 24 hours time horizon
- one shot unit commitment (OS-UC), consisting in the application of the unit commitment with a time horizon of 8760 hours, hourly time steps and perfect forecast.

The first three strategies have been already described. The last one represents the approach commonly used in Capacity planning methods, already presented in Sec.3.2.3. The costs related to the OS-UC approach are evaluated for two reasons: (i) it offers the most optimistic solution in terms of MG operation cost assuming perfect knowledge of one year ahead events and, for this reason, it can be used as a reference benchmark; and (ii), in the literature it is frequently used to evaluate the operational cost of a MG, as already mentioned in Sec.3.2.3.

It is important to remark that the OS-UC is not a dispatch strategy, but only a tool to assess operational costs over a certain time span, assuming perfect forecast. In fact, in real applications, it is not possible to have a perfect forecast for the whole year, and a realistic time horizon is limited to few days. Sub hourly fluctuations, limited time horizon and erroneous forecast lead in reality to a cost increase which is not actually accounted for by the OS-UC method.

All simulations are performed with a 12-core 2.6 GHz desktop computer with 32 GB of RAM. The optimization based approaches (PS and OS-UC) were simulated in a Julia environment, using Gurobi as solver for Mixed Integer Linear Programming (MILP) problems. The NPSs were implemented in a MATLAB environment.

Reference case - PV=60 kW, BESS=60 kWh

The first scenario considers the hybrid MG described in Section 5.2.2 in operation with a 60 kW PV plant and a 60 kWh battery. Results of the simulations for this specific case are reported in Figure 5.9.

For perfect forecast, the operational cost evaluated with the PS is only 0.4% higher than the one evaluated with the OS-UC. This suggests that, in this application, the knowledge of 24 hours-ahead forecast is sufficient to optimally manage the MG. The small increase in operational cost is due mainly to the sub hourly fluctuations (the time step for PS is 1 minute) which are not considered by the OS-UC. These results support that under the assumption of perfect forecast the OS-UC (which has a lower computational cost than the PS simulation) is a valid approach to assess long-term operation of a MG.

A comparison between the results obtained by the NPSs and the PS with perfect forecast shows a PS cost saving of 7.3% compared with CC (which is the best NPS in this case) suggesting that, in the ideal case with perfect forecast, the use of a strategy based on forecast is clearly advantageous for the system.

Regarding simulation with erroneous forecast, it is clear from Figure 5.9 that an increase of forecast error leads to an increase of operational cost for the predictive strategy. In the case of PV forecast, the effect is present but not very significant; going from exact forecast to a forecast with 60% NRMSE entails only a cost increase of 1.2%. The accuracy of load forecast has a greater impact. In fact, in the worst case considered (40% NRMSE), the operation cost was determined to be 5.3% higher than when perfect load forecast was used. This difference can be explained considering that the PS takes decisions on the base of the aggregate energy forecast trends within the time horizon. Error on PV forecast have a smaller impact than load ones because the total amount of energy within the time horizon is smaller and because for more than 12 hours a day (depending on the season) the solar radiation forecast is intrinsically exact since the sun is not shining.

As a consequence, in a scenario with forecast errors using OS-UC may lead to a considerable operation cost underestimation. In the worst case of forecast accuracy (PV NRMSE=60%, Load NRMSE=40%), the simulated operational cost is 6.6% higher than those obtained by the OS-UC method.

In summary, the comparison between the PS and the NPSs for this system shows that the PS allows achieving a considerable cost reduction if the forecast errors are small. For higher unpredictability of loads (i.e. small villages) the savings are smaller and probably not sufficient to justify spending resources in forecasts, measurement and automation. However, it is important to underline that, even with very considerable errors in forecast, the PS performs better than NPSs in this case.

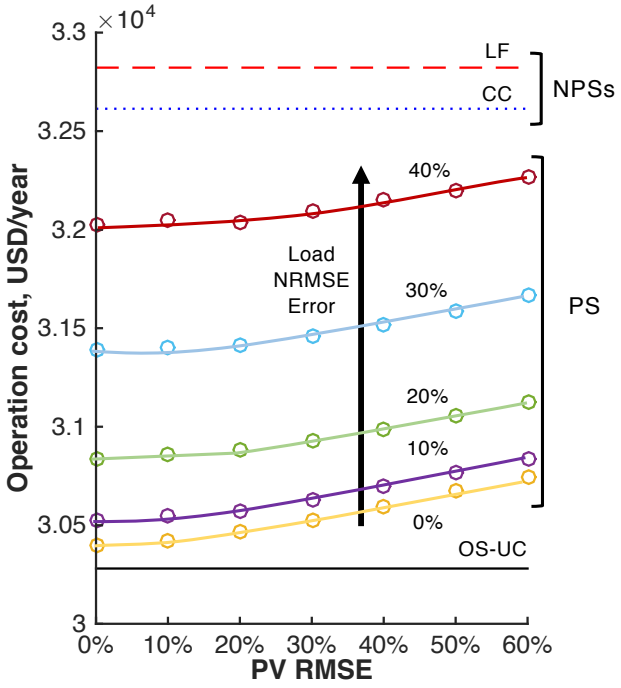

FIGURE 5.9: Yearly operation cost evaluated with different methods and assumptions: load following (LF), cycle charging (CC), one shot unit commitment (OS-UC) and the predictive strategy (PS) with different load forecast accuracy. (Mazzola, Vergara, et al., 2017)

Impact of MG configuration

With the results obtained for the reference case as the baseline, the same cost saving evaluation is performed with different PV and BESS sizes. Figure 5.10 depicts the relative cost saving of the PS compared against the best NPS for each combination of PV and BESS sizes. Excluding the case without a PV plant (row 1), the value of implementing a forecast based strategy increases on average by increasing the size of the PV, which can be related to the advantage of knowing about future PV production in preventing PV energy spillage. This rationale can be extended to expect that forecast-based methods will in most times perform better than non predictive dispatch strategies for systems with a high share of intermittent RES. The results show a similar trend with respect to the size of the BESS, arguably because larger storage begets a stronger coupling between present decisions and future events, a condition that only multi-period decision support tools can take advantage of.

The impact of the error in load forecast is relevant and present in each MG configuration: an increase of 10% of the NRMSE entails a reduction in cost saving from 1% to 2%, and hence has a noticeable effect on the total operation cost. These results suggest that there will be an economic advantage in load aggregation and deploying larger MGs to take advantage of better load forecast since the accuracy of load forecast is expected to increase as the number of households served increases (Sevlian and Rajagopal, 2014).

On the other hand, the impact of the PV forecast is related to the PV size. When the share of energy produced by PV increases, the solar forecast accuracy has a higher impact on the operational costs, in the range of 1-2% for configuration with PV size exceeding 60 kW. In

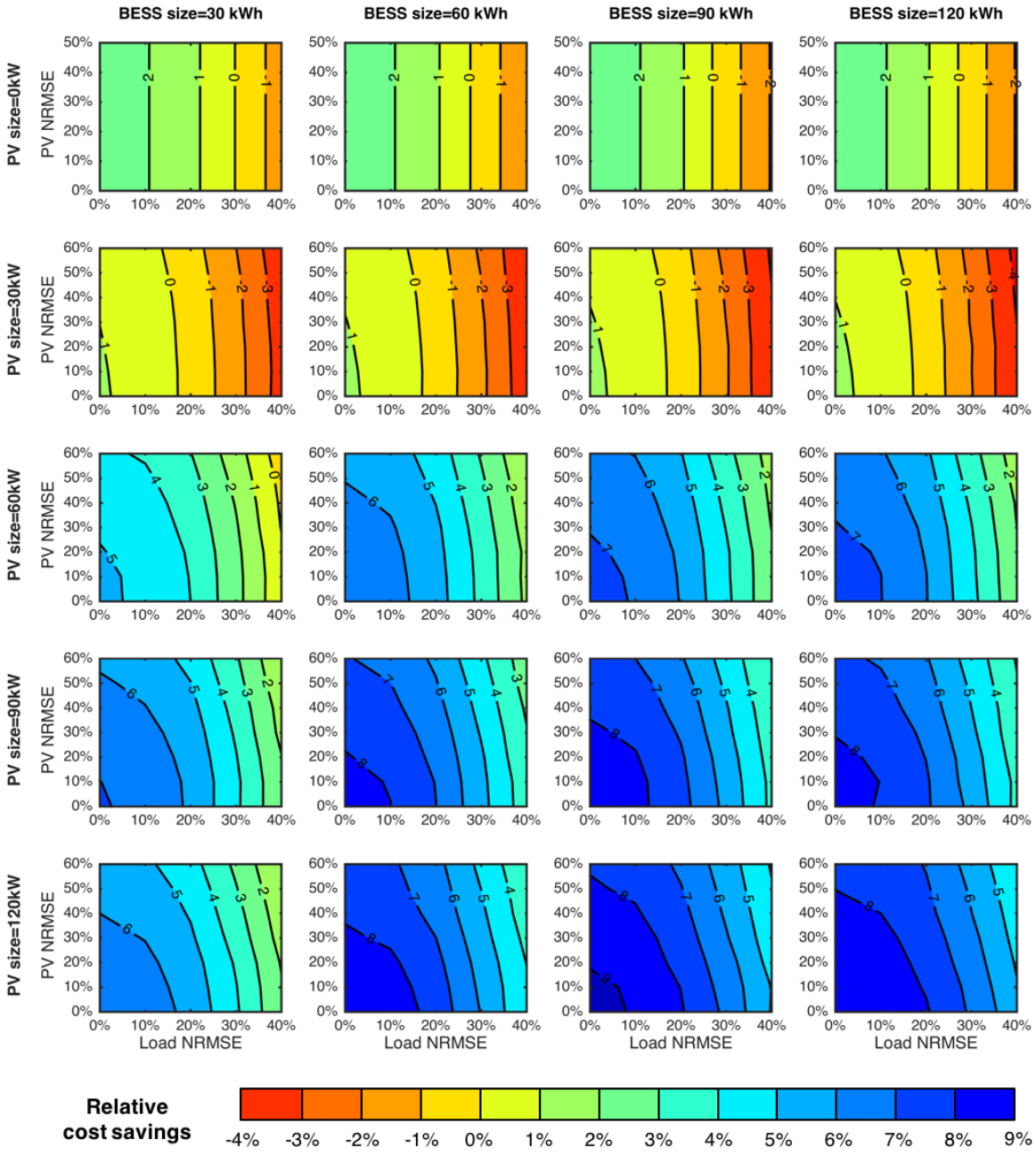

FIGURE 5.10: Relative cost saving of RH respect of best heuristic for different PV and BESS combinations. Positive values are relative cost savings, negative values relative cost increases. (Mazzola, Vergara, et al., 2017)

conclusion, for a MG in which PV forecast NRMSE is smaller than 20% and solar energy plays a relevant role (PV size greater than 60 kW corresponding to an installed capacity greater than 200 % of the peak load), a cost saving in the range of 4-8% is attainable using PS. In the other cases the cost saving is not so relevant, and under certain conditions (low load forecast accuracy and small PV), it is even possible to incur in an operational cost increase.

Design implications

As shown in previous sections, the dispatch strategy and the forecast accuracy assumptions lead to different operational cost. In this section, we'll show how the dispatch strategy selected for simulation affects the MG optimal design. For this purpose, the components sizes that, for each case (OS-UC, PS and NPSs), minimize the Annualized Net Present Cost (ANPC) have been found, assuming a discount rate of 9% and using the economic data summarized in Table 5.3. The design analysis has been conducted only varying BESS and PV sizes over a grid with a resolution of, respectively, 5 kWh and 5 kW. Note that, even if OS-UC is not a dispatch strategy, it has been considered in the analysis as benchmark and to evaluate its capability to find a optimal design which is practically efficient. Regarding PS, the accuracy of forecast has a considerable impact on operation costs. For this reason,the optimal design is evaluated using reasonable values of forecast accuracy (PV NRMSE=50%, Load NRMSE=10%) and, in addition, the ANPC is calculated for each optimal case with the assumptions of perfect forecast and very bad forecast (PV NRMSE=60%, Load NRMSE=40%). The four optimal MG configurations (one for each case) and the related economic performance of each strategy are those displayed in Figure 5.11.

	Investment	**Lifespan**	**Fixed O&M**
	USD/kW	years	related to investment
ICE	250	10	20%
Inverter	250	20	2%
PV	1100	20	2%
Lead acid BESS	180	8[2]	4%

Table 5.3: Economic assumptions for the ANPC evaluation. (Mazzola, Vergara, et al., 2017)

The lowest ANPC is found with the OS-UC approach, with a design consisting on a 70 kW PV plant and 60 kWh BESS. As expected, the perfect knowledge of future events favours solutions with high share of RES without the need of a huge energy storage.

However,a considerable cost increase is expected if this configuration is implemented and operated with the PS. This makes the solution suboptimal compared to optimal PS case,

[2]The value in the table is the maximum lifespan of the battery under the assumption of very limited usage. The real battery lifetime could be significantly lower according to the battery wear, which is calculated during simulation

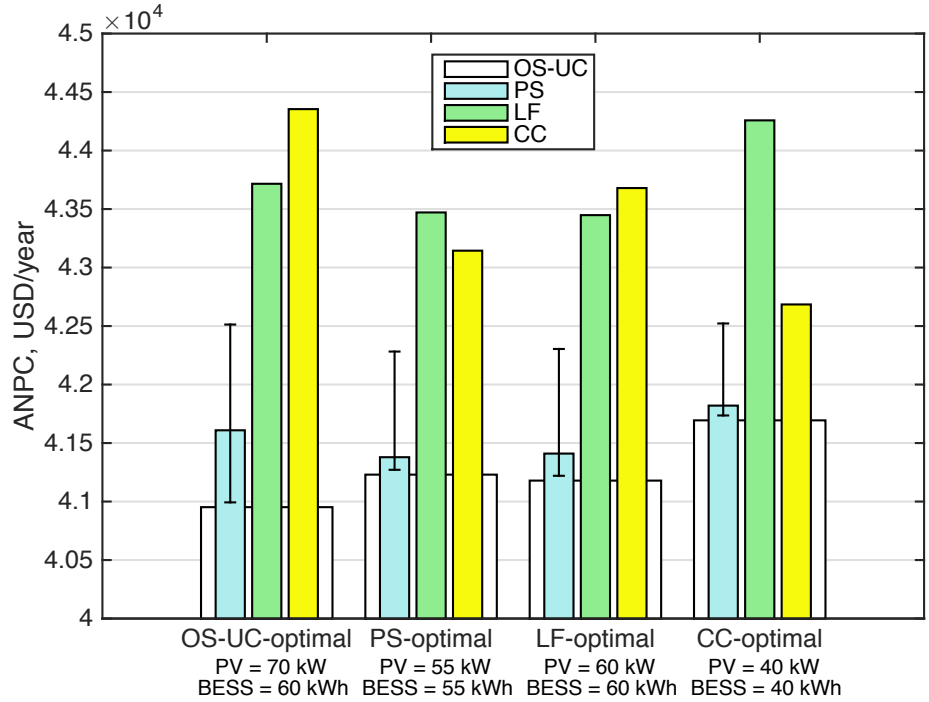

FIGURE 5.11: ANPC for four different MG configurations (each one found as optimum for one strategy) using different strategies. Different forecast qualities are used for PS, ranging from perfect forecast (lower bound) to bad forecast with PV NRMSE=60% and load NRMSE=40% (upper bound). (Mazzola, Vergara, et al., 2017)

which has slightly lower PV power (PV=55 kW BESS=55 kWh, which is the best solution found with PS).

On the other extreme is the CC strategy, where the lowest cost design has 40 kW PV and 40 kWh BESS. In this case, the use of a strategy which does not rely on forecast limits the RES share because it can not handle the unpredictable PV production.

Using LF strategy and PS results in very similar MG optimal design with component sizes between OS-UC and CC cases. However, differently from LF, PS takes advantage from forecast of PV and loads and it manages the generators and the battery with less inefficiencies resulting in a lower ANPC. Note that operating a MG with a NPS different from the one used in design always leads to a considerable cost increase, while the adoption of PS for the energy management system of an existing microgrid always results in a cost reduction, more or less considerable according to the forecast accuracy and the MG configuration.

5.3 Conclusions

In this chapter, the potential benefit of predictive strategies (PSs) compared to non-predictive ones (NPs) has been evaluated.

In the first section, the different strategies are compared on a two-days test-case, highlighting that predictive strategies (at least in the case of perfect forecast) are able to manage better the MG components, limiting the battery wear and reducing the generators startup.

In the second section, a framework which allows for a quantitative comparison between dispatch strategies not based on forecast and predictive ones has been proposed. Changing the forecast accuracy, the effect of the error in forecast for a test system lead to the following general conclusions.

Regarding MG operation, the cost savings attainable with the PS in comparison with NPSs are related to the accuracy of forecast and the MG configuration. The impact of error in load forecast is more relevant than the one related to PV, which becomes relevant only in MGs with big size PV plant. These results suggest that clustering a higher number of households could be favorable to reduce operational costs through a lower load forecast NRMSE. The advantage of the PS is higher for systems with a higher RES share and, assuming decent forecast accuracy (load NRMSE less than 10% and PV NRMSE less than 50%), a cost saving in the range of 4-8% is expected. The benefits of forecast based approaches could be even higher with more complex MGs, made by more and different dispatchable generators (i.e. biomass gasifiers) and including programmable loads.

Regarding MG design, different assumptions about how a MG will be operated can lead to different design choices. OS-UC is a good tool to obtain a first approximation but it leads to an underestimation of operational cost with respect to an implementation operated using imperfect forecasts. This leads to design choices with higher RES share and smaller BESS but a substantial cost increase can be expected when the MG is operated with PS (with imperfect forecast) or NPSs. The PS leads to a solution closer to NPSs ones and, even in design obtained with NPSs, shows good performance. This suggests the forecast-based approaches can be implemented in existing MGs with benefits in terms of operational cost reduction.

Chapter 6

Test-case 1: biomass exploitation in rural areas

In this chapter, the methodology proposed in this thesis is applied for the techno-economic analysis of a stand-alone hybrid MG serving a 2000 inhabitants community located in a rural area of Bihar (India). The benchmark MG is made by different generators and programmable loads, able to satisfy all the community needs (electricity, heating, domestic hot water, cooling and water for irrigation and domestic use). A large number of goods and programmable units has been intentionally considered to test the capability of the proposed methodology to handle such a complex system.

Diesel generators are the most common solution to power isolated MGs in rural areas, because they are relatively inexpensive and capable to follow the variable grid demand. However, they take along several significant disadvantages, as the high cost per served kWh and the emissions (see Section 2.3.1).The addition of generators fed by renewable energy sources (RES) could support or either replace the electricity generation based on fossil fuels, thus alleviating or even removing the above mentioned disadvantages. In sunny locations, a significant improvement to all these drawbacks can be achieved by adding a PV array to diesel generators (see Section 2.3.2). The non-programmability of these energy sources requires the adoption of an electric energy storage to properly dispatch energy entailing charge/discharge losses and higher capital costs.

On the other hand, the production of electricity (and heat when appropriate) is efficiently dispatchable when the primary energy source can be easily and economically stored as for biomass. For small scale application (below 1 MW), which are of interest in this case, gasification and combustion are the most promising options. A detailed description of the two technologies is available in Section 2.3.3.

Although wood biomass is abundant in vast regions of the world where there is a strong need of electricity and irrigation, in literature there are few studies analyzing its application in MG for rural electrification. Buragohain, Mahanta, and Moholkar, 2010 performed a feasibility study regarding biomass gasification for decentralized power generation in India. The potential cost saving related to biomass integration in a standalone MG, evaluated using an approach not based on the simulation of real operation, is relevant and higher than that one related to intermittent RES. Similar results have been obtained by Montuori et al., 2014, who evaluated the economic performance simulating the MG operation with a non-predictive dispatch strategy. Final results show that biomass gasification is far more convenient than

traditional supply by diesel generators. Ho, Hashim, and Lim, 2014 applied a Capacity planning method to a biomass-based MG, obtaining the optimal generator sizes taking into account weather variation and biomass availability. The biomass-based generators are present in the optimal solution obtained for a specific test case, proving the competitiveness of these technologies.

Even if economic feasibility seems to be proven by the above-mentioned publications, the impact of a biomass-based generator in the real operation of a MG has not been investigated yet. In fact, biomass based generators are generally treated as perfectly dispatchable generators, omitting start-up and ramp constraints and/or part-load efficiency during the simulation. Considering that these constraints would deeply affect the operation using a NPS, the methodology described in Chapter 4 has been applied adopting time-steps of 10 minutes: in addition to fast fluctuations of power and loads, the reduced time-step allows to properly consider ramp constraints and units start-ups obtaining a more realistic behavior of "slow" components as gasifiers and boilers. The increase in computation time related to a smaller time-step has been softened resorting to a rolling horizon approach with variable time-steps and simulating the MG operation for 15 days representative of the whole year.

6.1 Test case description

Despite of being one the fastest growing district of India, the rural area still suffers the lack of a reliable electricity access since 33.5% of villages are not electrified (Oda and Tsujita, 2011). A summary of the environmental and weather conditions of the village location, a description of the needs of the community and the proposed MG architectures are reported in following sections.

6.1.1 Climatic condition

Bihar is characterized by a humid subtropical climate and average meteorological data are reported in Table 6.1. Three main periods can be detected during the year: (i) the monsoon season, with high temperature, abundant rainfall and lowest solar potential (from June to September); (ii) the winter, with low temperature, dry climate and medium solar potential (from December to February); (iii) the pre-monsoon and the post-monsoon seasons, with high temperature, low rainfalls and the highest solar potential (from March to May and from October to November). The feasibility of generators based on intermittent RES, as sun and wind, is strictly related to the potential of the source. The wind potential in this region is very low and consequently wind turbine technology will not be taken into account in this work. On the other hand, the solar potential in the region is noticeable. According to NASA database, the yearly average potential is around 5.7 kWh/m^2/day with high average daily radiation during the whole year and the lowest values during the monsoon season because of the frequent presence of clouds.

[1]Global radiation on optimally tilted surface

TABLE 6.1: Climatic data (minimum temperature average, maximum temperature average, rainfall and global radiation) of Patna district, India

		Winter			**Pre-monsoon**			**Monsoon**			**Post-monsoon**		
		Dec	Jan	Feb	Mar	Apr	May	Jun	Jul	Aug	Sept	Oct	Nov
Minimum T	°C	10	9	12	17	22	25	27	26	26	26	22	15
Maximum T	°C	24	22	26	32	37	38	36	33	33	33	32	29
Rainfall	$\frac{mm}{day}$	7.4	11.5	16.4	7.5	15.8	41.9	185.5	339.3	259.3	241.6	39.2	17.1
Radiation[1]	$\frac{kWh}{m^2 day}$	5.3	5.06	6.24	7.12	6.87	6.37	5.15	4.5	4.86	5.07	5.79	6.17

6.1.2 Community needs

The community taken into account is formed by 400 private households, one health-care center, one school and some little business activities. Differently from the majority of the studies conducted for rural electrification, we do not consider only electrical loads but we face the problem taking into account all the needs of the community. One of the most important advantages of this approach is the possibility to decouple the production and the consumption of different goods with storage systems more economic than electrical batteries. In addition, the capability to shift in time the usage of different units may allow a further reduction of operating cost.

The daily demand of the different goods consumed by the final users is reported in Table6.2 for each period. The demand of each good is considered as non-deferrable and it is always satisfied by means of the contextual production and/or the discharge of the relative storage. In addition, some of these goods can be consumed by dedicated units to produce other goods: an example is the reverse osmosis plant which consumes ground water and electricity to produce cold potable water.

The average daily pattern of the AC directly consumed by final users is reported in Figure 6.1 and it is assumed constant during the whole year. In average each household is equipped with 4 low power lamps (cfl), 1 radio and 1 television. The school consumption is limited to diurnal hours, as well as the business activities load, while public lights are switched on during nocturnal hours. The hospital, which operates the whole day has a peak of electricity consumption during diurnal hours. During weekend the school and the business activities consumption is set equal to zero.

The main activity of the community is agriculture which requires a large amount of water to ensure the highest field productivity (Sadras, Grassini, and Steduto, 2012). The water demand for agriculture (60 hectares in this case) in the different periods of the year has been evaluated with Blaney-Criddle equation (Allen et al., 1998), assuming a yearly rotation of three different crops (rice, wheat, vegetables): a part of this water need is obtained by rainfall (see Table 6.1), while the rest is extracted by pumps from a 10 meters depth groundwater basin.

In addition to ground water and electricity consumption, the public and private users consume potable water while the two public buildings (i.e. the school and the hospital)

demand for air-conditioning (fan coil units are used for both heating and cooling depending on the season) and hot water.

TABLE 6.2: Average daily consumption of the different goods

Good		End-user	Monsoon	Winter	Pre/post monsoon
Electricity	kWh_{el}	Households		487.6	
		Public lighting		298.8	
		Business act.		301.3	
		Hospital		367.0	
		School		192.8	
		total		1647.4	
Ground water	m^3	Irrigation	3805.5	2609.2	2171.4
Cold potable water	m^3	Households		170.0	
		Business act.		10.0	
		Hospital		12.0	
		School		9.6	
		total		201.6	
Hot potable water	m^3	Hospital		7.8	
		School		1.4	
		total		9.2	
Heating	kWh_{th}	Hospital	0.0	889.8	0.0
		School	0.0	275.1	0.0
		total	0.0	1164.9	0.0
Cooling	kWh_c	Hospital	392.2	0.0	910.2
		School	481.2	0.0	314.5
		total	1873.5	0.0	1224.7

6.2 Microgrid architectures

The base layout of the MG is shown in the right side of Figure 6.2: it consists of different subsystems (one for each good) connected by multi-input/multi-output units. The AC bus is connected to the diesel ICE and it provides electricity to the domestic and the public users appliances (i.e. household, hospital, school and business activities), to the public lighting and to all the other electrical devices required for the operation of the MG units. The AC bus exchange electricity through an inverter with the DC bus which is connected with the electric storage (a lead acid battery) and polycrystalline PV panels. Ground water is pumped from the well in a non-potable water tank and used mainly for irrigation and for potable water production which is obtained with an osmosis process, consuming AC electricity. The potable cold water (20 °C) is then stored in vessels and it is consumed by domestic and public users. In addition it can be heated up to produce sanitized hot water at 60 °C: the heat required is obtained from the high temperature stream of the cogenerative ICE or it is released by a Heat Pump (HP). The low-medium temperature storage consists of two water vessels at 45

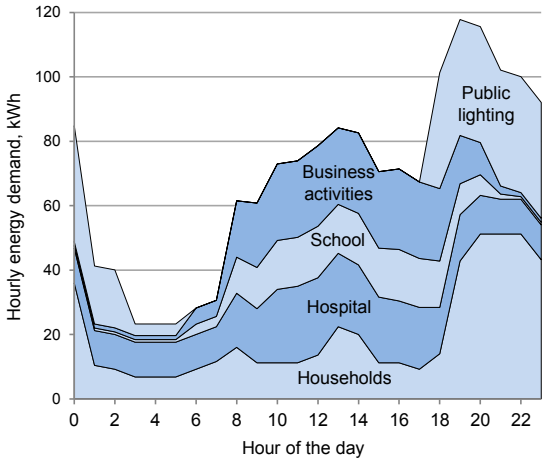

FIGURE 6.1: AC consumption daily pattern (week day). (Mazzola, Marco Astolfi, and Ennio Macchi, 2016)

°C and 35 °C respectively and it is used in the fan coil units for the heating of the school and the hospital. The ICE low temperature cogenerative heat can be used to store energy at medium temperature as well. Except for the winter season the two public buildings needs for air cooling and a chiller is used releasing heat to the ground water storage.

Finally the possibility to add a biomass dispatchable power generator to the genset is investigated. The two solutions here proposed are represented in the left side of Figure 6.2: the first one (A) is a boiler coupled with an Organic Rankine cycle (ORC), the second one (B) is a down-draft gasifier coupled with a cogenerative ICE. In both cases a chipper, powered by the AC bus, is used to chop the wood down to the size required by the gasifier unit and the biomass furnace. The gasifier and the ICE operate like a single unit because it is assumed that syngas cannot be stored. On the other hand, oil storage is considered and thus the operation of the biomass boiler is decoupled from the ORC one. The ORC can operate in two modes: in pure electric production mode, it condenses at low pressure releasing heat to the ground water tank; in cogeneration mode it condenses at higher temperature storing heat in the medium temperature water tank.

All the assumptions related to the programmable loads are reported in Appendix A.4 while the nominal and off-design performance of the programmable generators and the battery are represented in Figure 6.3. Nominal biomass boiler efficiency is equal to 88% based on LHV value (New York State Energy Research and Development Authority, 2010) while a fixed efficiency equal to 94% is assumed for the inverter. Finally, the properties of the different goods are reported in Table 6.3. The Oil-Heat and the woodchips storage sizes are expressed with the time span of nominal utilization while the cooling storage represents the building inertia.

The economic assumptions for each component are reported in Table6.4 as well as the life span. These data are mainly related to international manufacturers and retailers. Most of them have been obtained by public retail websites (internal combustion engines, lead-acid battery, PV and inverter) while the cost and the life span of the ORC system has been

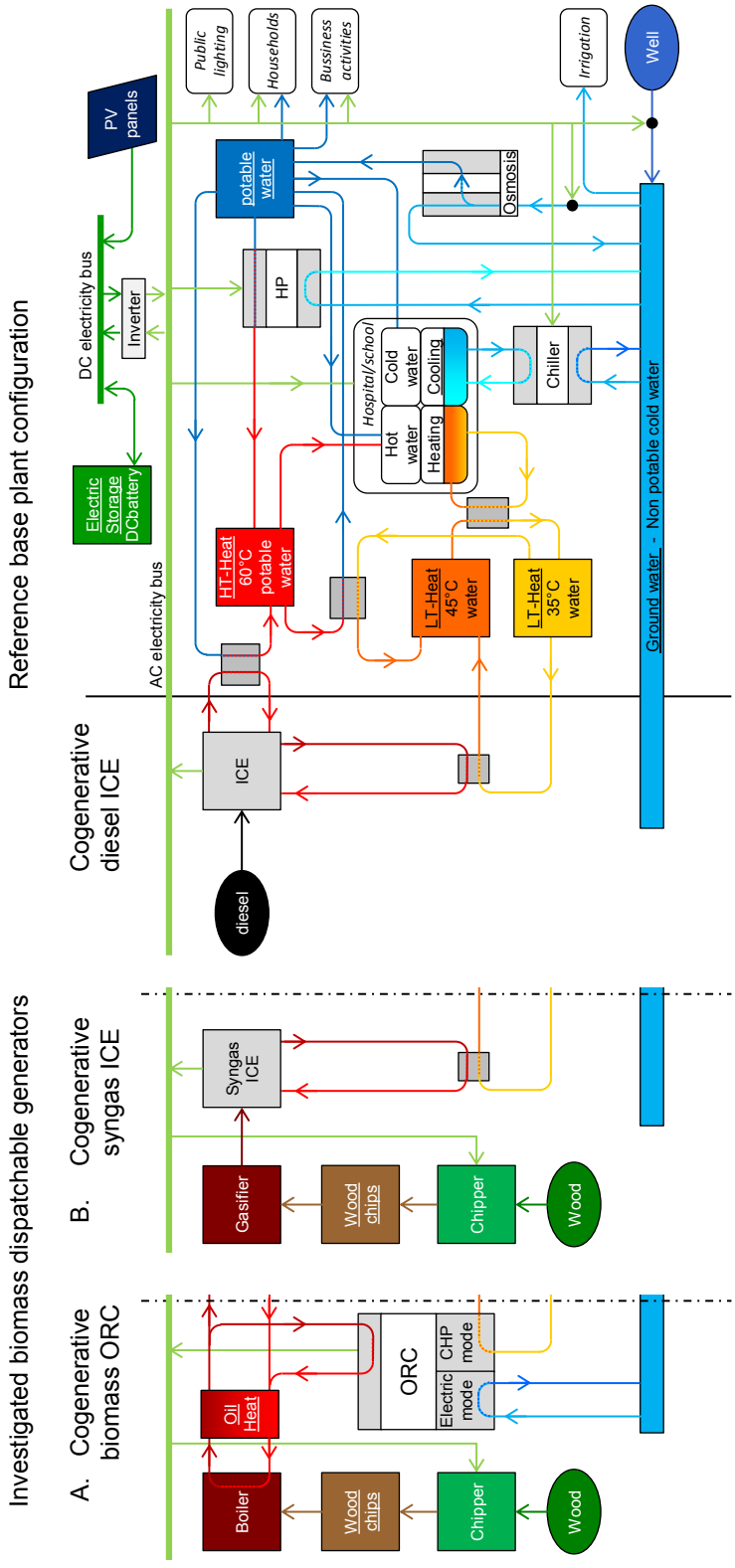

FIGURE 6.2: Schematic representation of the three MG architectures considered in the simulations. (Mazzola, Marco Astolfi, and Ennio Macchi, 2016)

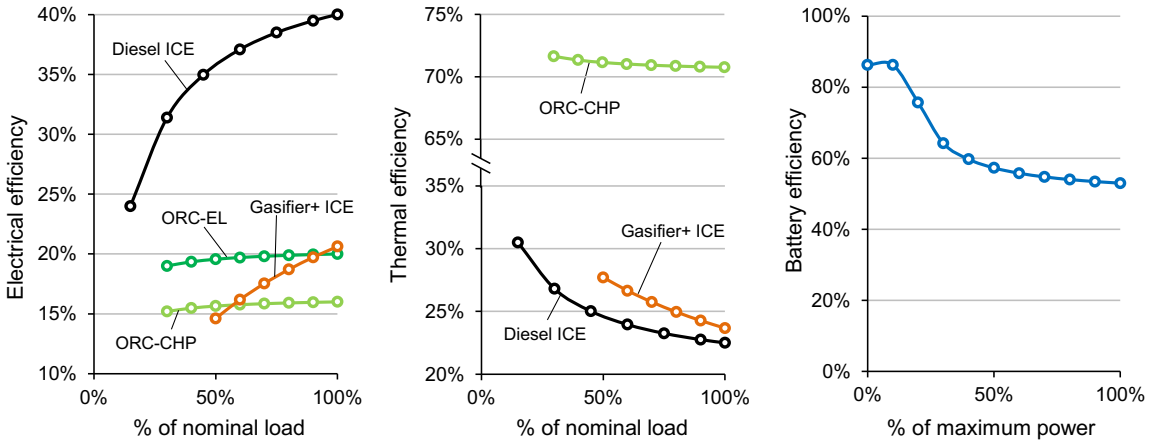

FIGURE 6.3: Electrical and thermal efficiency for the programmable generators and battery efficiency. (Mazzola, Marco Astolfi, and Ennio Macchi, 2016)

Good		Storage	Size	ϑ
AC	kWh	No	-	-
DC	kWh	No	-	-
$DC_{storage}$	kWh	Yes	Variable	0%
Ground water	m^3	Yes	600	0%
Potable water	m^3	Yes	100	0%
LT-Heat	kWh	Yes	150	1%
HT-Heat	kWh	Yes	100	1%
Oil-Heat	min	Yes	20	2%
Cooling	kWh	Yes	10	2%
Woodchips	h	Yes	18	0%

TABLE 6.3: Goods properties

Component	C^{inv}_{nom} USD	k -	O&M USD/year	LS years
Diesel ICE	20000	-	5000	10
PV	120000	0.9	1120	15
Gasifier+ICE	180000	0.7	18000	8
Boiler+ORC	500000	0.7	12000	15
Lead-acid BESS	19000	0.9	380	10
Inverter	25000	0.9	400	15

TABLE 6.4: Economic assumptions

obtained by private communications with a world leading company in the sector. The only exception is the gasifier system, whose assumptions are related to the Indian context and supported by two references already cited in Section2.3.3. Regarding O&M, the data about regular maintenance and the labor hours have been obtained by the above mentioned sources as well. The effect of the size on the investment cost is accounted with the exponential law in Eq.6.1 where the k coefficient (always smaller than 1) depends on the component type: PV panels are modular and so a exponent equal to 0.9 is assumed while a lower value is adopted for Boiler+ORC and Gasifier+ICE because of the favorable scale economies.

The nominal size for each unit is equal to 100 kW.

$$C^{inv}_{i} = C^{inv}_{nom}\left(\frac{size_i}{size_{nom}}\right)^{k} \tag{6.1}$$

The only exception is the lead-acid battery, whose lifespan (LS) in evaluated with the method already described in Section4.2.4.

6.3 Simulation framework

The simulations are carried out using the methodology described in detail in Chapter4. The length of the time step is a parameter of great influence and a 1-hour time-step is the common assumption for most of the studies in literature. In this work the simulations are carried out with a 10 min time-step with the advantage of catching the intermittent RES power fluctuations and the events which happen in a short time scale (i.e. units start-ups) but with the drawback of a dramatic increase of problem complexity and computational time.

For this reason, a variable time step is used in this case to cover the whole time horizon, with the goal to exploit the beneficial effect of a fine time discretization with a satisfactory computational time. A schematic representation of the rolling-horizon with variable time-steps pattern used in this work is reported in Figure 6.4. The time-step is progressively increased from 10 min to 4 h, covering a time horizon of 18 hours in 16 time-steps with a limited computational time effort. In spite of the adoption of a shorter time step, the results obtained by this approach cannot detect fluctuations below 10 minutes and regulations related to power quality, which would require a time-step around 1 second or less, are neglected in the simulation and are taken into account with an operating reserve constraints in the MILP problem.

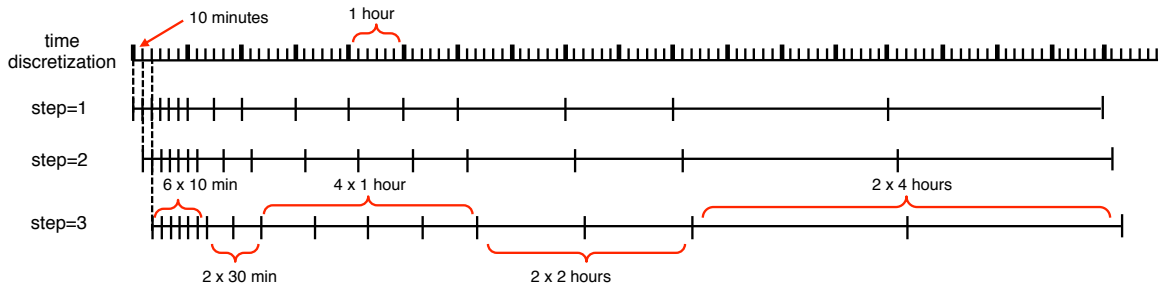

FIGURE 6.4: Variable time-steps pattern used in the simulation. (Mazzola, Marco Astolfi, and Ennio Macchi, 2016)

In Figure 6.5 a single day of simulation is represented for two MG configurations to highlight the capability of this approach in modeling fast fluctuations of generated and consumed power. A PV system (150 kW), a diesel ICE (200 kW) and a battery (200 kW h) are installed in both configurations. In the second one, a 100 kW biomass Gasifier+ICE is added to limit fossil fuel consumption. The fixed load follows the average profile in Figure 6.1 but a considerably random fluctuation is added to catch a realistic trend of power demand; PV production is not regular as well and a marked cloud passage can be noticed in the morning. In both cases the schedule of both the programmable loads and the dispatchable generators is defined by the EMS. The diesel engine mostly works in load following since it can cover the load peak by itself and it has a larger operation range compared to the gasifier system; as result the use of the battery is limited with small variation of the SOC level.

On the contrary, the biomass based generator needs to run a higher number of hours storing energy into the battery in order to face the night power demand. In spite of this, the diesel engine must operate for 30 minutes around 19 pm to assist the gasifier. Another

difference is related to the scheduling of the programmable loads: in the first case they are scheduled almost homogeneously during the whole day to limit the off-design of the diesel engine and the wear of the battery during the central hours of the day; in the second case, they are mainly placed during the first eight hours of the day (when the fixed load is low) with the aim to run the gasifier close to the nominal condition. The programmable loads are not scheduled in the night to reduce the use of the diesel engine with economic and environmental advantages.

Although the application of variable time-steps considerably reduces the computational time, the resolution the MILP problem requires in average 1 second to determinate the optimal MG operation for the consecutive 10 min. The simulation of an entire year of operation (365 days) would need more than 10 hours: a computational time effort that is not compatible with the objective of this work, which is the testing of a relevant number of MG configurations in order to find the most promising one. A representative year, made by 15 days has been defined to overcome this problem. As mentioned in previous chapter, the whole year has been split in three periods, representative of monsoon season, the dry winter and the intermediate seasons (pre and post monsoon). For each period the trends of the goods demand and of the solar radiation for 5 days have been created respecting the average values of each period. According to our results, 5 days is a good compromise between the good representation of the year (fluctuations of the goods demand and the sun radiation) and a relatively short simulated time span.

The operating cost over one year must take into account the availability of the components. During the year, the biomass-based generators are expected to be out of order for a certain number of days for scheduled maintenance and unpredictable failures: in these days the diesel ICE generator is used intensively to support the system and prevent power shortages. This additional operating cost is evaluated simulating the same system configuration (PV size, battery size) and assuming that the biomass-based generator is not available. We assumed an availability equal to 95% and 90% for ORC-based and Gasifier-based systems respectively since this parameter is in general higher for biomass combustion technologies in comparison with gasification ones (Environmental Protection Agency, 2007).

6.4 Results

In this study the research of the best MG design is realized with an enumerative approach instead of using an optimization algorithm in order to better describe the influence of the different variables on the final result. The size of the resulting multidimensional grid depends on both the MG configurations and the number of discrete sizes for each component. Three different cases are investigated: (i) the reference case with Diesel and PV, and two other configurations with the addition of (ii) a biomass boiler+ORC and a (iii) a gasifier+ICE. The size of the diesel ICE is equal to 200 kW for all the simulations since it must be able to cover the grid peak load by itself. The size of the PV ranges from 0 to 400 kW, battery from 0 to 500 kWh while ORC and Gasifier+ICE vary between 0 and 150 kW: a discrete step of 25 kW is assumed for the biomass-based generator size and 50 kW for PV and battery size. All

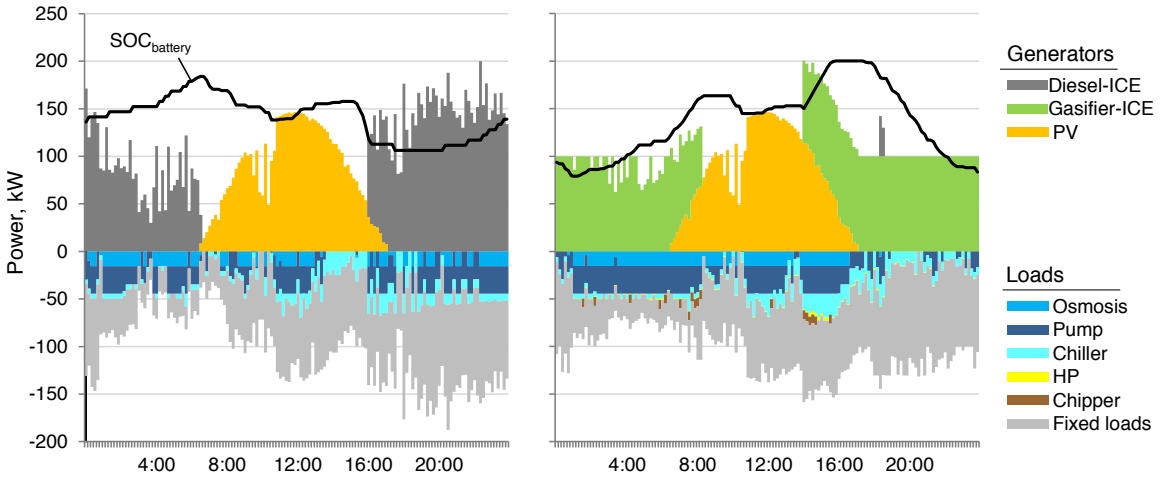

FIGURE 6.5: Single day simulation with 10 min time step for two different MG configurations. (left) MG based on diesel-ICE and (right) MG provided with a biomass gasifier-ICE. (Mazzola, Marco Astolfi, and Ennio Macchi, 2016)

the simulations have been performed by an i5 2.6 GHz desktop computer with 8 GB RAM, using Gurobi as solver for MILP problems. Each step of the rolling horizon strategy requires in average 1 second. The computational time generally increases in the ORC cases, because of the presence of an additional good (oil-heat). However, because in real management the problem is solved only once every 10 minutes, the computational time is fully compatible with practical implementation.

6.4.1 Integration of PV plant

In this section the integration of a PV plant in a MG provided with a diesel ICE is investigated. The aim is to understand the effects of the presence of a non-programmable renewable energy generator in terms of MG operation and system economy. The specific cost of the energy generated by PV, omitting the energy storage system, is considerably lower than the Diesel one and hence, this solution can lead to a substantial reduction of LCOE although it entails the use of a battery system. The contour map in Figure 7.a shows the LCOE attainable by varying the size of the PV plant and the storage. It is possible to point out that the optimal battery size changes depending on the PV system; for small PV nominal power, battery is not required and the intermittent PV power is handled by a proper scheduling of both the programmable loads and the diesel engine.

On the contrary, for a PV nominal power greater than 100 kW the use of a battery is mandatory to store the surplus of energy generated in the central hours of the day and to avoid energy dumping. The black line represents the locus of minimum LCOE varying the size of the PV plant and the detailed economic results for these cases are reported in Figure 7.b. Each group of stacked bars represents the LCOE breakup for a given PV size and optimal battery size: investment and operational costs are further divided in the contribution for each unit. A MG simply provided with a diesel ICE shows a very small investment and small

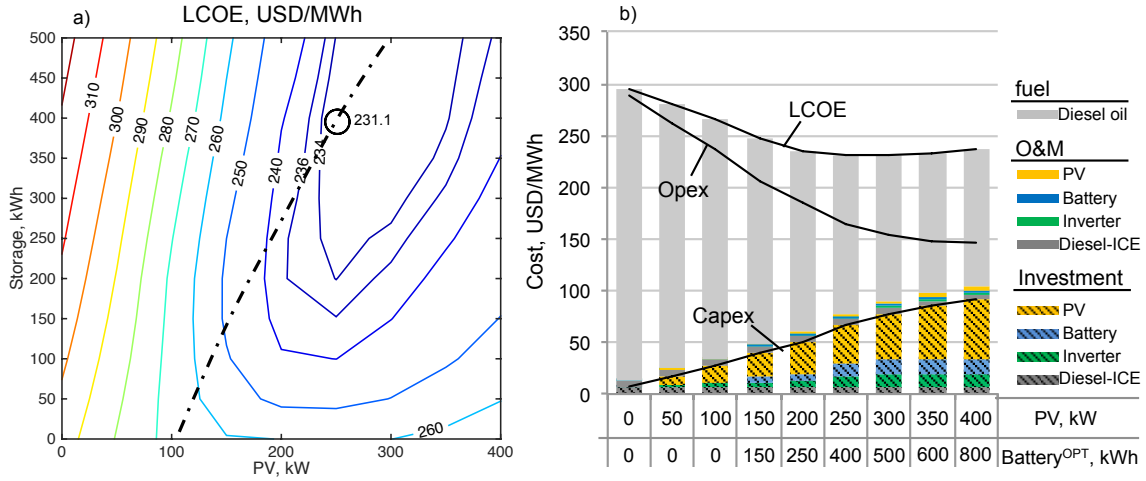

FIGURE 6.6: LCOE results for Diesel+PV system; a) LCOE map in function of PV and battery size and b) breakup of LCOE varying PV size with optimal battery size

O&M costs, but very high operational cost due to the use of an expensive fossil fuel (more than 95% of the LCOE). As result the LCOE is high, reaching a value of 295.1 USD/MWh. The introduction of a PV plant entails from one side a strong increase of the investment cost, mainly due to the PV panels followed by the inverter and the battery, and a slight increase of the maintenance costs. On the other side, the power production from a RES allows to reduce the consumption of fossil fuel with a relevant reduction of Opex cost. The trade-off between these two opposite effects leads to a minimum LCOE of 231.1 USD/MWh (-21.7% respect to the only-ICE case) for a 250 kW PV and 400 kWh battery.

A further increase of the PV size allows for a less marked reduction of fossil fuel savings because the diesel engine works anyway a relevant number of hours following the load and limiting the use of the battery. The RES penetration increases almost proportionally with the PV size reaching a value of 46% for the optimal case.

6.4.2 Integration of biomass based generators

In this section the use of a biomass based generator is investigated with the aim to further reduce fossil fuel consumption and to increase the electricity generation by RES. Two biomass-based systems are compared: (i) a gasifier+syngas ICE and (ii) a biomass boiler+ORC. Their specific investment cost are remarkably higher than PV because the more complex system architecture and their relatively small present market. However, the dispatchability of these units can play a relevant role in the reduction of LCOE, partially substituting the diesel ICE in the role of base generator. Figure 8.a and Figure 8.c show the trend of LCOE for the gasifier systems and the ORC respectively, varying the size of the biomass based generator and the PV plant; in each point the size of the battery is optimized. The two LCOE maps are very similar for the two cases (Gasifier system is in average cheaper of less than 5 USD/MWh) and common considerations can be addressed observing the trend of the minimum LCOE (dotted black line). Increasing the size of the biomass generator, the optimal size of the PV plant

and the battery decreases because the use of a reasonably priced programmable generator allows for an easier MG management without the necessity to adopt big capacity storage. PV is detrimental for big size (150 kW) biomass generators while a small battery is always recommended.

In Figure 8.b and Figure 8.d the LCOE breakup is reported for both cases. It is possible to note that the total investment cost is almost constant because the cost of the biomass generator is compensated by a reduction of PV plant size. Opex cost instead shows a minimum because for big size biomass based generators the higher investment cost is not repaid due to the limited number of operating hours. As a consequence, the LCOE trend has a minimum for both technologies; the optimal size for a gasifier system is slightly smaller than the ORC (100 kW vs 150 kW) according to its lower availability and higher off-design penalization. In the optimal configurations, the PV continues to play an important role with a nominal power of 100 kW and 150 kW respectively for ORC-based and Gasifier-based systems, providing an amount of cheap energy which can be easily matched by programmable loads. The Diesel engine is used in the energy-intensive seasons only for few hours at end of day and as backup generator when the biomass generator is out of order for maintenance or accidental failure. The optimal solutions show a RES share over 95% in both cases.

The final LCOE results are similar for both technologies but the generator management is considerably different, as reported in Table 6.5. The gasifier works with a higher average load factor respect to the ORC based system because of the higher part load penalization: this implies that the battery covers a more important role in load balancing as shown by the higher amount of energy stored in the battery coming by the programmable biomass based generator. The gasifier has in average more than one start-up every two days thanks to the faster start-up and because of the lower flexibility during operation. On the opposite, the ORC system exploits the additional degree of freedom offered by the oil storage: the boiler is shutdown with a lower frequency (1 start-up every 3 days in average) while the ORC shows a more intermittent operation following the load and using the heat stored in the oil tank.

6.4.3 Analysis of RES penetration cost

The results obtained in the simulations highlight the beneficial economic effect attainable by exploiting renewable energy sources whether intermittent (PV in this case) or dispatchable (biomass based generators) instead of fossil fuels. An additional investigation has been conducted to show the value of the dispatchability of a biomass-based system and the potential of hybrid solutions made by biomass and PV plants.

We calculated the specific cost of RES energy production for two MG configurations provided with a backup diesel engine and a single renewable energy power system: one with PV plant and the other with a Gasifier+ICE system. Different size of generators (and consequently of electricity generated) are investigated and the results are presented for the optimal size of the battery. The specific RES cost is calculated as the ratio between the life cost of the technology (generator plus the battery system) and the useful RES energy. This latter one is evaluated as the difference between the total electricity consumed by the village and the energy generated by the Diesel generator. This implies that the diesel engine never charges

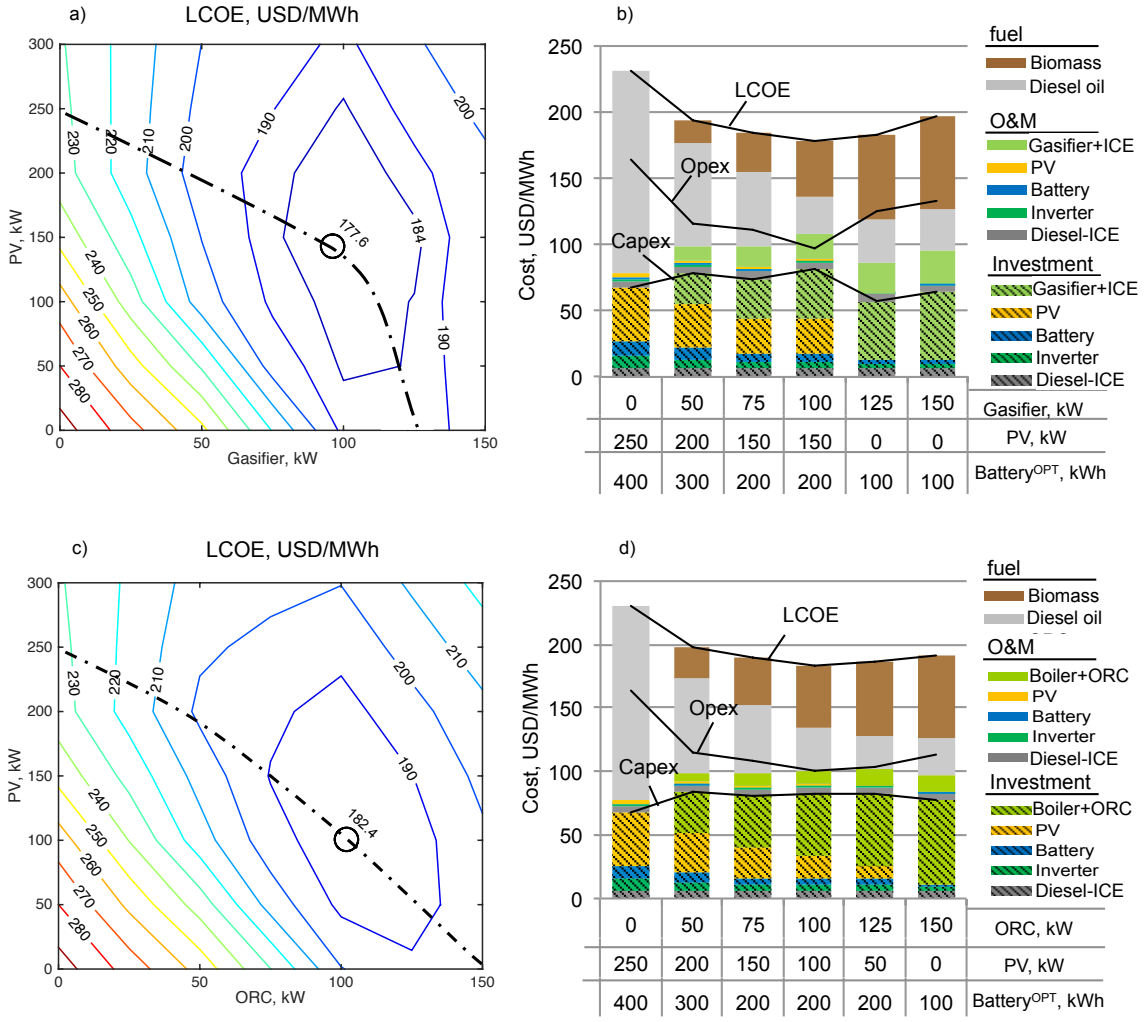

FIGURE 6.7: LCOE results for gasifier system (a,b) and ORC system (c,d); (a,c) LCOE map in function of PV and generator size and (b,d) breakup of LCOE varying generator size with optimal PV and battery size. (Mazzola, Marco Astolfi, and Ennio Macchi, 2016)

the battery and that the charge/discharge losses are totally allocated to the RES production: an assumption which is practically always verified as showed in the example in Table 8. In figure 9 three curves are presented: two for a PV system (in stand-alone and grid-connected configuration) and one for the biomass based plant.

As a general consideration, by increasing the installed power both stand-alone configurations show a trend formed by two different parts. Initially the specific cost of energy decreases, thanks to the favorable scale factor: the effect is more marked for PV plant since for small installed power (50 kW and 100 kW) battery is not required and grid balance is guaranteed by a correct management of schedulable loads. Increasing the RES share and hence the nominal RES installed power a bigger battery size is required leading to a specific cost increases: this figure soars for PV systems having a RES penetration higher than 20% (equivalent to 150 kW) while this effect is less pronounced for the biomass based system. The intermittent nature of solar source requires large energy storage systems with a relevant part

TABLE 6.5: Optimal MG design for the three configuration analysed with information about the operation of the different components and the use of the battery. Diesel ICE size is 200 kW for all cases

		Optimal size kW,kWh	LCOE USD/MWh		Load factor -	Daily Start-ups #/day	Working hours #/year	Electricity to battery MWh
Diesel only	Battery	0	295.1	D-ICE	49.0%	-	8760	-
PV system	PV	250	231.1	D-ICE	52%	1.45	4888	15.2
	Battery	400		PV	23%	-	-	177.6
ORC system	Boiler	500	182.42	Boiler	79.0%	0.25	7815	-
	ORC	100		ORC	81.7%	2	7800	0.78
	PV	100		D-ICE	31.5%	2.08	492	0.08
	Battery	200		PV	23%	-	-	15.62
Gasifier system	Gas+ICE	100	177.61	Gas-ICE	90.8%	1.6	6079	15.6
	PV	150		D-ICE	25.6%	1	453	0.12
	Battery	200		PV	23%	-	-	49.0

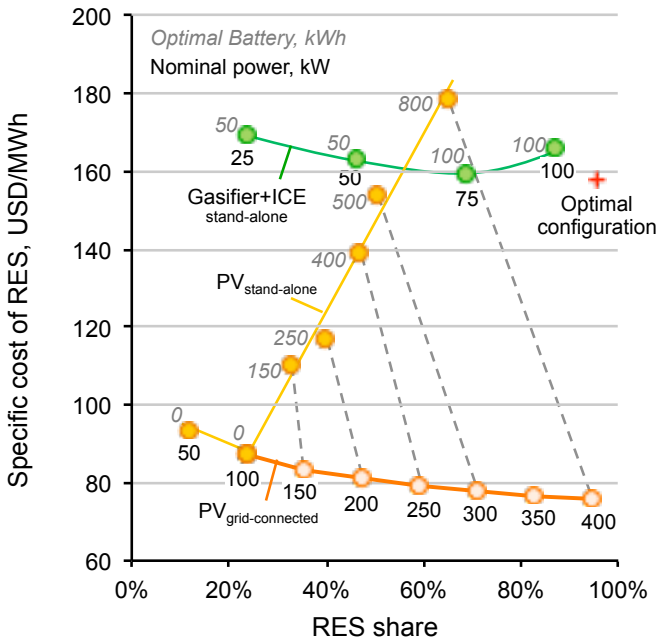

FIGURE 6.8: Specific cost of RES production as function of RES penetration for three microgrid based respectively on PV (grid-connected or stand-alone) or a Gasifier+ICE system. For each marker, black figures refer to the nominal installed power while grey ones to the size of the optimal energy storage. (Mazzola, Marco Astolfi, and Ennio Macchi, 2016)

of energy lost in charge/discharge process. A qualitative evaluation of this additional cost can be obtained comparing two PV systems with the same installed power: one in stand-alone configuration and the other one grid-connected. The difference in RES penetration is due to effect of charge/discharge losses which are not faced by a grid connected PV since the entire energy produced is injected in the grid without any limitation. Regarding the gasifier system, the slope inversion starts at a higher RES penetration (70%) and has a lower intensity. In fact, thanks to the dispatchability relevant amounts of energy are easily manageable without huge energy storage and charging/discharging losses.

With the goal of increasing the RES penetration, a prohibitive RES energy cost is obtained for PV plants while values up to 87% can be obtained with a Gasifier+ICE system at a reasonable cost underling once again that the only cost-effective solution for high RES sharing is to rely on a renewable dispatchable generator. However, biomass based generators benefit by the integration of relatively small PV systems as shown by the optimal design (red cross) and intermittent generators can play a relevant role in lowering the LCOE and increasing the RES share.

6.5 Conclusions

In this chapter the potential of RES technologies in reducing the LCOE of stand-alone microgrids for rural electrification has been investigated.

A proper mix of solar and biomass energy (with an optimized size of energy storage and management of the schedulable loads) leads to a LCOE reduction of about 40% respect to a system based only on diesel generator. In addition, the RES share is strongly increased up to more than 95%, restricting the fossil fuel electricity production to the marginal role of back-up system. These results show the importance of using RES dispatchable generators like biomass-based systems in stand-alone MGs and the benefits attainable in terms of cost reduction and RES share.

The results presented are obviously related to the assumptions made. In particular different input data on specific cost of fuels (diesel oil and biomass), daily variation of electricity demand, solar radiation, etc. would lead to different solutions. For instance, the presence of a relevant cooling demand related to air conditioning, moving electricity demand peaks in the sunny hours, would favor PV and reduces the size of the battery. However, other sensitivity analyses have been performed to assess the robustness of the solution in relation to reasonable changes of the input data and it has been found that, even if the optimum generators size can slightly change as the share of energy sources, the qualitative trends of the results remains the same over a wide range of variation. The following general conclusions, are hence valid for a wide range of cases:

- The addition of solar PV yields a relevant contribution to decrease the LCOE, as well as emissions, but cannot completely replace the diesel production: the optimal (minimum LCOE) mix of diesel generator, PV and electric batteries still allocates a relevant role to fossil fuel, which actively acts to shave the battery charge/discharge fluxes and during the nocturnal hours. A higher RES share and a lower LCOE can be obtained only

with an technology improvement of both PV panels (higher effi- ciency, lower cost) and energy storage (lower investment cost, smaller wear and longer life).

- Whenever biomass is available at reasonable cost, a better result is obtained with a RES dispatchable generator like a biomass Boiler+ORC or a biomass Gasifier+ICE, since they can almost totally replace the use of diesel engine, reducing the size of the electric storage and strongly increment the RES penetration. The possibility of reducing the LCOE strongly depends on the cost of these components, their efficiency and the cost of biomass.

- The best solution, in term of LCOE as well as RES penetration, is based on a proper mix of PV and biomass generators (with a reasonable size of energy storage and an optimized management of the schedulable loads), with a marginal role of back-up diesel generator. Varying the assumptions, the optimal mix may change leading to solutions with a different share of electricity produced by PV and by biomass but the beneficial effect of using a RES dispatchable generator is always confirmed except for the cases with a extremely high cost of the biomass.

Chapter 7

Test-case 2: energy access in islands

Electricity supply on most of small island communities is nowadays based on fossil fuels, especially diesel oil. Since grid extension is practically unfeasible or too costly in many cases, the energy needed to cover the community needs is produced locally using Diesel fueled internal combustion engines with numerous drawbacks. Because diesel oil has generally a high cost in remote locations (0.8-1.2 USD/liter) and diesel generators are forced to part-load operation, the resulting levelized cost of electricity (LCOE) is in average considerably higher (0.3-0.6 USD/kWh) than the one on mainland (IRENA, 2015c). Other relevant drawbacks are the strong dependency from an external source, with the related fluctuations and uncertainty, and the environmental concerns associated to diesel engines operation. In addition to this, this problem is even more important because of the scarcity of fresh water in many islands. Since the import is frequently an expensive option, fresh water is usually produced locally using processes which require considerable amount of electricity (Karagiannis and Soldatos, 2008). As a consequence, a relevant share of electricity is spent in water desalination, as happen in Canary Islands where 5 to 30% of electricity is spent to power reverse osmosis plants (Schallenberg-Rodriguez, Veza, and Blanco-Marigorta, 2014). The sum of all these factors leads to high expense for fossil fuel import, which in islands community consumes from 8 to 20% of GDP, a high value compared to mainland average (4.5%) (GREIN, 2016).

A possible option to be considered is the installation of power generators based on Renewable Energy Sources (RES). Thanks to the massive deployment of certain technologies (Photovoltaic above all), in the last decades a considerable cost reduction has been observed making these technologies competitive with fossil fuels counterparts. The competitiveness and the advantages are even more evident in remote locations, where the cost associated to energy production from diesel oil is very high. A lot of research and projects have been conducted to bring RES in islands (IRENA, 2015b), with numerous successful examples. Real cases show that the introduction of solar PV or wind turbines (WT) allows considerable fuel and money saving during the lifetime of projects (Bunker et al., 2015a). One of the most important example is El Hierro, which claims to become the first 100% renewable island, exploiting the wind resource in the island (Bueno and Carta, 2005). Many projects underline also the potential synergies between RES and desalination. Powering the desalination plant with energy coming from RES could allow in island context to reduce the cost related to fresh water production (IRENA, 2015c).

Hover, the most implemented technologies (PV and WT) are based on intermittent sources, challenging to be managed in an off-grid environment. El Hierro, whose objective is to reach

a very high RES penetration, has several problems to exceed 30% of penetration. This trend is confirmed in many islands and it is very rare that more than half of energy is produced by RES, even in presence of energy storage systems (Bunker et al., 2015b).

In this chapter the introduction of Concentrating Solar Power (CSP) power plant in an island is investigated and evaluated. Despite of the high installation costs, this technology is expected to reach higher RES penetration thanks to the possibility to store efficiently the thermal energy, decoupling the electricity production from the solar irradiation Another potential advantage is related to possible synergies with Multi Effect Distillation (MED) plants; this technology, used to produce fresh water, requires huge amount of thermal power during operation which could be produced efficiently by the CSP in cogenerative operation. This possibility, already investigated for other kind of Combined Heat and Power (CHP) plants (Cardona, Piacentino, and Marchese, 2007), could lead to a reduction of total fossil fuel consumption.

In order to have a fair and realistic comparison between the technologies, the whole hybrid system operation is simulated using a rolling horizon approach based on Unit Commitment. Operation costs are assessed simulating one year of operation using an optimization model which use the available units (both power generators and desalination plants) to cover the electricity and fresh water demand at the least feasible costs. This is an important novelty compared to other recent studies, in which the performances of the system are evaluated only at nominal load and do not take into account the yearly variability of electricity demand and RES productivity.

7.1 Test-case description

The test-case used to assess the different MG configurations consists of a small island community. The MG is responsible to satisfy both electricity and potable water needs. Due to the lack of comprehensive studies and data availability about one single real case, we built synthetic time series of the demand of both electricity and potable water considering both realistic weather data and a seasonal variability of the island inhabitants. Weather data are assumed the same of Tenerife (Canary Island) and SWEC hourly dataset is used as reference[1]. In addition, we assume that island occupancy ranges from 8400 in low season (October-May) to 12000 inhabitants in high season (August).

7.1.1 Community needs

Electricity demand per capita has been split in two different terms: basic needs (BN) and air conditioning needs (ACN). The basic needs comprise the domestic and the commercial users, the public lighting and the public buildings loads. We assume a daily pattern common to most of developed country users, with two demand peaks at the middle and at the end of the working day and a lower consumption during nocturnal hours (Pombeiro, Pina, and C. Silva, 2012) as reported in both Figures 7.1.b and 7.1.c. The daily base electrical load

[1]SWEC data set from `https://energyplus.net/weather`

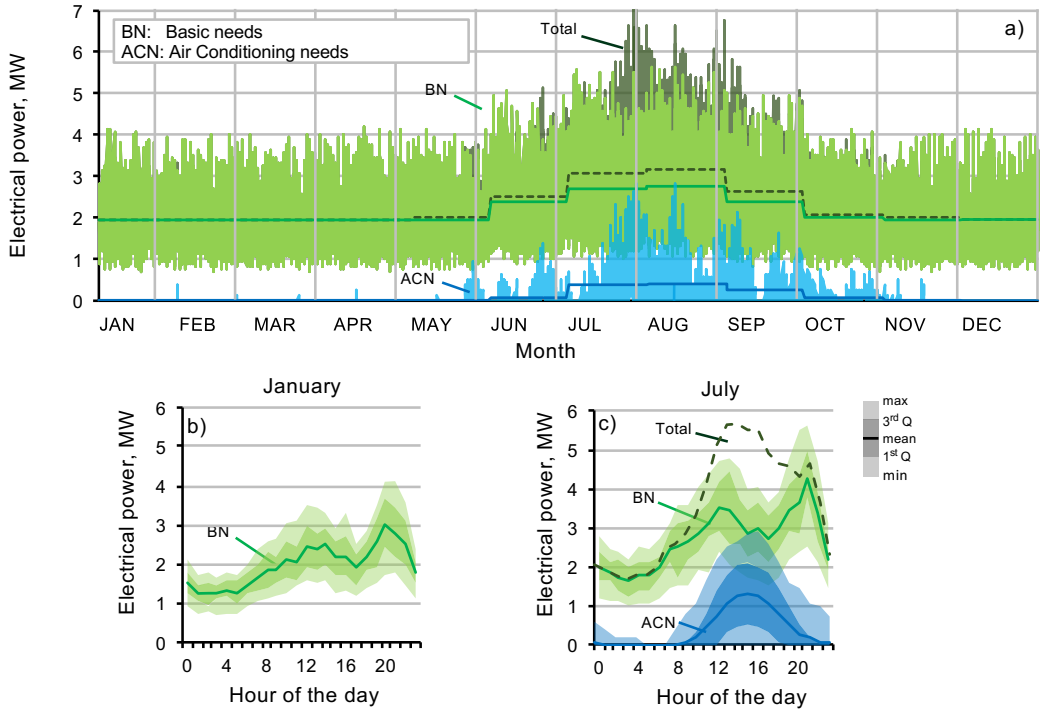

FIGURE 7.1: Trend of electricity consumption: a) hourly variability for the basics needs (light green) and the air cooling load (light blue) and monthly average values. b) and c) hourly variability range for the months of January and July. (Mazzola, Marco Astolfi, P. Silva, et al., 2017)

profile is obtained imposing an average electricity consumption of 5 kWh_{el}/(day person) as representative of a developed country. Figure 7.1.a depicts the hourly electrical load and the average monthly load along one representative year. The hourly demand peak is in summer and it is about 7 MW_{el} because of the increase of island inhabitants as well as of the presence of air conditioning load. In order to simulate the variability of electricity demand, a ±40% random deviation is added for the basic needs trend while the air condition load variation is exclusively due to ambient temperature change. Air conditioning need increases proportionally with the ambient temperature when it is higher than 26°C while vanishes at lower temperatures and its maximum value is assumed equal to the 50% of the BN yearly peak. As a result, ACN represents the 12% of electrical energy needs in summer months and 5% on a year base. Figures 7.1.b and 7.1.c depicts the data variability for January and July reporting for each hour of the day the monthly minimum, the average and the maximum values together with the 1^{st} and the 3^{rd} quartile of the distribution.The resulting total annual electricity demand (not including water related requests) is about 16.9 GWh.

Regarding potable water request, the daily pattern per person is assumed constant during the year and it is reported in Figure 7.2. It has been derived from Funk and DeOreo, 2011, considering that most of the consumption is related to residential and commercial sector (restaurants, hotels) and that the average consumption of potable water is 500 liter/(day person), with small seasonality related to ambient temperature. A random variation of ±10% is added as for the electrical demand. The resulting annual water request is about 1.600.000 m^3.

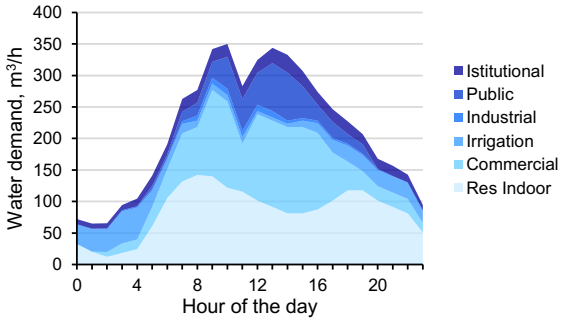

FIGURE 7.2: Daily pattern of community water consumption in the 15th of July. (Mazzola, Marco Astolfi, P. Silva, et al., 2017)

Table 7.1 summarizes the monthly data for the test-case in terms of weather information, and microgrid requests.

7.2 Microgrid configurations

The simplest plant layout able to satisfy both community basic needs (i.e. electricity and potable water) is made by a fossil fuel generator and a desalination plant. In the specific case, the microgrid (MG) base configuration is provided with three diesel Internal Combustion Engines (ICE) of the same size and a Reverse Osmosis plant (RO). The RO plant is design to cover the maximum daily demand along the year while the ICEs must cover the MG peak load working together at nominal load. The choice to adopt different ICEs in parallel is motivated by the large load variation along the year and with the aim of increasing the annual fuel consumption by limiting part load operation. This assumption also reflects the common practice adopted in islands where a multiple engine configuration is preferred for availability purposes.

In the RO plant, seawater is pumped from sea and it flows through a series of filters and water treatment units in order to remove the suspended materials and to limit biofouling (Schallenberg-Rodriguez, Veza, and Blanco-Marigorta, 2014). After that, it flows in a pressure exchanger device where the pressure is increased at the expenses of the high pressure brine released from the membrane retentate side[2]. The high pressure sea water is then divided in a set of osmosis membranes working in parallel where pure water is separated and eventually stored in a pool or a tank. Generally, a second stage at a lower pressure is used to maximize the system productivity. The RO specific electric consumption ranges between 3.5 and 5 kWh_{el}/m^3 (IRENA, 2012b) depending on many factors like turbomachine efficiency, membrane configuration and retentate-feed ratio. In the future RO consumption is expected to touch 2.5 kWh_{el}/m^3 (Bartels and Andes, 2013; Schallenberg-Rodriguez, Veza, and Blanco-Marigorta, 2014), but in this work a value of 4.2 kWh_{el}/m^3 is considered to represent the current average scenario. This is the most common MG configuration for production

[2]In recent years, pressure exchangers are the most common solutions and have replaced turbopumps because of the higher system efficiency (Schallenberg-Rodriguez, Veza, and Blanco-Marigorta, 2014)

Month			Jan	Feb	Mar	Apr	May	Jun	Jul	Aug	Sep	Oct	Nov	Dec	Year
Ambient temperature		°C	17.9	18.1	18.6	19.2	20.5	22.3	24.6	25	24.3	22.4	20.7	18.7	21
GHI		kWh/m^2day	4.93	5.76	6.15	6.14	6.81	6.72	7.17	7.35	6.58	6.06	5.41	4.82	6.16
DNI		kWh/m^2day	3.69	4.52	5.56	6.17	6.89	7.12	7.27	6.95	6.05	4.92	3.94	3.43	5.55
Inhabitants		-	8400	8400	8400	8400	8400	10200	11400	12000	10200	8400	8400	8400	9256
Water		m^3/day	3424	3424	3995	3995	4565	5543	6196	6522	5543	4280	3424	3424	4536
	Peak	$m^3/hour$	240	243	276	284	320	388	434	457	388	300	242	241	457
Electricity		MWh/day	40.2	40	40.2	40	41	52.7	71	75.4	60.1	43.5	40.5	40	48.7
	BN	MWh/day	40.2	40	40.2	40	40.4	50.6	62.1	65.2	54	42.1	40.3	40	46.3
	ACN	MWh/day	0	0	0	0	0.6	2.1	8.9	10.2	6.1	1.4	0.2	0	2.5
	Peak	MW	4.12	4.04	4	4.19	4.16	5.16	7.08	6.77	5.84	4.16	4.02	4.16	7.08

TABLE 7.1: Monthly weather data and microgrid goods demand

of both electricity and potable water but it totally relies on fossil fuel with issues in terms of sustainability and operational costs.

One possible improvement of this MG configuration is to exploit the available heat recoverable from the ICEs to produce potable water with a Multi Effect Distillation (MED) system. MED consists in a series of chambers at different pressure where pure water is evaporated from brine. The highest temperature chamber uses the heat provided by an external source while in the other chambers the heat is provided by the condensation of the steam produced in the previous one. To produce 1 cubic meter of desalinated water the MED technology requires 60 $kWh_t h$ (usually in the range 55-70 °C) and 1.5 kWh_{el} (Ophir and Lokiec, 2005; Gude, Nirmalakhandan, and Deng, 2010) thus allowing for a considerable reduction of the electrical consumptions compared to RO technology.

Considering reasonable values for a MW-scale diesel CHP engine we assume an electrical and thermal efficiencies respectively equal to 43.7% and 35.9%[3]. With these efficiencies and assuming to use the electricity only for water production, we calculated that the installation of an integrated ICE+(RO&MED) instead of an ICE+RO system allows to produce a higher amount of water (+3.70%) starting from the same fossil fuel amount thanks to the possibility of exploiting the waste heat with potential economic as well as environmental benefits.

With the aim of further reducing the fuel consumptions, renewable energy generators can be introduced. The present work is focused on the exploitation of solar energy by comparing two different technologies namely photovoltaic panels (PV) and Concentrating Solar Power technology coupled with an Organic Rankine Cycle (CSP-ORC).

In the first case, electricity is produced by conventional policrystalline silicon cell modules in DC and it is converted in AC with an inverter and/or directly stored in an electrochemical storage made by a set of lithium-ion batteries.

In the second case, instead, solar energy is collected by a Solar Field (SF) made by arrays of SkyFuel-SkyTrough collectors loops with 2008 Schott PTR70 Vacuum receiver. Dowtherm A is used as Heat Transfer Fluid (HTF) because of its low freezing point temperature and it is heated up in the SF from a temperature of 180°C up to 300°C. The solar field area is calculated knowing the thermal power required by the ORC at full load, assuming a Direct Normal Irradiation (DNI) equal to 800 W/m^2 and possibly considering an opportune Solar Multiple (SM)[4]. The thermal energy can directly feed an Organic Rankine Cycle (ORC) or it can be stored in a thermal Energy Storage (TES). The TES system is designed as a single tank thermocline filled with quartzite sand with the goal of reducing the total mass of HTF.

ORC is a well-established technology that it is able to efficiently exploit medium low temperature heat sources having a small available heat. Compared to geothermal and biomass fields, CSP-ORC applications are still limited (E. Macchi and M. Astolfi, 2016) because this technology shows a nominal sun-to-electric efficiency comparable to PV but it requires a more complex and costly system. However, CSP-ORC can use a high efficiency storage with a high efficiency storage. It is expected that, in off-grid application, this capability could play a

[3]Low temperature heat is available from the cooling of (i) the flue gases, (ii) the engine cooling water and lubricating oil circuits, (iii) the Exhaust Gas Recirculation loop and (iv) the Charge Air Cooler

[4]Solar multiple is the ratio between the actual solar field area and the solar field area required to operate the power block at full load with nominal DNI. It is always greater than one

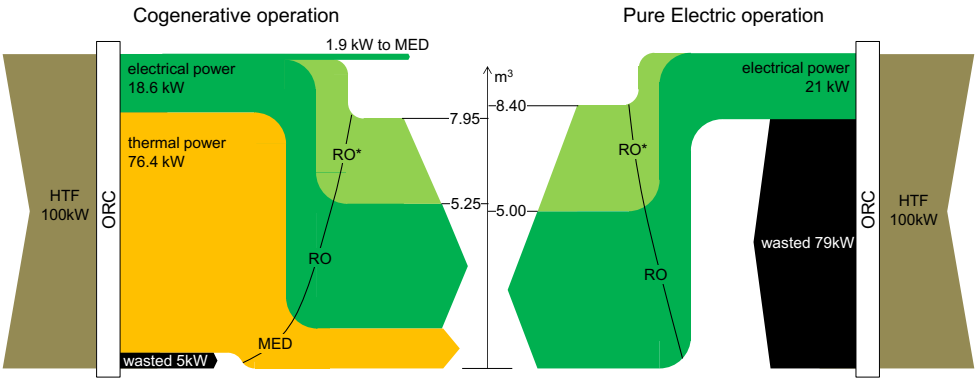

FIGURE 7.3: Sankey diagrams for potable water production for the ORC working in cogenerative mode (on the left) and in pure electric mode (on the right). Light green represents the additional potable water produced with a more efficient RO system. (Mazzola, Marco Astolfi, P. Silva, et al., 2017)

relevant role, leading to higher annual performance and possibly a lower Levelized Cost of Electricity (LCOE).

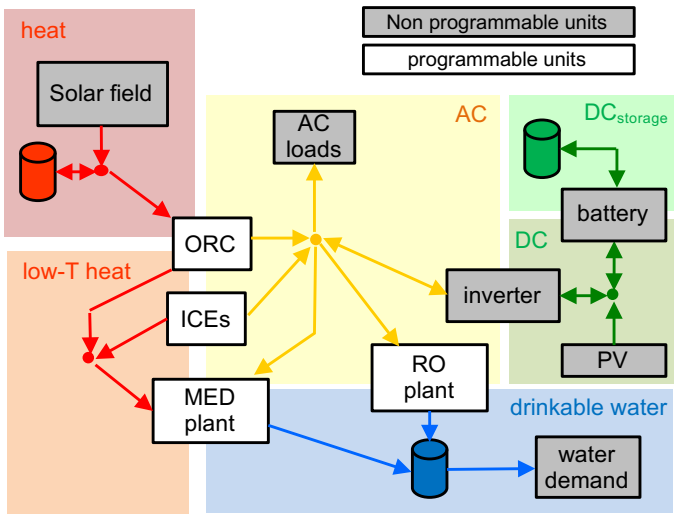

FIGURE 7.4: Multigood model representation of the system

In the present case, the ORC is arranged as a subcritical saturated cycle working with an organic fluid (e.g. pentane). The cycle is recuperative and condensation heat is released to a closed loop of water. Water can eventually release the heat to a MED system or to the sea water with the possibility to operate the ORC in both cogenerative and pure electric production mode. The nominal ORC electrical efficiency is computed assuming a second law efficiency equal to 55%[5] for the cogenerative mode leading to an efficiency value equal to 18.6%. In pure electric production mode, the turbine is expected to have a lower efficiency

[5]Second law efficiency is computed with respect to the reversible Lorenz cycle working between the HTF mean logarithmic temperature and the condensation temperature equal to 65 °C and 30 °C for the cogenerative and the pure electric operation mode respectively

because of the larger enthalpy drop: a small penalization (3 percentage points of the second law efficiency) is accounted and the resulting efficiency is 21%. Fig.7.3 depicts the Sankey diagram of the ORC in both cogenerative and pure electric operation. In case of a RO specific consumption of 4.2 kWh_{el}/m^3 it is convenient to operate the ORC in cogenerative mode recovering the available heat with the MED system. On the opposite, with more efficient RO system (2.5 kWh_{el}/m^3) it is more convenient to produce potable water only by reverse osmosis.

Finally a last MG configuration is analyzed considering both PV and CSP-ORC plants for a higher penetration of Renewable Energy Sources (RES). In all the three hybrid diesel/solar MG configurations a combination of RO and MED can be used in order to better exploit the heat available from both the diesel engines and the ORC in cogenerative operation. The optimal ratio between MED and RO nominal capacities changes depending on the efficiency of RO system and the size of the ORC. Figure 7.4 reports the interconnection between the different components and the goods handled by the MG namely (i) the electricity, (ii) the high temperature heat (stored in the TES), (iii) the low temperature heat and (iii) the potable water. Regarding the above mentioned goods, only DC electricity, high temperature heat and water are considered storable. Among these ones the high temperature heat is the only good which has a loss factor: each hour, 2% of energy stored is lost due to environmental heat transfer. Figure 7.5 depicts the most comprehensive MG while Table 7.2 reports the assumed efficiencies of the different MG components considered in this study.

TABLE 7.2: Nominal and off design performance of the different microgrid components and their minimum load constraints.a) Part load efficiency is defined with a parabolic function in the form $y = A \cdot x^2 + B \cdot x + C$ where x is the percentage of maximum power.

		Nominal index	**value**	**Min load value**	**Part load** ($y = Ax^2 + Bx + c$) **A**	**B**	**C**
ICE		η_{el}	43.7%	25%	-0.17	0.32	0.31
		η_{th}	35.9%		0.17	-0.32	0.51
ORC	**Pure electric**	η_{el}	21.0%	30%	-0.05	0.1	0.16
	T_{cond}=30C				-	-	-
	Cogenerative	η_{el}	18.6%		-0.05	0.09	0.14
	T_{cond}=65C	η_{th}	76%		0.05	-0.091	0.81
RO		kWh_{el}/m^3	4.2	20%	-	-	-
MED		kWh_el/m^3	1.5	40%	-		-
		kWh_{th}/m^3	60		-	-	-
Battery		η_{charge}	95%		-0.05	0.02	0.95
Inverter		$\eta_{AC–DC}$	90%		-	-	-
		$\eta_{DC–AC}$	94%		-	-	-

All the economic assumptions of this study are reported in Table 7.3. The cost of traditional components (ICEs, PV plant, Li-on battery and bi-directional inverters) are obtained from retailers' public websites while Solar Field costs are derived from SAM default values (Kurup and Turchi, 2015). The module cost of the ORC is assumed equal to 1400 USD/kW_el with an exponential coefficient of 0.8, as representative of a multi megawatts cheap ORC unit

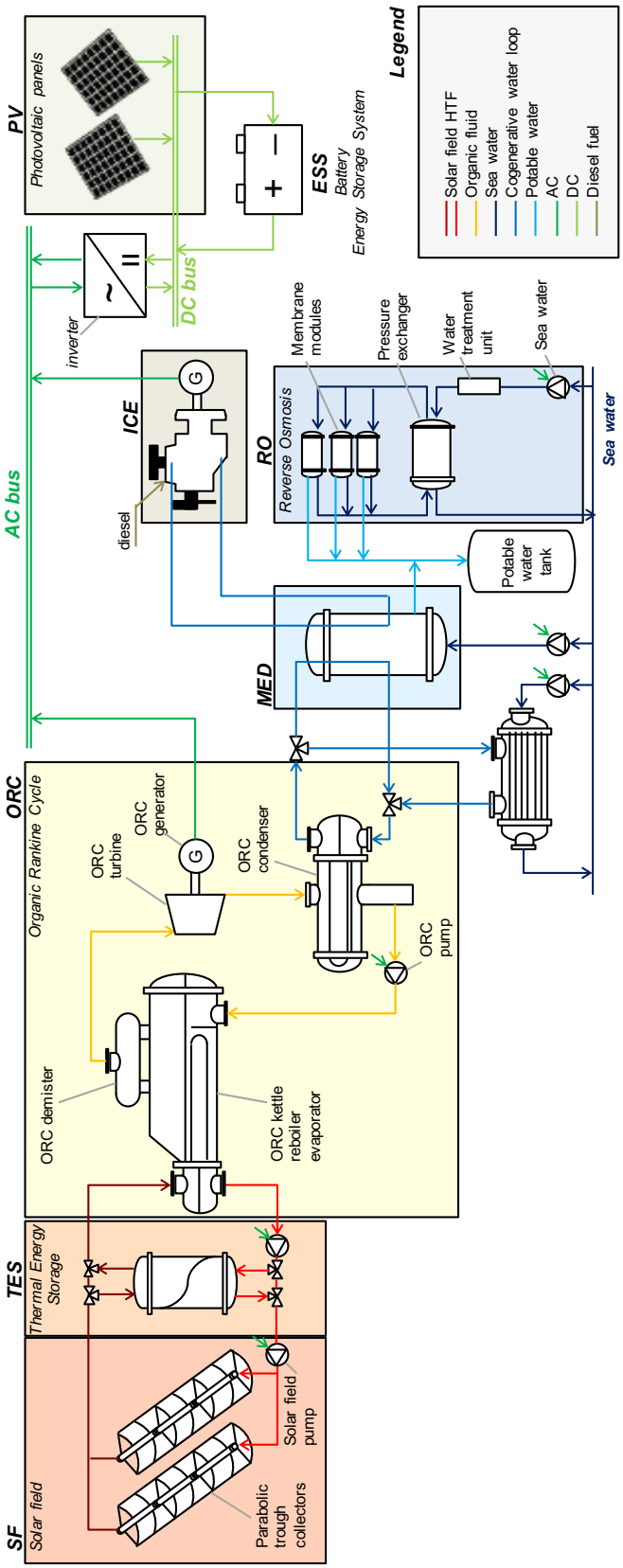

FIGURE 7.5: Scheme of the most comprehensive microgrid analyzed in the study. (Mazzola, Marco Astolfi, P. Silva, et al., 2017)

(Lemmens, 2015). Regarding desalination plants, economic data are obtained from Banat, 2007. In literature no commercial information is available about thermocline storage cost in this range of temperature and sizes because nowadays the two-tanks storage is basically the sole technology adopted in large CSP plants. Few examples of thermocline storages are available for small solar ORC (few kW) with a lower temperature. The specific cost of the present thermocline system is obtained starting from cost information of both conventional double tank storage (Herrmann, Kelly, and Price, 2004) and high temperature thermocline (Pacheco, Showalter, and Kolb, 2002) and applying appropriate scaling factors for the tank material, the fluid and the filling material inventory.

TABLE 7.3: Economic assumptions of the MG components. O&M costs are reported as fraction of up-front costs.

	Up-front costs		**Fixed O&M**	**Lifetime, years**	**k**
ICE	500	USD/kW	10%	10	-
PV	1300	USD/kW	2%	25	0.95
Li-on battery	550	USD/kWh	2%	-	0.95
Inverter	400	USD/kW	2%	15	0.95
ORC	1400	USD/kW	4%	25	0.8
Solar field	260	USD/m^2	4%	25	0.9
TES	43	USD/kWh_{th}	1%	25	0.8
RO	800	USD/(m^3/day)	7%	20	0.95
MED	950	USD/(m^3/day)	4%	20	0.9

7.3 Simulation framework

The methodology used to assess the techno-economic performance of the different MG configurations is the one proposed in Chapter 4. In order to reduce computation time, a time-step of 1 hour have been adopted for the simulation routine. Rolling horizon strategy is based on a sliding time (T_s) of 6 hours, a time horizon (T_h) of 24 hours and a variable time-steps pattern already reported in the last row of Table 4.3.

The optimal MG design is found by investigating different combinations of component size. Except for the ICEs whose sizes are fixed, the MG design requires the definition of 7 parameters: the nominal power of both (i) the PV and (ii) the ORC plants, (iii) the Solar Multiple of the solar field, the capacity of both (iv) the battery and the (v) TES and the nominal productivity of both (vi) the RO and (vii) the MED systems. Water storage capacity is another variable, but we decided to fix to 13000 m^3 (equivalent to 2-days water request in the most demanding month), since it is expected to have a low cost compared to other components and the simulations do not show any advantage in a further increase of the capacity. Many different combinations of components size must be analyzed with the aim of minimizing the MG total annualized cost.

In the present study the latter approach is implemented in order to obtain a clearer representation of the influence of the different variables and avoid local minimum. Table

Table 7.4: Minimum and maximum size of the MG components subject to optimization and step used for the discretization

	Unit		**Min**	**Step**	**Max**
Generation	PV	MW	0	1	16
	ORC	MW	0	1	5
Solar field	Solar multiple	-	1	0.5	3
Storage	Battery	MWh	0	0.5	32
	TES	hours	6	2	12
Desalination	RO	m^3/day	0	500	8000
	MED	m^3/day	0	500	8000

7.4 reports the range of components size investigated in this work. A preselection of the combinations is required in order to exclude those designs that are not feasible like large PV plants without battery or a total desalinated water capacity largely above the maximum daily request.

7.4 Results

In this section, the results of the simulations are shown, highlighting the most important insights.

7.4.1 PV and CSP impact

The influence of size of the two renewable components is shown in Figure 7.6: figures on the left column depict the sensitivity analysis on the PV plant size, figures on the right column the influence of the ORC power output.

Figures 7.6.a and 7.6.b illustrate the influence of the renewable plant size on the RES penetration and on the total yearly expenses respectively. Installing a PV plant has the main advantage of reducing the diesel consumption leading to economic benefits but, on the other hand it involves the use of a battery. For big PV plants the increment of battery size required to properly handle the solar production would strongly penalize the MG economy. As result, the optimization algorithm prefers to dump energy in the central hours of the day instead to adopt a big battery bank that would be over-designed for most of the year. For PV size above 6 MW, a large amount of solar energy is wasted with a consequent limitation of RES penetration and electricity production that still largely relies on diesel engines. We find that the optimal solution for PV is an installed capacity of 6 MW with a battery of 1.5 MWh and a RES penetration close to 40%. A further increase of PV size reduces the savings with respect to the reference (only-Diesel) case because of the limited number of equivalent hours of the PV and almost constant fossil fuel consumption.

Similar considerations can be highlighted for the CSP case: the larger is the ORC the higher is the RES penetration and the lower the fossil fuel consumption. Differently from the

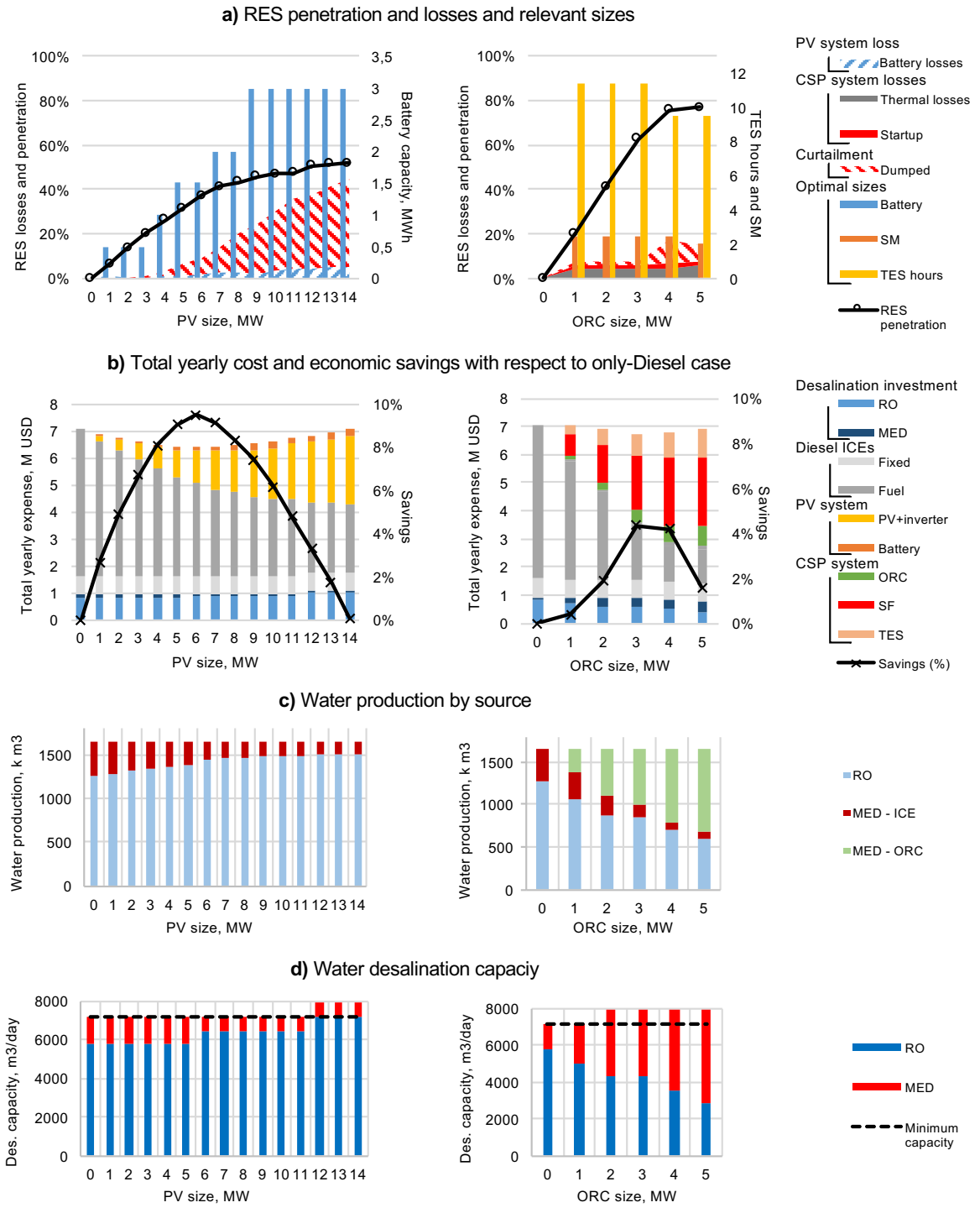

FIGURE 7.6: Optimal configuration properties and performance changing PV size (left column) and ORC size (right column). (Mazzola, Marco Astolfi, P. Silva, et al., 2017)

PV case, the cheaper and more efficient storage system (TES) guarantees a high dispatchability of the solar energy and it allows pushing the RES penetration up to values close to 80%. The optimal size of the ORC is 3 MW with 2.5 SM and 11 hour of TES. Maximum savings in this case are lower than for the PV because of the higher specific cost (USD/kW) of the CSP but this configuration is certainly attractive with the goal of increasing the RES penetration.

Figure 7.6.c depicts the optimal size of both the MED and the RO systems increasing the PV and the ORC size while Figure 7.6.d shows the contribution to water desalination of the two technologies. When all electricity production is obtained by only Diesel engines the most convenient configuration is represented by a MED system that matches the thermal power released by a single ICE and a RO system able to cover the remaining water demand. ICE runs always in cogeneration (unless the water tank is full) and about 20% of potable is produced by MED. Increasing the size of PV, the contribution of MED decreases, following the decrease of available heat from Diesel. However, the MED capacity remains the same until the reduction of the diesel running hours makes a smaller and cheaper MED more attractive.

On the other hand, when a CSP system is added, the MED can be also fed by the condensation heat of the ORC. Increasing the size of the ORC leads to a large size of the MED system, a large share of potable water produced by MED and a reduction of both RO capacity and production.

7.4.2 Intra-day analysis

According to the results obtained, PV and CSP seem to have a different impact on MG operation. For a better understanding of the capabilities of the optimization algorithm in handling different kinds of MG assets, the operation of four different MG configurations are reported in Figure 7.7.a.-d. for two typical days (representative of winter and summer conditions respectively). The first three configurations refer to the cases already described :a) only diesel ICE, b) ICE+PV, c) ICE+CSP while the last configuration d) ICE+PV+CSP is introduced to highlight the synergies achievable using both solar energy plants. For each configuration, we refer to the optimum combination of design parameters.

The upper part of each figure depicts the diagram of the hourly electrical energy generated by the various components and the charge status of the electrochemical and thermal storages, while the lower part depicts how the electricity is used. In the first configuration battery is not used and the optimization algorithm only defines the RO schedule in order to increase the average load and the efficiency of the diesel engines in operation. Potable water production, and hence RO consumption, is modulated during the day and it is usually higher when the electrical consumption (BN+ACN) are low or when the two diesel engines are running together. For a relevant number of hours two engines are in operation while in very demanding days (peak hours in summer high season) the use of all the three generators is required.

For the second configuration (ICE+PV) a battery is indispensable to avoid energy dump. It can be seen that in winter, the energy generated by PV is mainly used in the daily hours: most of the power flows across the inverter while only a small fraction is stored to be used during evening hours. RO is scheduled in the central hours of the day in order to limit the power fluxes through the battery and the associated loss. One diesel engine operates

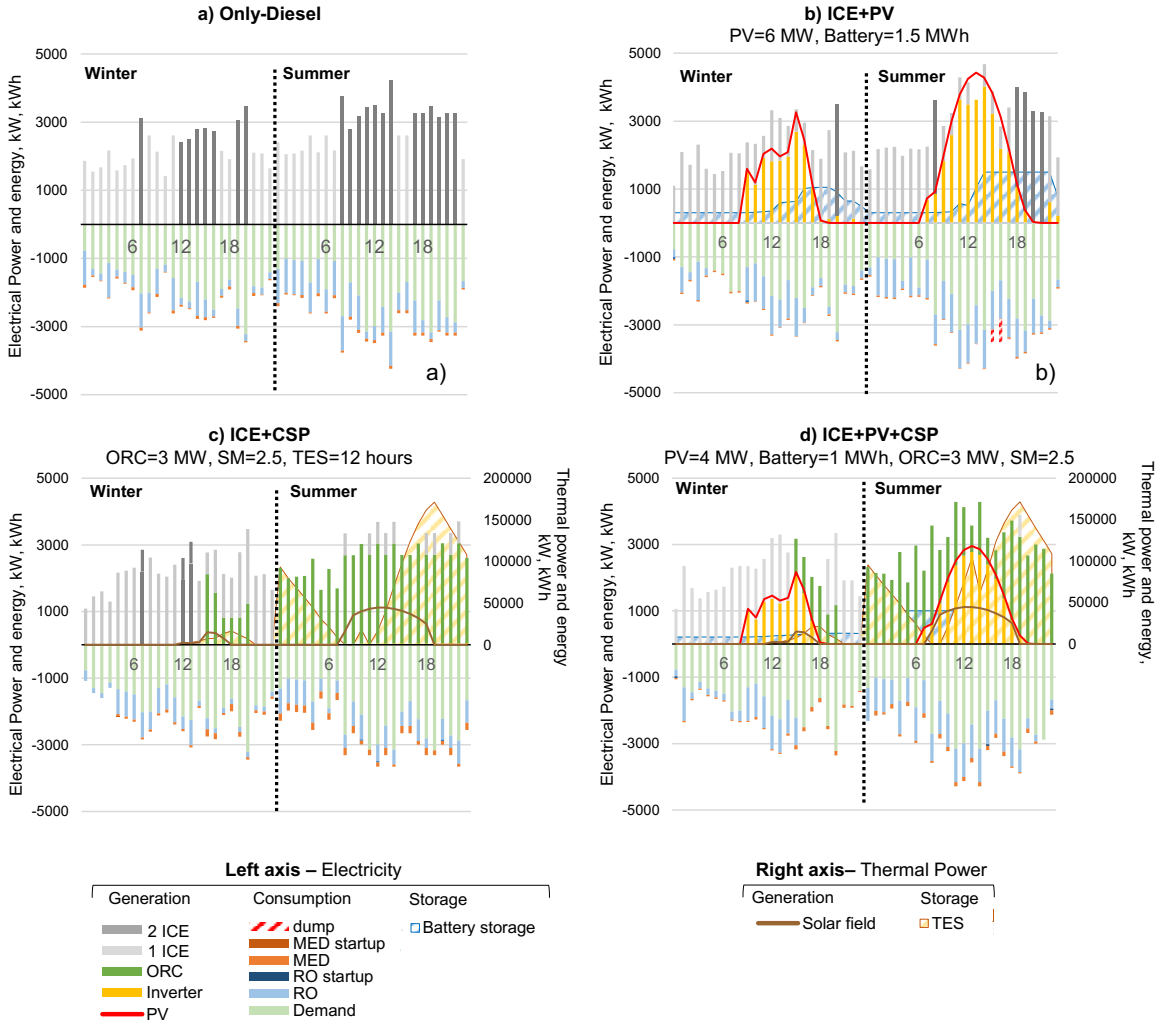

FIGURE 7.7: Two-days optimal schedule for 4 different MG configurations. (Mazzola, Marco Astolfi, P. Silva, et al., 2017)

continuously, while a second one is required only for one hour in the evening. In summer, the PV contribution is larger, but a small amount of energy is dumped due to the limited size of both electrochemical storage and RO. The diesel engine contribution is still large and the algorithm keeps one ICE in operation for most of the day in order to limit the startup cost.

For the third configuration (ICE+CSP), the solar contribution in winter is very limited because of the optical losses that strongly affect liner concentrating collectors. Most of the heat collected feeds directly the ORC, which works in cogenerative mode, while a small fraction is stored in TES to extend the ORC operation in evening hours. In winter season Diesel engines still play a relevant role. On the contrary, in summer the ORC production is capable to cover the majority of the electricity demand thanks to the higher available solar energy and the higher solar collectors' efficiency. A single ICE runs close to the minimum load during the central hours of the day guaranteeing a proper power reserve and during the evening (when the basic needs are higher). During nocturnal hours the diesel is switched off and the battery is discharged. as a general observation, PV technology is characterized by large savings (small

capital cost) but it shows severe issues in dispatching energy because of an expensive storage with a low round trip efficiency leading in the end to a poor RES penetration. On the other hand, the CSP system capital cost is relevant but the high dispatchability of the stored thermal energy gives a great flexibility to the MG management with a consistent reduction of fossil fuel consumption.

In order to mitigate the drawbacks of both PV and CSP plant while combining their strengths a last configuration is investigated. Results are reported in Figure 7.7.d. In winter time PV directly feeds the load assisted by a diesel engine while thermal energy from solar field is stored in the TES. The ORC starts up when the PV production decreases and allows to temporary switch off the ICE. During summer the MG operation almost totally relies on solar energy: in particular PV power directly flows through the inverter while the TES is filled. ORC is in continuous operation in order to limit start up penalizations: it works in load-following during the night while during the day it reduces it load working in cogeneration feeding the MED system.

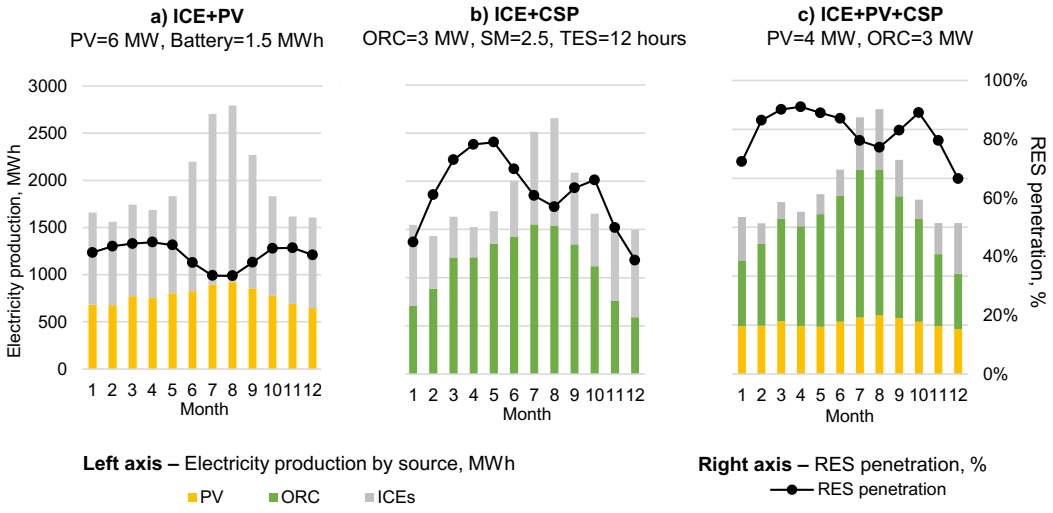

FIGURE 7.8: Monthly trends of electricity production and RES penetration for three MG configurations (ICE+PV, ICE+CSP, ICE+PV+CSP). (Mazzola, Marco Astolfi, P. Silva, et al., 2017)

Figure 7.8.a.-c. illustrate the share of electricity produced by the solar energy and the diesel engine for the two optimal MG configurations and the hybrid configuration (ICE+PV+CSP). PV production is more constant along the year leading to a RES penetration slightly above 40% in the low season and lower values during the summer when the island inhabitants and the electrical load increase. A similar trend is shown for CSP case with a marked drop of RES penetration in winter time because the poor optical efficiency of the Solar Field. Figure 8.c depicts the benefits attainable with the synergic adoption of both PV and CSP. The addition of a CSP system to a PV plant allow to almost double the RES penetration, with values of about 60% in December and January and value close to 80% during all the other months.

7.4.3 RES specific cost and LCOE trends

Additional hints about RES impact can be found evaluating the RES specific cost. The index is representative of the specific annualized cost of the RES power plant and it is equal to the sum of all the expenses (annualized fixed and variable costs) of the RES system divided by the fraction of energy produced which is effectively used to cover the electricity demand, defined as the difference between the total electricity consumed and the electricity produced from diesel generators (see Eq. 7.1). Battery and TES costs are considered as well in the calculation of PV and CSP specific cost respectively. Moreover this index includes the energy losses due to the efficiency of the storage system and the energy dumps due to its limited size.

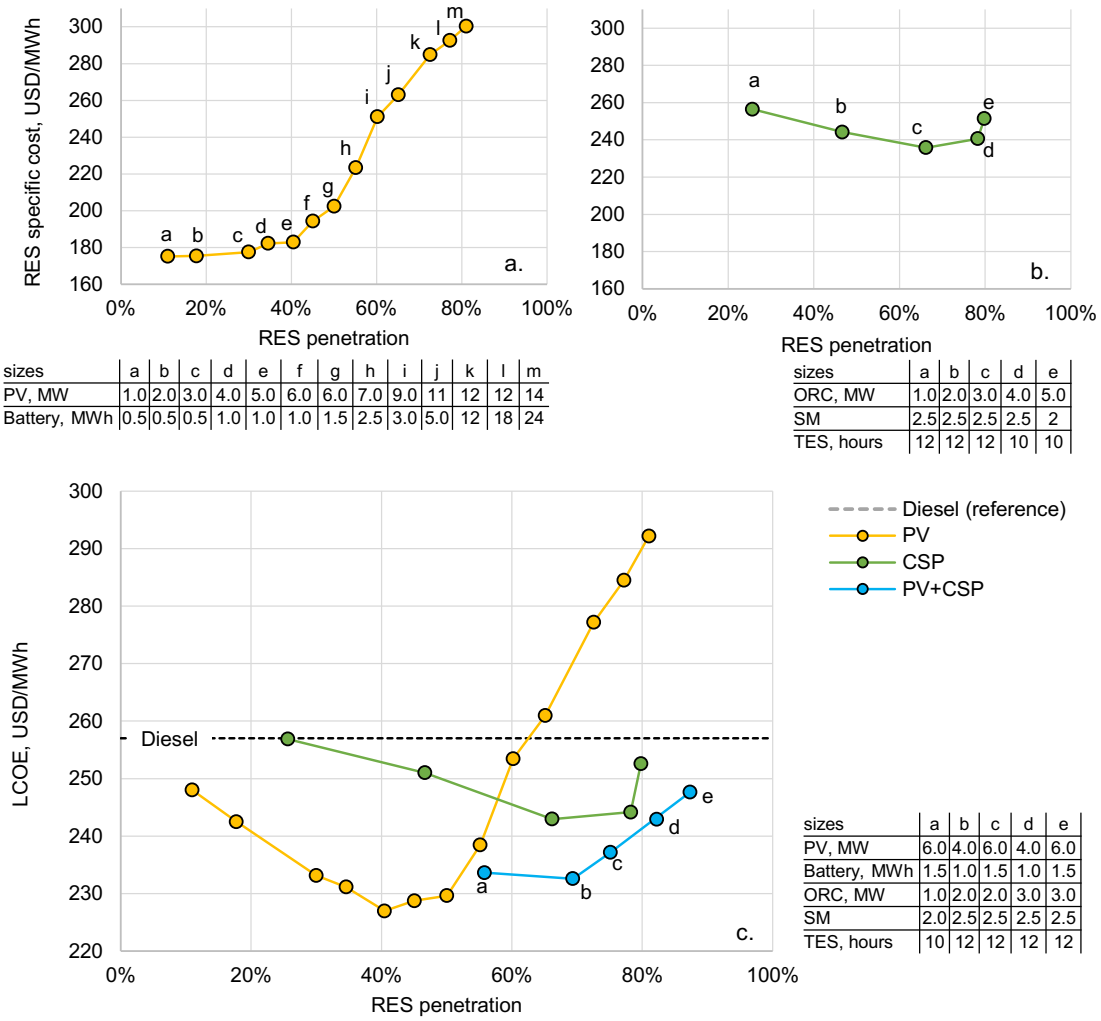

sizes	a	b	c	d	e	f	g	h	i	j	k	l	m
PV, MW	1.0	2.0	3.0	4.0	5.0	6.0	6.0	7.0	9.0	11	12	12	14
Battery, MWh	0.5	0.5	0.5	1.0	1.0	1.0	1.5	2.5	3.0	5.0	12	18	24

sizes	a	b	c	d	e
ORC, MW	1.0	2.0	3.0	4.0	5.0
SM	2.5	2.5	2.5	2.5	2
TES, hours	12	12	12	10	10

sizes	a	b	c	d	e
PV, MW	6.0	4.0	6.0	4.0	6.0
Battery, MWh	1.5	1.0	1.5	1.0	1.5
ORC, MW	1.0	2.0	2.0	3.0	3.0
SM	2.0	2.5	2.5	2.5	2.5
TES, hours	10	12	12	12	12

FIGURE 7.9: RES specific cost and LCOE as a function of RES penetration. The single points represent the optimal sizes for a given RES penetration range. (Mazzola, Marco Astolfi, P. Silva, et al., 2017)

$$\text{RES specific cost} = \frac{C_{fix,RES} + C_{var,RES}}{E_{consumed} - E_{ICE}} \tag{7.1}$$

Figure. 7.9.a-b illustrate the RES specific cost for MGs provided by a PV plant and a CSP plant respectively. The configurations shown in this case represent the most cost-effective sizes combination for a given RES penetration (on the x-axis).

PV is the solar technology with the lowest specific cost (around 175 USD/MWh) but it allows achieving a limited RES penetration. In order to reduce the fossil fuel consumption the size of the PV must be increased and this lead to a rapid soar of the battery capacity and a consequent increment of capital and maintenance costs. For small PV sizes the energy produced can be easily handled by a proper schedule of the dispatchable loads or with a small battery, while if the PV rated power is largely above the AC load peak a very big battery is required to accommodate the energy surplus and to increase RES penetration. Battery is used more intensively with a marked wear that impact on the RES specific cost. For RES penetration above 40% we assist to a marked soar of the PV specific cost highlighting that a MG cannot rely only on PV technology and be economically feasible at the same time.

CSP technology instead is more capital intensive, hence its specific cost is higher than PV for small plant sizes. However, increasing the size of both the solar field and the ORC allows achieving high RES penetration values with a RES specific cost that decreases thanks to the favorable scale economies. In this case it is possible to reach RES penetration close to 80% but a further increase leads is not possible because of the availability and reliability of the system and the solar mirrors defocusing in the days with high DNI.

Finally, Figure 7.9.c depicts the LCOE trends in relation to RES penetration for three MG configurations: the first provided with PV, the second with CSP and the third with a combination of both. LCOE is defined considering the annual expenses for all the MG components (including the desalination systems) divided for a constant amount of energy in order to fairly compare the different configurations. The LCOE of a MG provided only by diesel engines is reported for comparison.

ICE+PV configuration shows the highest savings for a RES penetration around 40-50%, but becomes noncompetitive respect to diesel for RES penetration above 60%. CSP, despite the lower attainable savings, allows to strongly reduce the fossil fuel consumption still remaining competitive up to 80%. Finally, calculations show that with a synergic use of both solar systems it is possible to reach values close to 230 USD/kWh, similar to the ones obtained by the best PV solution, but with a much higher RES penetration (about 70% vs 40%). Moreover it would be possible to break the limit of 80% RES penetration with still relevant economic savings respect to the reference only Diesel case.

7.5 Conclusions

This chapter aims at highlighting the advantages of combining different desalination technologies and different solar power systems in a stand-alone microgrid for both electricity and potable water production. Although the study focuses only on single test case, it is expected that the found qualitative trends are representative of a common situation for relatively high

irradiation islands whereby a significant fraction of the energy demand is devoted to water desalination. The conclusions can be summarized in the following points:

- Solar energy plants and desalination units can be integrated in a synergic way provided that their schedule must be optimized by an advanced Energy Management System (EMS). The EMS should be able to take into account weather and loads forecast exploiting the possibility of translating the energy required by RO plants in the sunniest hours and limiting the use of the battery. The rolling horizon approach developed in this thesis coupled with a 24h Unit Commitment problem formulated as MILP resulted in an accurate and fast method for this case

- Both PV and CSP-ORC technologies allow reducing overall electricity cost while increasing the penetration of RES. In particular the PV panels + inverter specific cost have been consistently reduced in the last ten years making this technology extremely attractive until the energy produced can be directly used by the RO plant instead of stored. PV technology is indicated for RES penetration below 40%. Above this threshold the combined effects of larger energy storages and a higher amount of dumped energy lead to a soars of annualized cost. CSP technology allows for smaller savings compare to PV because the very high investment cost. On the other hand, the use of a TES permits to operate the ORC in a flexible way with the possibility to dispatch energy in an easy and cheap way. This technology benefits from scale economies and working in cogeneration allows for an effective integration with MED system.

- Synergies between all the above mentioned technologies are very promising. The combination of the two solar plant systems, i.e. PV and CSP-ORC, takes advantage from the characteristics of both technologies: the former that generates electricity at a low cost during high irradiation hours and the latter that permits to extend the operation in night hours thanks to low the cost thermal storage. On the other hand, the combination of the two desalination plant technologies, i.e. reverse osmosis and multi effect distillation, leads to a synergic integration with the solar power systems. RO is adequate for peak-shaving allowing for a reduction of electrochemical battery capacity while the MED is capable of benefiting of "free" low temperature heat recoverable by power cycles.

The result is the possibility of fulfilling the electricity and potable water demand of the island community with a very high (>80%) RES penetration at lower overall cost than the traditional, fossil fuel based, solution.

Chapter 8

Conclusions

As already reported in the Introduction, the core objectives of this thesis are two. The first one was to develop innovative mathematical tools to efficiently operate and simulate off-grid microgrids operation. The most important capabilities and features are the following:

- units scheduling based on forecast-based optimization
- detailed representation of components behavior (e.g. startups, battery wear)
- capability to handle advanced microgrids architectures, with multiple valuable goods
- limited computation time, compatible with real operation and long-term simulation

The state of the art analysis showed that such a tool was not present in literature and it has been developed from scratch using AMPL optimization language. The final model is capable to operate and simulate advanced microgrid architectures taking into account not only electricity request, but also other valuable goods as heating and potable water. This capability represents an innovative aspect in forecast-based optimization of off-grid microgrids, since it allows to efficiently exploit the possible synergies among all the components and it has the potential to reduce the operation costs (see Figure 4.5 on page 64 for a multi-good system example). In addition to this, the forecast-based optimization model has been embedded in a simulation framework based on a rolling horizon approach, which allows to simulate the long-term behavior of complex microgrids using an optimization model for scheduling with a limited time horizon for forecasts (as in reality).

State of the art models describing the wear and the kinetics of the battery energy storage, which is one of the key component of an off-grid energy system, have been embedded in the optimization problem, as well as start-up constraints and costs for components as diesel generators and biomass boilers. Despite of the increasing complexity of the optimization problem, computation time are sufficiently low for real operation and, using expedients as variable time steps unit commitment, the model can be effectively used to perform long-term simulations and system design. As shown in Table 4.3, variable time steps allow to reduce computation time up to 80% with a very limited increase of the operation costs calculated (less than 2.3%) and, for this reason, they have been successfully applied in the final steps of the work, more focused on long-term simulations and design optimization.

The potential cost savings in operation related to the developed model in comparison with standard non-predictive approaches was evaluated. The first example considered was a

two-days operation of a standard microgrid simulated using the proposed model with exact forecast and the most common non-predictive strategies. The results show that the model proposed allows to obtain a cost saving around 10% compared with traditional approaches (see Figure 5.2); if start-up penalization are considered the potential saving is even higher (13%). In a second example, the effect of forecast accuracy is investigated, performing long-term simulations (365 days). Results show that considerable cost savings on microgrid operation (4-8%) are achievable, especially in microgrids with a high share of renewable energy sources (RESs). On the other hand, the study highlights that these savings are strictly related to the forecast accuracy and the potential advantage could vanish in the case of low quality forecasts. Another important point emerged from calculations is that the dispatch strategy used for the simulation has an impact of the optimal sizing of the microgrid. In fact, using standard non-predictive approaches lead to conservative sub-optimal solutions, in which the share of RES is limited. Note that these results have been obtained temporally removing some key features of the models only to make it comparable with state of the art models. The advantages obtainable in advanced multigood microgrids are expected to be higher, as shown in the two final test cases of the thesis.

The second main objective was to investigate the possibility to increase RES penetration in remote contexts in a cost-effective way, exploring the two following alternatives:

- load scheduling to cope with the intermittency of RES as PV
- feasibility of dispatchable RES generators, taking into account biomass-based systems and CSP[1]

Both possibilities were studied applying the developed mathematical model on two test-cases, a rural village in a developing country and a community in an island. Despite of the considerable differences between the two test-cases, the insights coming from the results are the same. First of all, the studies show that advanced models used for microgrid operation allows to handle efficiently a large amount of intermittent RES, as PV. In fact, the possibility to shift in time a part of the loads helps match the RES production, reducing the curtailment and the battery usage. In the case of the rural village this possibility is given mostly by the irrigation needs (see Figure 6.5 on 108); thanks to a relatively inexpensive water tank, it is possible to shift in time the energy consumption by the pumps without changing the water supply schedule. In the case of the island, same synergy can be found with desalination units, which are responsible of a relevant share of total electricity consumption (10-20%) and can be shifted in time using a potable water storage. However, even using this possibility, the RES share reachable using only PV is limited (<50%) due to the fact that a massive usage of battery storage, with the consequent expenses, is requested to increase RES penetration.

The other possibility investigated is the use of programmable RES generators. In particular, the implantation of wood biomass generators was considered for the rural village while

[1]CSP can be dispatchable only if a thermal energy storage is present. However, due to the low cost of thermal energy storage (TES) compared to other energy storages (as batteries), the TES has always been considered and the CSP has been listed as a dispatchable source.

the use of Concentrating solar power technology (provided with a thermal energy storage) was taken into account for the island community. In both cases, the dispatchable generators are able to reach considerably higher RES share (>60%) offering a considerable cost reduction compared to the only-diesel case. Despite these technologies have a higher LCOE than PV if connected to a grid with infinite capacity, their capability to produce energy when it is really needed represents an important advantage in off-grid contexts. Finally, test-cases show that the most cost-effective configurations to reach high RES penetration are hybrid ones. A proper balance of intermittent and dispatchable RESs is the best option, benefiting of low energy cost of the former and the dispatchability of the latter to cover most of the electricity requests (see Figure 7.9 on page 132).

List of acronyms

ANPC . . . . . Annualized net present cost
BESS . . . . . Battery energy storage system
BOS . . . . . Balance of system
CAES . . . . . Compressed air energy storage
CC . . . . . Cycle charging
CHP . . . . . Combined heat and power
CSP . . . . . Concentrating solar power
DoD . . . . . Depth of discharge
ES . . . . . Energy storage
HTF . . . . . Heat transfer fluid
ICE . . . . . Internal combustion engine
IEA . . . . . International Energy Agency
IRENA . . . . . Internation Renewable Energy Agency
LCOE . . . . . Levelized cost of electricity
LCOS . . . . . Levelized cost of storage
Li-ion . . . . . Lithium ion
LF . . . . . Load following
MED . . . . . Multi-effect distillation plant
MG . . . . . Microgrid
MILP . . . . . Mixed-Integer Linear Programming
MINLP . . . . . Mixed-Integer Non-Linear Programming
NRMSE. . . . . Normalized root mean square error
NPS . . . . . Non-predictive strategy
NPV . . . . . Net present value
ORC . . . . . Organic Rankine Cycle
OS-UC . . . . . One-shot unit commitment
PS . . . . . Predictive strategy
PV . . . . . Photovoltaic
RES . . . . . Renewable energy source
RH . . . . . Rolling horizon
RO . . . . . Reverse osmosis
SM . . . . . Solar multiple
TES . . . . . Thermal energy storage
T_h . . . . . Time horizon
T_s . . . . . Sliding time
USD . . . . . United States dollar
WT . . . . . Wind turbine

Appendix A

Table A.1: List of CSP projects below 5 MW worldwide in 2015

Project name	**Country**	**Technology**	**TDN cycle**	**Year**	**HTF**	**Power, MW**
Maricopa Solar Project	US	Dish/Engine	Stirling	2010	-	1.5
Tooele Army Depot	US		Stirling	2013	Helium	1.5
Augustin Fresnel 1	FR	Linear Fresnel	Steam Rankine	2012	Water	0.25
Rende-CSP Plant	IT		Organic Rankine	2014	Diathermic oil	1
Kimberlina Solar Thermal Power Plant	US		Steam Rankine	2008	Water	5
Saguaro Power Plant	US	Parabolic trough	Organic Rankine	2006	Xceltherm 600	1
National Solar Thermal Power Facility	IN		Steam Rankine	2012	Therminol VP-1	1
City of Medicine Hat ISCC Project	CA		-	2014	Xceltherm®SST	1.1
Holaniku at Keahole Point	US		Steam Rankine	2009	Xceltherm-600	2
Colorado Integrated Solar Project	US		Solar hybrid	2010	Xceltherm® 600	2
Stillwater GeoSolar Hybrid Plant	US		Organic Rankine	2015	-	2
Airlight Energy Ait-Baha Pilot Plant	MA		Organic Rankine	2014	Ambient air	3
Archimede	IT		-	2010	Molten salt	4.72
Thai Solar Energy 1	TH		-	2012	Water/Steam	5
Dahan Power Plant	CN	Power tower	Steam Rankine	2012	Water/Steam	1
Greenway CSP Mersin Tower Plant	TR		Steam Rankine	2012	Water	1
Jülich Solar Tower	DE		-	2008	Air	1.5
Sundrop CSP Project	AU		Steam Rankine	2016	Water/Steam	1.5
ACME Solar Tower	IN		Steam Rankine	2011	Water/Steam	2.5
Lake Cargelligo	AU		Steam Rankine	2011	Water/Steam	3
Sierra SunTower	US		Steam Rankine	2009	Water	5

Table A.2: Test-case components properties - Chapter 4.1.3

UNIT	Produced good	P_{min}		P_{rate}		Consumed good		$C(P_{min})$	$C(P_{max})$	$c_{startup}$	PW	m	q
Boiler	Heat	400	-	800	kWh	Woodchips	kg	100.6	193.2	25	1	0.23	8.05
						Money	USD	4.0	6.8	4	1	0.01	1.24
RO plant	Water	3.5	-	7	m^3	AC	kWh	14.0	28.0	0	1	4.00	0.00
Inverter	AC	0	-	250	kWh	DC	kWh	0.0	260.4	0	1	1.04	0.00
	DC	0	-	250	kWh	AC	kWh	0.0	260.4	0	1	1.04	0.00
Battery	DC	0	-	250	kWh	$DC_{storage}$	kWh	0.0	396.4	0	1	1.18	0.00
											2	1.63	-10.86
	$DC_{storage}$	0	-	250	kWh	DC	kWh				1	1.18	0.00
											2	1.63	-10.86
Icemaker	Ice	250	-	250	kg	AC	kWh	10.0	10.0	1	1	0.00	10.00
						Water	m3	0.0	0.0	0	1	0.00	0.01
Chipper	Woodchips	250	-	500	kg	AC	kWh	2.5	5.0	0.2	1	0.01	0.00
						Money	USD	1.0	1.0	1	1	0.00	1.00
ORC	AC	50	-	100	kWh	Heat	kWh	482.5	852.8	0	1	7.80	73.10
											2	7.02	131.58
						Money	USD			0.5	-	-	-

UNIT	Produced good	P_{min}		P_{rate}		Consumed good	$C(P_{min})$	$C(P_{max})$	$c_{startup}$	PW	m	q
ICE	AC	50	-	100	kWh	Money	9.8	15.7	1.88	1	0.11	4.12
										2	0.12	3.55
ICE_{aux}	AC	50	-	100	kWh	Money	9.8	15.7	1.88	1	0.11	4.12
										2	0.12	3.55
RO plant	Water	0	-	7	m3	AC	0.0	28.0	-	1	4.00	0.00
						Money	-	-	0.2	-	-	-
Inverter	AC	0	-	180	kWh	DC	0.0	187.5	-	1	1.04	0.00
	DC	0	-	180	kWh	AC	0.0	187.5	-	1	1.04	0.00
Battery	DC	0	-	50	kWh	$DC_{storage}$	0.0	58.8	-	1	1.18	0.00
										2	1.63	-36.20
	$DC_{storage}$	0	-	50	kWh	DC	0.0	58.8	-	1	1.18	0.00
										2	1.63	-36.20

Table A.3: Test-case components properties - Section 5.1

TABLE A.4: Test-case components properties - Section 6

UNIT	Produced good	P_{min}		P_{rate}		Consumed good		$C(P_{min})$	$C(P_{max})$	$c_{startup}$	Time
Water pump	Ground water	0	-	259	m^3	AC	kWh	0.0	30.0	-	-
RO plant	Potable water	3.5	-	14	m^3	AC Ground water	kWh m3	3.8 3.9	15.0 15.4	-	-
Chipper	Woodchips	500	-	500	kg	AC	kWh	6.3	6.3	-	-
Heat pump	HT-Heat	4.2	-	14	kWh	AC	kWh	0.7	3.4	-	-
Chiller	Cold	53.4	-	178	kWh	AC	kWh	4.9	24.8	-	-
ICE	AC LT-Heat HT-Heat	30 38 38	-	200 112.5 112.5	kWh kWh kWh	Diesel	USD	12.6	50.3	8.4	10 min
Boiler	Oil-Heat	0.5	-	variable	kWh	Woodchips	kg/kW USD/kW	0.1 0.007	0.3 0.014	0.3	60 min
ORC (EL)	AC	0.3	-	variable	kWh						
ORC (CHP)	AC LT-Heat	0.24 1.0	-	0.8 3.2	kWh/kW kWh/kW	Oil-Heat	kWh_{oil}/kW	1.6	5.0	3.3	40 min
Gasifier+ICE	AC LT-Heat	0.5 1.0	-	variable 1.2	kWh/kW kWh/kW	Woodchips Money	kg/kW USD/kW	0.9 0.0	1.3 0.1	0.6 0.0	30 min

Bibliography

Aguiar, R and M Collares-Pereira (1992). "TAG: A time-dependent, autoregressive, Gaussian model for generating synthetic hourly radiation". In: *Solar Energy* 49.3, pp. 167–174.

Allen, R G et al. (1998). "Crop evapotranspiration: guidelines fo computing crop water requirements. Irrigation and Drainage Paper 56." In: p. 300.

Astolfi, Marco (2014). "An innovative approach for the techno-economic optimization of organic rankine cycles". PhD. Politecnico di Milano.

Baldick, R. (1995). "The generalized unit commitment problem". In: *IEEE Transactions on Power Systems* 10.1, pp. 465–475.

Banat, Fawzi (2007). "Economic and technical assessment of desalination technologies". In: *IWA Conference-New Technologies for Water and ...*

Barbato, Antimo et al. (2014). "A framework for home energy management and its experimental validation". In: *Energy Efficiency* 7.6, pp. 1013–1052.

Bartels, Craig R. and Keith Andes (2013). "Consideration of energy savings in SWRO". In: *Desalination and Water Treatment* 51.4-6, pp. 717–725.

Bekele, Getachew and Björn Palm (2010). "Feasibility study for a standalone solar–wind-based hybrid energy system for application in Ethiopia". In: *Applied Energy* 87.2, pp. 487–495.

Bertsimas, Dimitris et al. (2013). "Adaptive Robust Optimization for the Security Constrained Unit Commitment Problem". In: *IEEE Transactions on Power Systems* 28.1, pp. 52–63.

Bhuiyan, M. M H and M. Ali Asgar (2003). "Sizing of a stand-alone photovoltaic power system at Dhaka". In: *Renewable Energy* 28.6, pp. 929–938.

Bischi, Aldo et al. (2014). "A detailed MILP optimization model for combined cooling, heat and power system operation planning". In: *Energy* 74, pp. 12–26.

BP (2016). *BP Statistical Review of World Energy*. Tech. rep. June, pp. 1–48.

Bracco, Stefano, Federico Delfino, et al. (2014). "A mathematical model for the optimal operation of the University of Genoa Smart Polygeneration Microgrid: Evaluation of technical, economic and environmental performance indicators". In: *Energy* 64, pp. 912–922.

Bracco, Stefano, Gabriele Dentici, and Silvia Siri (2013). "Economic and environmental optimization model for the design and the operation of a combined heat and power distributed generation system in an urban area". In: *Energy* 55, pp. 1014–1024.

Bruno, J C et al. (1998). "A Rigorous {MINLP} Model for the Optimal Synthesis and Operation of Utility Plants". In: *Chem. Eng. Res. Des.* 76.3, pp. 246–258.

Bueno, C. and J.A. Carta (2005). "Technical–economic analysis of wind-powered pumped hydrostorage systems. Part II: model application to the island of El Hierro". In: *Solar Energy* 78.3, pp. 396–405.

Bunker, Kaitlyn et al. (2015a). *Renewable Microgrids: Profiles from Islands and Remote Communities Across the Globe*. Tech. rep. November. Rocky Mountain Institute.

Bunker, Kaitlyn et al. (2015b). "Renewable Microgrids: Profiles from Islands and Remote Communities Across the Globe". In: November.

Buragohain, Buljit, Pinakeswar Mahanta, and Vijayanand S. Moholkar (2010). "Biomass gasification for decentralized power generation: The Indian perspective". In: *Renewable and Sustainable Energy Reviews* 14, pp. 73–92.

Carapellucci, Roberto and Lorena Giordano (2013). "A methodology for the synthetic generation of hourly wind speed time series based on some known aggregate input data". In: *Applied Energy* 101, pp. 541–550.

Cardona, E., A. Piacentino, and F. Marchese (2007). "Performance evaluation of CHP hybrid seawater desalination plants". In: *Desalination* 205.1-3, pp. 1–14.

Chaouachi, Aymen et al. (2013). "Multiobjective Intelligent Energy Management for a Microgrid". In: *IEEE Transactions on Industrial Electronics* 60.4, pp. 1688–1699.

Chen, C. et al. (2011). "Smart energy management system for optimal microgrid economic operation". In: *IET Renewable Power Generation* 5.3, p. 258.

Chung, Donald et al. (2015). "U.S. Photovoltaic Prices and Cost Breakdowns : Q1 2015 Benchmarks for Residential , Commercial , and Utility-Scale Systems". In: *National Renewable Energy Laboratory* September.

Dai, Ran and Mehran Mesbahi (2013). "Optimal power generation and load management for off-grid hybrid power systems with renewable sources via mixed-integer programming". In: *Energy Conversion and Management* 73, pp. 234–244.

D'Ambrosio, Claudia, Andrea Lodi, and Silvano Martello (2010). "Piecewise linear approximation of functions of two variables in MILP models". In: *Operations Research Letters* 38.1, pp. 39–46.

Dasappa, S. et al. (2011). "Operational experience on a grid connected 100kWe biomass gasification power plant in Karnataka, India". In: *Energy for Sustainable Development* 15.3, pp. 231–239.

Delarue, Erik and William D'haeseleer (2008). "Adaptive mixed-integer programming unit commitment strategy for determining the value of forecasting". In: *Applied Energy* 85.4, pp. 171–181.

Demirbas, M. Fatih, Mustafa Balat, and Havva Balat (2009). "Potential contribution of biomass to the sustainable energy development". In: *Energy Conversion and Management* 50.7, pp. 1746–1760.

Dennis Barley, C. and C. Byron Winn (1996). "Optimal dispatch strategy in remote hybrid power systems". In: *Solar Energy* 58.4-6, pp. 165–179.

Domingo, Carlos Mateo et al. (2011). "A Reference Network Model for Large-Scale Street Map Generation". In: *IEEE Transactions on Power Systems* 26.1, pp. 190–197.

Dong, Leilei, Hao Liu, and Saffa Riffat (2009). "Development of small-scale and micro-scale biomass-fuelled CHP systems – A literature review". In: *Applied Thermal Engineering* 29.11-12, pp. 2119–2126.

Drouilhet, Stephen et al. (1997). "A battery life prediction method for hybrid power applications". In: *35th Aerospace Sciences Meeting and Exhibit*. Reston, Virigina: American Institute of Aeronautics and Astronautics.

Dufo-López, Rodolfo and José L. Bernal-Agustín (2005). "Design and control strategies of PV-Diesel systems using genetic algorithms". In: *Solar Energy* 79.1, pp. 33–46.

Dufo-López, Rodolfo, José L. Bernal-Agustín, et al. (2011). "Multi-objective optimization minimizing cost and life cycle emissions of stand-alone PV–wind–diesel systems with batteries storage". In: *Applied Energy* 88.11, pp. 4033–4041.

Dvorkin, Yury et al. (2015). "A Hybrid Stochastic/Interval Approach to Transmission-Constrained Unit Commitment". In: *IEEE Transactions on Power Systems* 30.2, pp. 621–631.

Elhadidy, M.A. and S.M. Shaahid (2000). "Parametric study of hybrid (wind + solar + diesel) power generating systems". In: *Renewable Energy* 21.2, pp. 129–139.

Elsied, Moataz et al. (2014). "An advanced energy management of microgrid system based on genetic algorithm". In: *2014 IEEE 23rd International Symposium on Industrial Electronics (ISIE)*. IEEE, pp. 2541–2547.

Energy Avicenne (2014). *Battery Market Development for Consumer Electronics, Automotive, and Industrial*. Tech. rep.

Environmental Protection Agency (2007). "Biomas Combined Heat and Power Catalog of Technologies". In: September, pp. 11–20.

Farhangi, H. (2010). "The path of the smart grid". In: *IEEE Power and Energy Magazine* 8.1, pp. 18–28.

Faxas-Guzmán, J. et al. (2014). "Priority load control algorithm for optimal energy management in stand-alone photovoltaic systems". In: *Renewable Energy* 68, pp. 156–162.

Fossati, Juan P et al. (2015). "A method for optimal sizing energy storage systems for microgrids n". In: *Renewable Energy* 77, pp. 539–549.

Funk, Andrew and William B. DeOreo (2011). "Embedded Energy in Water Studies Study 3: End-use Water Demand Profiles". In: 1, p. 215.

Godina, R et al. (2015). "Sustainable Energy System of El Hierro Island". In: 13.

Graham, V A and K G T Hollands (1990). "A method to generate synthetic hourly solar radiation globally". In: *Solar Energy* 44.6, pp. 333–341.

GREIN (2016). *Global renewable energy islands network*.

Groh, S. et al. (2014). "The Battle of Edison and Westinghouse Revisited: Contrasting AC and DC microgrids for rural electrification". In: *MES-BREG 2014*.

GTM-research (2015). *U.S. Solar Market Insight Report, Q1 2015*. Tech. rep. Washington, DC: Solar Energy Industries Association.

Gu, Wei et al. (2014). "Modeling, planning and optimal energy management of combined cooling, heating and power microgrid: A review". In: *International Journal of Electrical Power & Energy Systems* 54, pp. 26–37.

Gude, Veera Gnaneswar, Nagamany Nirmalakhandan, and Shuguang Deng (2010). "Renewable and sustainable approaches for desalination". In: *Renewable and Sustainable Energy Reviews* 14.9, pp. 2641–2654.

Gupta, R.A. and Nand Kishor Gupta (2015). "A robust optimization based approach for microgrid operation in deregulated environment". In: *Energy Conversion and Management* 93, pp. 121–131.

Hafez, Omar and Kankar Bhattacharya (2012). "Optimal planning and design of a renewable energy based supply system for microgrids". In: *Renewable Energy* 45, pp. 7–15.

Hatziargyriou, Nikos et al. (2007). "Microgrids". In: *IEEE Power and Energy Magazine* 5.4, pp. 78–94.

Herrmann, Ulf, Bruce Kelly, and Henry Price (2004). "Two-tank molten salt storage for parabolic trough solar power plants". In: *Energy* 29.5-6, pp. 883–893.

Hittinger, Eric et al. (2015). "Evaluating the value of batteries in microgrid electricity systems using an improved Energy Systems Model". In: *Energy Conversion and Management* 89, pp. 458–472.

Ho, W.S., H. Hashim, and J.S. Lim (2014). "Integrated biomass and solar town concept for a smart eco-village in Iskandar Malaysia (IM)". In: *Renewable Energy* 69, pp. 190–201.

Hrayshat, Eyad S. (2009). "Techno-economic analysis of autonomous hybrid photovoltaic-diesel-battery system". In: *Energy for Sustainable Development* 13.3, pp. 143–150.

IEA (2012). "World energy outlook 2012". In:

— (2014). *Technology Roadmap: Solar thermal electricity*. Tech. rep. Berlin/Heidelberg, p. 52.

IEA PVPS (2015). *Trends in photovoltaic application - 2015*. Tech. rep., p. 64.

IEA-PVPS (2013). *Photovoltaic and Solar Forecasting: State of the Art*. Tech. rep.

IRENA (2012a). "Biomass for Power Generation".

— (2012b). *Water Desalination Using Renewable Energy*. Tech. rep. March.

— (2014). *Solar Photovoltaics*. Tech. rep. 4/5.

— (2015a). "Battery storage for renewables: market status and technology outlook". In: January, p. 60.

— (2015b). "Off-Grid Renewable Energy Systems: Status and Methodological Issues".

— (2015c). *Renewable Desalination : Technology Options for Islands*. Tech. rep. October.

— (2015d). *Renewable Power Generation Costs in 2014*. Tech. rep.

IRENA-GREIN (2014). *A Path to Prosperity: Renewable Energy for Islands*. Tech. rep. June, pp. 22–24.

ISE (2016). *Photovoltaics report*. Tech. rep. March. Fraunhofer Institute for Solar Energy Systems.

Javadi, F.S. et al. (2013). "Global policy of rural electrification". In: *Renewable and Sustainable Energy Reviews* 19, pp. 402–416.

Jenkins, DP, J Fletcher, and D Kane (2008). "Lifetime prediction and sizing of lead-acid batteries for microgeneration storage applications". In: *Renewable Power Generation ...* April, pp. 191–200.

Kagiannas, Argyris G., Dimitris Th Askounis, and John Psarras (2004). "Power generation planning: a survey from monopoly to competition". In: *International Journal of Electrical Power & Energy Systems* 26.6, pp. 413–421.

Kanagawa, Makoto and Toshihiko Nakata (2007). "Analysis of the energy access improvement and its socio-economic impacts in rural areas of developing countries". In: *Ecological Economics* 62.2, pp. 319–329.

— (2008). "Assessment of access to electricity and the socio-economic impacts in rural areas of developing countries". In: *Energy Policy* 36.6, pp. 2016–2029.

Karagiannis, Ioannis C. and Petros G. Soldatos (2008). "Water desalination cost literature: review and assessment". In: *Desalination* 223.1-3, pp. 448–456.

Katiraei, Faridaddin, M.R. Iravani, and P.W. Lehn (2005). "Micro-Grid Autonomous Operation During and Subsequent to Islanding Process". In: *IEEE Transactions on Power Delivery* 20.1, pp. 248–257.

Katiraei, Farid et al. (2008). "Microgrids management". In: *IEEE Power and Energy Magazine* 6.3, pp. 54–65.

Kim, Jong Suk and Thomas F. Edgar (2014). "Optimal scheduling of combined heat and power plants using mixed-integer nonlinear programming". In: *Energy* 77, pp. 675–690.

Kousksou, T. et al. (2014). "Energy storage: Applications and challenges". In: *Solar Energy Materials and Solar Cells* 120, pp. 59–80.

Kriett, Phillip Oliver and Matteo Salani (2012). "Optimal control of a residential microgrid". In: *Energy* 42.1, pp. 321–330.

Kuravi, Sarada et al. (2013). "Thermal energy storage technologies and systems for concentrating solar power plants". In: *Progress in Energy and Combustion Science* 39.4, pp. 285–319.

Kurup, Parthiv and Craig S Turchi (2015). "Parabolic Trough Collector Cost Update for the System Advisor Model (SAM)". In: November.

Kwasinski, Alexis and Philip Krein (2006). "Optimal Configuration Analysis of a Microgrid-Based Telecom Power System". In: *INTELEC 06 - Twenty-Eighth International Telecommunications Energy Conference*. IEEE, pp. 1–8.

Kyriakarakos, George et al. (2013). "Intelligent demand side energy management system for autonomous polygeneration microgrids". In: *Applied Energy* 103, pp. 39–51.

Lambert, T (2006). *Micropower system modeling with HOMER*. Tech. rep.

Lau, K.Y. et al. (2010). "Performance analysis of hybrid photovoltaic/diesel energy system under Malaysian conditions". In: *Energy* 35.8, pp. 3245–3255.

Lazard (2015). "Lazard's levelized cost of storage analysis — version 1.0". In: *Lazard* November.

Lee, Kyoung-Ho et al. (2012). "Preliminary determination of optimal size for renewable energy resources in buildings using RETScreen". In: *Energy* 47.1, pp. 83–96.

Lemmens, S. (2015). "A perspective on costs and cost estimation techniques for Organic Rankine Cycle systems". In: *3rd International Seminar on ORC Power Systems*. Brussels.

Lopes, J.A.P., C.L. Moreira, and A.G. Madureira (2006). "Defining Control Strategies for MicroGrids Islanded Operation". In: *IEEE Transactions on Power Systems* 21.2, pp. 916–924.

Lowery, C and M O'Malley (2012). "Impact of Wind Forecast Error Statistics Upon Unit Commitment". In: *IEEE Transactions on Sustainable Energy* 3.4, pp. 760–768.

Ma, Yiwei et al. (2015). "Optimal Economic Operation of Islanded Microgrid by Using a Modified PSO Algorithm". In: *Mathematical Problems in Engineering* 2015, pp. 1–10.

Macchi, E. and M. Astolfi, eds. (2016). *Organic Rankine Cycle (ORC) Power Systems, 1st Edition*. Woodhead Publishing.

Madduri, P. Achintya et al. (2013). "Design and verification of smart and scalable DC microgrids for emerging regions". In: *2013 IEEE Energy Conversion Congress and Exposition, ECCE 2013*, pp. 73–79.

Magdalena, L. (2010). "What is Soft Computing? Revisiting Possible Answers". In: *International Journal of Computational Intelligence Systems* 3.2, p. 148.

Mainali, Brijesh and Semida Silveira (2013). "Alternative pathways for providing access to electricity in developing countries". In: *Renewable Energy* 57, pp. 299–310.

Malheiro, André et al. (2015). "Integrated sizing and scheduling of wind/PV/diesel/battery isolated systems". In: *Renewable Energy* 83, pp. 646–657.

Mandelli, Stefano, Marco Merlo, and Emanuela Colombo (2016). "Novel procedure to formulate load profiles for off-grid rural areas". In: *Energy for Sustainable Development* 31, pp. 130–142.

Manwell, James F. and Jon G. McGowan (1993). "Lead acid battery storage model for hybrid energy systems". In: *Solar Energy* 50.5, pp. 399–405.

Manzolini, Giampaolo and Paolo Silva (2013). "Solar energy conversion with thermal cycles". In: *Solar Energy Sciences and Engineering Applications*. CRC Press. Chap. Solar ener, pp. 413–484.

Mariam, Lubna, Malabika Basu, and Michael F. Conlon (2013). "A Review of Existing Microgrid Architectures". In: *Journal of Engineering* 2013, pp. 1–8.

Marzband, Mousa et al. (2013). "Experimental validation of a real time energy management system for microgrids in islanded mode using a local day-ahead electricity market and MINLP". In: *Energy Conversion and Management* 76, pp. 314–322.

Maurer, E. (2013). *Advancing Military Microgrids Two-Day Workshop To Support Naval Facilities Engineering*. Tech. rep. Rocky Mountain Institute.

Mazzola, Simone, Marco Astolfi, and Ennio Macchi (2015a). "A detailed model for the optimal management of a multigood microgrid". In: *Applied Energy* 154, pp. 862–873.

— (2015b). "Techno-Economic Optimization of a Stand-alone Hybrid Microgrid for the Rural Electrification in Sub Saharan Africa". In: *3rd Southern African Solar Energy Conference*.

— (2016). "The potential role of solid biomass for rural electrification: A techno economic analysis for a hybrid microgrid in India". In: *Applied Energy* 169, pp. 370–383.

Mazzola, Simone, Marco Astolfi, Paolo Silva, et al. (2017). "Solar energy for electricity and water production in islands". In: *under review*.

Mazzola, Simone, Claudio Ricardo Vergara, et al. (2017). "Assessing the value of forecast-based dispatch in the operation of off-grid rural microgrids". In: *under review*.

Meng, Lexuan et al. (2016). "Microgrid supervisory controllers and energy management systems: A literature review". In: *Renewable and Sustainable Energy Reviews* 60, pp. 1263–1273.

Montuori, Lina et al. (2014). "Integration of renewable energy in microgrids coordinated with demand response resources: Economic evaluation of a biomass gasification plant by Homer Simulator". In: *Applied Energy* 132, pp. 15–22.

Morais, Hugo et al. (2010). "Optimal scheduling of a renewable micro-grid in an isolated load area using mixed-integer linear programming". In: *Renewable Energy* 35.1, pp. 151–156.

Navigant Research (2014). *Micro-grid deployment tracker 2Q14*. Tech. rep. Navigant Research.

Neves, Diana, Carlos A. Silva, and Stephen Connors (2014). "Design and implementation of hybrid renewable energy systems on micro-communities: A review on case studies". In: *Renewable and Sustainable Energy Reviews* 31, pp. 935–946.

New York State Energy Research and Development Authority (2010). *European Wood-Heating Technology Survey: An Overview of Combustion Principles and the Energy and Emissions Performance Characteristics of Commercially Available Systems in Austria, Germany, Denmark, Norway, And Sweden*. Tech. rep.

Nouni, M. R., S. C. Mullick, and T. C. Kandpal (2007). "Biomass gasifier projects for decentralized power supply in India: A financial evaluation". In: *Energy Policy* 35.November 2004, pp. 1373–1385.

Oda, Hisaya and Yuko Tsujita (2011). "The determinants of rural electrification: The case of Bihar, India". In: *Energy Policy* 39.6, pp. 3086–3095.

Olivares, Daniel E. et al. (2014). "Trends in Microgrid Control". In: *IEEE Transactions on Smart Grid* 5.4, pp. 1905–1919.

Olivares, Daniel E et al. (2015). "Stochastic-Predictive Energy Management System for Isolated Microgrids". In: *IEEE Transactions on Smart Grid* 6.6, pp. 2681–2693.

Ophir, A. and F. Lokiec (2005). "Advanced MED process for most economical sea water desalination". In: *Desalination* 182.1-3, pp. 187–198.

Pacheco, James E., Steven K. Showalter, and William J. Kolb (2002). "Development of a Molten-Salt Thermocline Thermal Storage System for Parabolic Trough Plants". In: *Journal of Solar Energy Engineering* 124.2, p. 153.

Palma-Behnke, Rodrigo et al. (2013). "A Microgrid Energy Management System Based on the Rolling Horizon Strategy". In: *IEEE Transactions on Smart Grid* 4.2, pp. 996–1006.

Parisio, Alessandra and Luigi Glielmo (2012). "Multi-objective optimization for environmental/economic microgrid scheduling". In: *2012 IEEE International Conference on Cyber Technology in Automation, Control, and Intelligent Systems (CYBER)*. IEEE, pp. 17–22.

Parisio, Alessandra, Evangelos Rikos, and Luigi Glielmo (2014). "A Model Predictive Control Approach to Microgrid Operation Optimization". In: *IEEE Transactions on Control Systems Technology* 22.5, pp. 1813–1827.

Parker, C.D. (2009). "Applications - stationary | Energy Storage Systems: Batteries". In: *Encyclopedia of Electrochemical Power Sources*. Elsevier, pp. 53–64.

Pombeiro, Henrique, André Pina, and Carlos Silva (2012). "Analyzing Residential Electricity Consumption Patterns Based on Consumer's Segmentation". In: *CEUR Workshop Proceedings*, pp. 29–38.

Quoilin, S. et al. (2011). "Performance and design optimization of a low-cost solar organic Rankine cycle for remote power generation". In: *Solar Energy* 85.5, pp. 955–966.

Rehman, Shafiqur and Luai M. Al-Hadhrami (2010). "Study of a solar PV–diesel–battery hybrid power system for a remotely located population near Rafha, Saudi Arabia". In: *Energy* 35.12, pp. 4986–4995.

Rivarolo, M., A. Greco, and A. F. Massardo (2013). "Thermo-economic optimization of the impact of renewable generators on poly-generation smart-grids including hot thermal storage". In: *Energy Conversion and Management* 65, pp. 75–83.

Rivarolo, M., L. Magistri, and A. F. Massardo (2014). "Hydrogen and methane generation from large hydraulic plant: Thermo-economic multi-level time-dependent optimization". In: *Applied Energy* 113, pp. 1737–1745.

Rivarolo, M. and A. F. Massardo (2013). "Optimization of large scale bio-methane generation integrating "spilled" hydraulic energy and pressurized oxygen blown biomass gasification". In: *International Journal of Hydrogen Energy* 38.12, pp. 4986–4996.

Ruetschi, Paul (2004). "Aging mechanisms and service life of lead–acid batteries". In: *Journal of Power Sources* 127.1-2, pp. 33–44.

Ruiz, P.A. et al. (2009). "Uncertainty Management in the Unit Commitment Problem". In: *IEEE Transactions on Power Systems* 24.2, pp. 642–651.

Sadras, Victor O, Patricio Grassini, and Pasquale Steduto (2012). "Status of water use efficiency of main crops ". In: *SOLAW Background Thematic Report - TR07* 2013.October.

Sauer, Dirk Uwe and Heinz Wenzl (2008). "Comparison of different approaches for lifetime prediction of electrochemical systems—Using lead-acid batteries as example". In: *Journal of Power Sources* 176.2, pp. 534–546.

Schallenberg-Rodriguez, Julieta, Jos?? Miguel Veza, and Ana Blanco-Marigorta (2014). "Energy efficiency and desalination in the Canary Islands". In: *Renewable and Sustainable Energy Reviews* 40, pp. 741–748.

Schnitzer, D. et al. (2014). "Microgrids for Rural Electrification : A critical review of best practices based on seven case studies". In: *United Nations Foundation*.

Sethi, Suresh and Gerhard Sorger (1991). "A theory of rolling horizon decision making". In: *Annals of Operations Research* 29.1, pp. 387–415.

Sevlian, Raffi and Ram Rajagopal (2014). "Short Term Electricity Load Forecasting on Varying Levels of Aggregation". In: pp. 1–8.

Shi, L., Y. Luo, and G. Y. Tu (2014). "Bidding strategy of microgrid with consideration of uncertainty for participating in power market". In: *International Journal of Electrical Power and Energy Systems* 59, pp. 1–13.

Strasser, Matthew N. and R. Paneer Selvam (2014). "A cost and performance comparison of packed bed and structured thermocline thermal energy storage systems". In: *Solar Energy* 108, pp. 390–402.

Szabó, S et al. (2011). "Energy solutions in rural Africa: mapping electrification costs of distributed solar and diesel generation versus grid extension". In: *Environmental Research Letters* 6.3, p. 034002.

Terna (2016). "Energia da fonti rinnovabili in Italia 2016". In:

Tian, Y. and C. Y. Zhao (2013). "A review of solar collectors and thermal energy storage in solar thermal applications". In: *Applied Energy* 104, pp. 538–553.

Unamuno, Eneko and Jon Andoni Barrena (2015). "Hybrid ac/dc microgrids—Part I: Review and classification of topologies". In: *Renewable and Sustainable Energy Reviews* 52, pp. 1251–1259.

Urtasun, Andoni et al. (2014). "Energy management strategy for a battery-diesel stand-alone system with distributed PV generation based on grid frequency modulation". In: *Renewable Energy* 66, pp. 325–336.

U.S. Department of Energy (2012). *Summary Report: 2012 DOE Microgrid Workshop*. Tech. rep.

Üster, Halit and Şebnem Dilaveroğlu (2014). "Optimization for design and operation of natural gas transmission networks". In: *Applied Energy* 133, pp. 56–69.

Valencia, Felipe et al. (2015). "Robust Energy Management System Based on Interval Fuzzy Models". In: *IEEE Transactions on Smart Grid*, pp. 1–18.

Vergara, Claudio Ricardo (2015). "Representing Battery Energy Storage in Electric Power Systems Studies". PhD. University of Porto.

Wang, J. et al. (2011). "Wind power forecasting uncertainty and unit commitment". In: *Applied Energy* 88.11, pp. 4014–4023.

Wang, Kangli et al. (2014). "Lithium–antimony–lead liquid metal battery for grid-level energy storage". In: *Nature* 514.7522, pp. 348–350.

Werner, C. and C. Breyer (2012). "Analysis of Mini-Grid Installations: An Overview on System Configurations". In: *27th European Photovoltaic Solar Energy Conference and Exhibition*, pp. 3885–3892.

Wood, A J and B F Wollenberg (1996). *Power Generation, Operation, and Control*. A Wiley-Interscience publication. Wiley.

Wouters, Carmen, Eric S. Fraga, and Adrian M. James (2015). "An energy integrated, multi-microgrid, MILP (mixed-integer linear programming) approach for residential distributed energy system planning – A South Australian case-study". In: *Energy* 85, pp. 30–44.

Yan, Jinyue, ed. (2015). *Handbook of Clean Energy Systems*. Chichester, UK: John Wiley & Sons, Ltd.

Zhang, Mingrui and Jie Chen (2014). "The Energy Management and Optimized Operation of Electric Vehicles Based on Microgrid". In: *IEEE Transactions on Power Delivery* 29.3, pp. 1427–1435.

Zhao, Bo, Xuesong Zhang, Jian Chen, et al. (2013). "Operation Optimization of Standalone Microgrids Considering Lifetime Characteristics of Battery Energy Storage System". In: *IEEE Transactions on Sustainable Energy* 4.4, pp. 934–943.

Zhao, Bo, Xuesong Zhang, Peng Li, et al. (2014). "Optimal sizing, operating strategy and operational experience of a stand-alone microgrid on Dongfushan Island". In: *Applied Energy* 113, pp. 1656–1666.

Zhao, C. Y., W. Lu, and Y. Tian (2010). "Heat transfer enhancement for thermal energy storage using metal foams embedded within phase change materials (PCMs)". In: *Solar Energy* 84.8, pp. 1402–1412.